NASA TM X-350

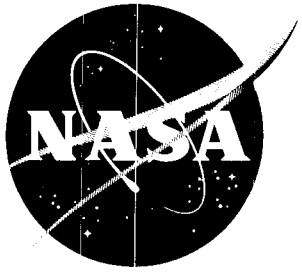

TECHNICAL MEMORANDUM
X-350

DYNAMIC STABILITY AND DISPERSION OF A PROJECT MERCURY TEST CAPSULE UPON ENTERING THE ATMOSPHERE, WITH EFFECTS OF ROLL RATE, CENTER-OF-GRAVITY DISPLACEMENT, AND THRESHOLD OF A RATE-REACTION CONTROL SYSTEM

By Byron M. Jaquet

Langley Research Center
Langley Field, Va.

NATIONAL AERONAUTICS AND SPACE ADMINISTRATION
WASHINGTON

January 1961

CONFIDENTIAL

NATIONAL AERONAUTICS AND SPACE ADMINISTRATION

TECHNICAL MEMORANDUM X-350

DYNAMIC STABILITY AND DISPERSION OF A PROJECT MERCURY TEST CAPSULE UPON ENTERING THE ATMOSPHERE, WITH EFFECTS OF ROLL RATE, CENTER-OF-GRAVITY DISPLACEMENT, AND THRESHOLD OF A RATE-REACTION CONTROL SYSTEM*

By Byron M. Jaquet

SUMMARY

An analytical investigation was made to determine the effects of initial roll rate, relative displacement between the center of gravity and the center of pressure, and threshold of a reaction control system responding to pitch, yaw, and roll rates on the dynamic stability of a Project Mercury test capsule during reentry from an altitude of 450,000 feet. The dispersion area at a Mach number of 1.0, the point of first parachute deployment, also was determined. Although dispersion areas are somewhat elliptical, circular areas were used herein for convenience.

With the control system operative at all times the angle of attack at a Mach number of 1.0 was in all cases less than about $2\frac{1}{2}^{\circ}$; whereas, with the control system inoperative at all times the capsule attained an angle of attack of about 20°. When the relative displacement between the center of gravity and the center of pressure was increased from 1/4 to 1/2 inch (control system operative), the trim angle of attack was generally doubled for altitudes below about 300,000 feet but had a negligible effect on the amplitude of oscillation. An increase in control-system threshold from 0.5 deg/sec to 1.0 deg/sec allowed the capsule to reach greater amplitudes of oscillation but did not appreciably affect the trim angle of attack.

For a 1/4-inch center-of-gravity offset and a 1.0 deg/sec threshold, the use of an initial roll rate of 1 rpm reduced the dispersion area from

*Title, Unclassified.

a circle of approximately 8.9 nautical miles in diameter for the no-spin case to one of about 0.25 nautical mile in diameter for the rolling case. For the rolling capsule, with a 1.0 deg/sec threshold, an increase in center-of-gravity offset from 1/4 to 1/2 inch about doubled the diameter of the dispersion circle.

The control system, in general, reduced the pitch and yaw rates to within the threshold after arbitrary disturbances were introduced in the angle of attack and the rates. The time required to reduce these rates varied considerably with the altitude at which the disturbances were introduced. With the control system inoperative at all times the capsule, with an initial reentry angle of attack of 0°, experienced maximum pitch and yaw rates at about a Mach number of 1.0, the point of first parachute deployment. The peak rates were 41 deg/sec and 24 deg/sec for pitch and yaw, respectively.

INTRODUCTION

In the development program of Project Mercury a number of preliminary unmanned flights of the capsule are contemplated. Among these flights are various simulated entries into the atmosphere from an orbital path. In order to obtain some indication of the expected behavior of the capsule during its reentry and descent through the atmosphere, the Space Task Group of the National Aeronautics and Space Administration has requested the Langley Missile Systems Section to investigate the dynamic behavior of a Mercury type test capsule during descent from an altitude of 450,000 feet. Reference 1 gives the results of a general study of the behavior of such capsules. The present investigation included the effects of initial roll rate, relative lateral displacement between the center of pressure and the center of gravity, and control-system threshold on the dynamic behavior of the capsule. Since the first parachute deployment was to occur when the capsule velocity decreased to a Mach number of 1.0, the dispersion area at this point was determined. The control system used in this investigation was a jet-reaction on-off type responding to pitch, yaw, and roll rates. The effect of initial roll rate on the condition of resonance that occurs when roll rate and pitch or yaw frequencies are coincident (refs. 2 and 3) was determined with the control system inoperative.

In addition to the complete trajectory calculations, the effects of arbitrary step disturbances in angle of attack and in pitch and yaw rates on the stability of the capsule and on the ability of the control system to handle such disturbances were investigated.

All calculations were made on an IBM 704 electronic data processing machine for a spherical nonrotating earth.

SYMBOLS

The symbols and coefficients used with the equations of motion given in appendices A and B are referred to the axes system shown in figure 1.

A	reference area (area at maximum diameter), sq ft
A_{V_R}	deceleration, $\frac{-\Delta V_R}{g\Delta t}$
a	speed of sound, ft/sec
C_X	coefficient of force along X_b-axis, $\frac{\text{Force along } X_b\text{-axis}}{QA}$
C_Y	coefficient of force along Y-axis, $\frac{\text{Force along Y-axis}}{QA}$
C_{Y_α}	rate of change of side-force coefficient with angle of attack in XY-plane, $\frac{\partial C_Y}{\partial \alpha_Y}$, per radian
C_Z	coefficient of force along Z-axis, $\frac{\text{Force along Z-axis}}{QA}$
C_{Z_α}	rate of change of normal-force coefficient with angle of attack in XZ-plane, $\frac{\partial C_Z}{\partial \alpha_Z}$, per radian
C_m	moment coefficient about Y-axis, $\frac{\text{Moment about Y-axis}}{QAd}$
C_{m_q}	damping-in-pitch coefficient, $\frac{\partial C_m}{\partial\left(\frac{qd}{2V_R}\right)}$
C_{m_α}	variation of pitching-moment coefficient with angle of attack in XZ-plane, $\frac{\partial C_m}{\partial \alpha_Z}$, per radian

$C_{m_{\dot{\alpha}}}$ acceleration derivative due to rate of change of angle of attack in X_bZ_b-plane, $\frac{\partial C_m}{\partial\left(\frac{\dot{\alpha}d}{2V_R}\right)}$

C_n moment coefficient about Z-axis, $\frac{\text{Moment about Z-axis}}{QAd}$

C_{n_r} damping-in-yaw coefficient, $\frac{\partial C_n}{\partial\left(\frac{rd}{2V_R}\right)}$

C_{n_α} variation of yawing-moment coefficient with angle of attack in XY-plane, $\frac{\partial C_n}{\partial \alpha_Y}$, per radian

$C_{n_{\dot{\beta}}}$ acceleration derivative due to rate of change of angle of attack in X_bY_b-plane, $\frac{\partial C_n}{\partial\left(\frac{\dot{\beta}d}{2V_R}\right)}$

D relative lateral displacement between center of pressure and center of gravity measured initially along Y-axis, ft

d maximum diameter of capsule, ft

g acceleration of gravity at earth's surface, 32.2 ft/sec^2

H heading angle (positive when measured from east toward south), deg

h altitude above surface of earth, ft

I_{X_b} moment of inertia about X_b-axis, slug-ft^2

I_{Y_b} moment of inertia about Y_b- and Z_b-axes, slug-ft^2

K control-system threshold, deg/sec

M Mach number, V_R/a

$M_{X_b}, M_{Y_b}, M_{Z_b}$	torque about X_b-, Y_b-, and Z_b-axis, respectively, produced by control system, ft-lb
m	mass of capsule, slugs
p,q,r	angular rate about X-, Y-, and Z-axis, respectively, radians/sec, deg/sec, or rpm
p_b, q_b, r_b	angular rate about X_b-, Y_b-, and Z_b-axis, respectively, radians/sec or deg/sec
Q	dynamic pressure, $\frac{\rho}{2} V_R^2$, lb/sq ft
R	radial distance from center of earth to center of gravity of capsule, ft
R_e	radius of earth, 20.909×10^6, ft
t	time, sec
u,v,w	component of velocity along X-, Y-, and Z-axis, respectively, ft/sec
V_R	resultant velocity, fps
X,Y,Z	reference axes with origin at capsule center of gravity; plane containing Z-axis is always parallel to Z'X'-plane (see fig. 1)
X_b, Y_b, Z_b	body system of axes with origin at capsule center of gravity and rolling through an angle ϕ about X-axis which is coincident with X_b-axis
X_i, Y_i, Z_i	reference axes with origin at center of earth
X',Y',Z'	reference axes with origin at capsule center of gravity at distance R from center of earth and parallel to X_i-, Y_i-, and Z_i-axes
x,y,z	distance from origin along X_i-, Y_i-, and Z_i-axis, respectively, to center of gravity of capsule
α	total angle of attack, angle between capsule longitudinal axis and resultant velocity, deg

α_Y angle of attack in XY-plane, deg

α_Z angle of attack in XZ-plane, deg

β angle of sideslip, radians

δ inclination of flight path from local horizontal, positive for nose up, deg

θ angle of elevation of X- and X_b-axes above a plane parallel to X_iZ_i-plane, radians

$\bar{\theta}$ angle of latitude of capsule, radians

ρ density of air (standard atmosphere tables for density variation with altitude, from Rocket Panel Proposal of April 1955), slugs/cu ft

ϕ roll angle about X- and X_b-axes, radians or deg

ψ angle in X'Z'-plane between plane containing X- and Y-axes and X'-axis, radians

$\bar{\psi}$ angle in X_iZ_i-plane of orientation of position vector to capsule, radians (see fig. 1)

Subscript:

o indicates initial conditions

A dot over a symbol indicates the derivative with respect to time. The prefix Δ indicates a change or increment.

CALCULATIONS

General Considerations

Two types of calculations were made in the present investigation of the dynamic behavior of a Project Mercury test capsule. The first group of calculations were made in order to determine the effect of various design and initial conditions on the dynamic behavior of the capsule. These calculations were continuous trajectory calculations from reentry at an altitude of 450,000 feet down to an altitude where the Mach number

decreased to a value appreciably below 1.0. The second group of calculations were made to evaluate the ability of the control system to compensate for arbitrarily imposed disturbances which were initially introduced at six different altitudes along the trajectory.

Included in the first group of calculations were the effects on the capsule behavior of initial roll rate, relative lateral displacement between the center of pressure and the center of gravity (hereinafter referred to as center-of-gravity offset), and threshold of a jet-reaction on-off control system responding to pitch, yaw, and roll rates. Since the initial roll angle at reentry would not be known exactly, calculations were made with various initial roll angles in combination with center-of-gravity offsets. Because the various combinations of initial roll angle and center-of-gravity offset provide different initial trim angles of attack, the dispersion area as well as the dynamic behavior could be determined from these calculations. Inasmuch as the first parachute deployment was to occur at $M = 1.0$, this point was selected for the dispersion study. Calculations were also made to determine the behavior of the capsule with the control system inoperative after the peak heating region was passed; the control system for this case was inoperative after reaching $A_{V_R} = 5.0$. Also, a calculation was made to determine the behavior of the capsule with the control system inoperative at all times. In order to determine the significance of resonance on the behavior, additional calculations were made with initial roll rates of 0, 1, and 6 rpm with the control system inoperative. All of the trajectories of the first group of calculations were computed by use of 10 to 20 points per half-cycle (depending on the frequency of oscillation) when an oscillation was present in the angle of attack. Also, these calculations were made with a given initial heading to a prescribed impact area and with the initial conditions given in appendix B.

For the second group of calculations a reference trajectory was first calculated, by the previously described procedure, for flight along the equator. This case had an initial roll rate of 1 rpm, no center-of-gravity offset, and the control system inoperative. Six altitudes were selected from this trajectory in which ϕ_o was an even multiple of 360° in order to facilitate the introduction of arbitrary step disturbances in angle of attack and in pitch and yaw rates. Calculations were then made at these six altitudes in order to determine the effectiveness of the control system in handling arbitrary disturbances. Calculations were made with constant computing intervals for the cases of (a) no disturbances with the control system inoperative, (b) step disturbances introduced with the control system inoperative, and (c) step disturbances introduced with the control system operating outside of a threshold of 1.0 deg/sec. The calculations with the control system inoperative and without disturbances also provided information on the peak rates that would exist at points along the trajectory.

Initial conditions for both groups of calculations are given in appendix B and other pertinent data are given in tables I and II. All calculations were made on an IBM 704 electronic data processing machine for a spherical nonrotating earth. Above an altitude of 390,000 feet zero density was used.

Aerodynamic, Mass, and Dimensional Characteristics

The general arrangement of the capsule is shown in figure 2. The aerodynamic derivatives and coefficients used in the calculations are shown in figure 3 as functions of Mach number. These curves are based on derivatives experimentally determined in various NASA facilities (refs. 4 and 5) and on values supplied by the NASA Space Task Group. Changes in derivatives were made during the calculations in the manner indicated in figure 3. The derivatives C_{m_q} and C_{n_r} were obtained from oscillation tests and therefore represent the total damping derivatives $C_{m_q} + C_{m_{\dot{\alpha}}}$ and $C_{n_r} - C_{n_{\dot{\beta}}}$. The curve of C_{m_α} against Mach number is also based on oscillatory derivatives (refs. 4 and 5). All derivatives were obtained at $\alpha \approx 0^\circ$ and some would probably vary considerably with angle of attack. At the time the calculations were made only these values were available.

The following mass and dimensional parameters were used for all calculations:

m, slugs	65.2
S, sq ft	30.272
d, ft	6.208
I_{X_b}, slug-ft^2	200
I_{Y_b}, slug-ft^2	360
D (fig. 1(b)), in.	0, 1/4, 1/2

RESULTS AND DISCUSSION

Presentation of Results

Some trajectory characteristics V_R, M, A_{V_R}, Q, and h are plotted as a function of time in seconds in figures 4 to 8 for several of the calculations of reentry at an initial altitude of 450,000 feet. The effects of control-system threshold, initial roll rate, center-of-gravity offset, initial roll angle, cutting the control system off at

A_{V_R} = 5.0, and having the control system inoperative at all times on the variation of angle of attack with time are shown in figures 9 to 16.

The effect of initial roll rate on resonance in angle of attack for the capsule with the control system inoperative is shown in figure 17.

The dispersion area, as affected by initial roll rate and center-of-gravity offset, is shown in figure 18 for the capsule with a control-system threshold of 1.0 deg/sec.

The characteristics of a trajectory on equatorial flight, made for the purposes of obtaining initial conditions at various altitudes for additional calculations, are shown in figure 19. Based upon the initial conditions obtained from figure 19 at six altitudes along the trajectory, the effects of arbitrary step disturbances in angle of attack and in the pitch and yaw rates on the variation of α, q_b, and r_b with time and the effectiveness of the control system in compensating for the disturbances are shown in figures 20 to 25.

General Remarks

The trajectory characteristics of figures 4 to 8 are presented for the sake of completeness. In general, it can be said that peak values of deceleration and dynamic pressure occur at essentially the same time for all cases. The magnitude of the peak values is somewhat lower for the cases in which the nose of the capsule is pointed downward.

Dynamic Stability Over Entire Reentry

From $t = 0$ (450,000-foot altitude) to $t \approx 80$ seconds, the region where air density was zero, all cases show the same essentially linear increase in angle of attack (figs. 9 to 16). This increase in angle of attack is attributable to the flight path curving downward while the capsule attitude remains unchanged because an aerodynamic restoring moment does not exist due to the lack of air. After reaching the air the restoring moment causes an oscillation in angle of attack to develop, the period and amplitude of which are functions of dynamic pressure (the variation of dynamic pressure with time is shown in figs. 4 to 8) and are affected to some extent by the conditions imposed on the capsule at reentry.

Abrupt changes in the derivatives were made at M = 5.0, 3.5, 2.5, 1.5, and 1.0 (fig. 3) and it appears that these changes have noticeable effects only for Mach numbers of 2.5 and less (figs. 9 to 16). For Mach numbers above 3.5 the derivative C_{m_q} was the only one changed. The

positive shift in the trim angle of attack at $M = 2.5$ can be attributed to the decrease in C_{m_α} and the change in C_{Z_α} from negative to positive. The change in C_{m_q} at this Mach number is stabilizing and causes a decrease in amplitude of oscillation. At $M = 1.5$, the decrease in trim angle of attack is due to the decrease in C_X which causes a decrease in moment because there is a relative displacement between the center of pressure and the center of gravity. The only other derivative changed at $M = 1.5$ was C_{m_q}; this change causes the amplitude to increase. For the $M = 1.0$ change, C_{m_α} is decreased again and the trim angle of attack again increases, and the change in C_{m_q} is of such a nature that the amplitude decreases. The effects of these changes in derivatives on the motions are modified, of course, by control-system threshold, initial roll rate, and relative lateral displacement between the center of pressure and the center of gravity. The effect of these and other conditions at reentry on the behavior are discussed in the sections that follow.

Effects of control-system threshold and initial roll rate.- For both the nonrolling (fig. 9) and the rolling (fig. 10) capsule, an increase in control-system threshold from 0.5 deg/sec to 1.0 deg/sec in general doubles the amplitude of oscillation in angle of attack but has essentially no effect on the frequency. At the high altitudes after the first peak angle of attack is reached, the rolling capsule has a somewhat higher amplitude of oscillation than the nonrolling capsule. This behavior can be seen directly from figure 11 for a control-system threshold of 0.5 deg/sec and by a comparison of figures 9 and 10 for a threshold of 1.0 deg/sec.

At a Mach number of 1.0, the point of first parachute deployment, the use of different threshold values had essentially no effect on the trim angle of attack for either the rolling or nonrolling capsule (figs. 9 and 10). The rolling capsule, however, did have a lower trim angle of attack than did the nonrolling capsule at Mach number 1.0 (fig. 14). For all cases with the control system operating outside of a given threshold the angle of attack at Mach number 1.0 was less than about 2.5°.

Effects of center-of-gravity offset and initial roll angle.- Since the effects of initial roll angle are coupled to the effects of center-of-gravity offset, they are discussed together in this section. With the capsule rolling initially at 1 rpm and with a control-system threshold of 1.0 deg/sec, an increase in center-of-gravity offset from 1/4 to 1/2 inch approximately doubles the trim angle of attack for altitudes below about 300,000 feet (fig. 12) and has essentially no effect on the amplitude of oscillation about the trim value or on the frequency of oscillation. At Mach number 1.0 the trim angles of attack are about 1.0° and 2.0° for 1/4- and 1/2-inch center-of-gravity offsets, respectively.

As previously mentioned, the dispersion area at $M = 1.0$ was determined by varying the initial roll angle ϕ_o for a given center-of-gravity offset. Since this produced various initial trim angles of attack, these cases are also of interest from a stability standpoint. For the nonrolling capsule with 1/4-inch center-of-gravity offset (fig. 13), a change in ϕ_o from 0° to 180° results in somewhat larger amplitudes of oscillation at the higher altitudes and smaller amplitudes at the lower altitudes corresponding to Mach numbers less than 1.0. For the rolling capsule (fig. 14) initial roll angles of 60° and 240° were selected. By the time the rolling capsule reached an altitude of 390,000 feet where the density first had a value, the rolling vehicle with $\phi_o = 240^\circ$ reached a position corresponding to $\phi_o = 0^\circ$ of the nonrolling capsule and the rolling vehicle with $\phi_o = 60^\circ$ corresponded to $\phi_o = 180^\circ$ of the nonrolling capsule. With this in mind it can be seen that the effects of initial roll angle for the rolling capsule (fig. 14) are generally similar to the effects of initial roll angle for the nonrolling capsule (fig. 13).

Effects of terminating control-system operation at $A_{V_R} = 5.0$ and of completely inoperative control system.- Since it has been previously mentioned that the capsule would have passed the peak heating region at the time when $A_{V_R} = 5.0$, the control-system operation was terminated at this point in order to determine the behavior thereafter without stability augmentation. The data of figure 15 show that, after the control system was made inoperative at $A_{V_R} = 5.0$, the angle of attack begins to diverge almost immediately and, although the angle of attack at $M = 1.0$ is still under 5°, very large angles are reached thereafter. By comparison, when the control system was operating throughout the trajectory, the angle of attack was much lower especially at the subsonic Mach numbers (fig. 15).

With the control system inoperative throughout the trajectory (fig. 16), much larger oscillations in the angle of attack were generally obtained although the trim angle of attack was about the same down to $M = 10$ as for the case with the control system in operation. At $M = 1.0$ the maximum angle of attack is about 20° for the case with the control system inoperative compared with about 2° with the control system operating. Although the aerodynamic derivatives were changed in the step-function pattern shown in figure 3, it is believed that the actual behavior of the capsule would be similar to that represented herein. The periodic appearance of the angle-of-attack envelope for Mach numbers above 3 is attributable to the combined effects of roll rate and center-of-gravity offset. It is more pronounced for the capsule with the inoperative control system because the effective damping of the control system is unavailable. This type of oscillation did not occur for either the nonrolling capsule with center-of-gravity offset (fig. 9) or the rolling capsule without center-of-gravity offset (fig. 19(b)).

Resonance Effects With Control System Inoperative

When the roll rate and the pitch or yaw frequency are in coincidence, resonance phenomenon can occur in the angle-of-attack motion (refs. 2 and 3). Calculations were made for initial roll rates of 0, 1, and 6 rpm for 1/4-inch center-of-gravity offset and $\phi_o = 0^o$ with the control system inoperative over an altitude range from 450,000 feet to about 275,000 feet. Since the roll rates are relatively low, resonance is likely to occur only at high altitudes where the pitch and yaw frequencies are low; it actually occurs only for the 6-rpm case (fig. 17). The onset of resonance begins for this case at an altitude of about 325,000 feet where the amplitude of oscillation begins to increase rapidly, with the peak occurring at an altitude of about 300,000 feet. At an altitude of 300,000 feet the pitch frequency is 0.1 cycle/sec which coincides with the roll frequency of 0.1 cycle/sec for the 6-rpm case. The additional peak angles of attack that occur at lower altitudes are similar to those that were previously described (control system inoperative) with an initial roll rate of 1 rpm and 1/2-inch center-of-gravity offset. The higher peak angle of attack for the 6-rpm case is due to the increased gyroscopic effect as compared with the 0-rpm and 1-rpm cases.

Dispersion

As previously mentioned, the dispersion area was determined by providing various amounts of initial trim angle of attack at an altitude of 450,000 feet. These initial trim angles of attack were obtained from combinations of initial roll angle and center-of-gravity offset. Since initial parachute deployment was to occur at Mach number 1.0, this point was selected for the dispersion study. Dispersion areas are usually elliptical in shape with the major axis of the ellipse extending down range. In the present investigation, circles were used for dispersion areas because enough points to define the actual elliptical area were not calculated. For the particular computation program used herein, range could only be computed for equatorial or meridional flight. For flights with headings other than these, only the impact coordinates could be computed. The actual range would be similar to that shown in figure 19(e) for equatorial flight.

The impact coordinates are plotted in figure 18 for various initial conditions for the capsule with the control system operating outside of a threshold of 1.0 deg/sec. With $p_o = 0$ rpm and 1/4-inch center-of-gravity offset, the dispersion area is contained within a circle of about 53,900 feet in diameter or about 8.9 nautical miles. However, when a roll rate of 1 rpm is used, this area is reduced to a circle of about 1,500 feet in diameter (0.25 nautical mile). When the center-of-gravity offset is increased from 1/4 to 1/2 inch for the rolling vehicle, the

circle is increased to a diameter of 2,480 feet (0.41 nautical mile). The angles of attack that exist at the points of dispersion are presented in table III and are the values just prior to the change in derivatives at $M = 1.0$. In all cases the angle of attack is $2\frac{1}{2}^{\circ}$ or less.

Dynamic Stability at Six Altitudes

In order to determine the effectiveness of the control system in overcoming arbitrary step disturbances, calculations were made in which step disturbances were introduced in the angle of attack and the pitch and yaw rates about the body axes at six altitudes selected along the equatorial trajectory described in figure 19. Pertinent data concerning these calculations are given in table II.

Angle of attack and pitch and yaw rates about the body axes are plotted against time for the six altitudes in figures 20 to 25. All data are for an initial roll rate of 1 rpm and no center-of-gravity offset.

Angle-of-attack characteristics.- At the highest altitude (407,146 ft, fig. 20(a)), no oscillation exists for the undisturbed case (control system inoperative) because of a lack of air density. Shortly after the introduction of the disturbances the angle of attack decreases as a result of the manner in which the q_b disturbance was introduced. Thereafter, the spin about the X_b-axis causes the angle of attack to increase to 34° before sufficient aerodynamic restoring moment is available to cause the angle to decrease. When the control system is operative, the first peak angle is reduced to 13° and thereafter the oscillation damps rapidly to amplitudes that are less than the undisturbed values.

For the other altitudes, the control system generally reduces the angle of attack of the disturbed cases to those of the undisturbed cases but the time required varies with altitude (figs. 21(a) to 25(a)). In the region of maximum dynamic pressure (fig. 23(a)) over 10 seconds is required to reduce the magnitude of the disturbed amplitudes to the magnitude of the undisturbed amplitudes.

Rate characteristics.- In the altitude range from 450,000 to 390,000 feet the pitch and yaw rates are zero for the undisturbed case (figs. 20(b) and (c)) because of the lack of air. When the capsule enters the air, it pitches and yaws because of the angle of attack which had been attained up to this point (fig. 20(a)). When disturbances are introduced into α, q_b, and r_b, the rates increase in amplitude and the amplitudes in general increase with time because, in this region, the damping derivatives (fig. 3) have destabilizing values. When the

control system is operative the disturbed rates are reduced to within the threshold in about 0.10 second. Control-system operation is again indicated in the middle time region by the saw-tooth type of curves because the rates tended to exceed the threshold values. Similar effects are shown at an altitude of 315,960 feet (figs. 21(b) and (c)). The on-off type of control system used herein responds instantaneously and reduces the rates to the threshold values.

As the altitude decreases, the rates increase in magnitude and exceed the threshold values (figs. 22 to 25) for both the undisturbed and the disturbed cases when the control system is inoperative. When the control system is operative, the pitch rates in most cases were not contained to threshold values but the yaw rates, in general, were reduced to threshold values in the time studied.

For both the undisturbed and disturbed cases with the control system inoperative, peak rates occur near Mach number 1.0 (figs. 25(b) and (c)). The undisturbed peak rates at $M = 1.0$ were about 41 deg/sec and 24 deg/sec for pitch and yaw, respectively. These are the values that would occur for the capsule just prior to parachute deployment if the control system was inoperative throughout the trajectory.

CONCLUSIONS

An analytical investigation to determine the dynamic behavior of a Project Mercury test capsule during reentry from an altitude of 450,000 feet and the dispersion area at a Mach number of 1.0 has been made, and the results indicate the following conclusions:

1. With the control system operative at all times the angle of attack at a Mach number of 1.0, the point of first parachute deployment, was in all cases less than about $2\frac{1}{2}^{\circ}$; whereas, with the control system inoperative at all times the capsule attained an angle of attack of about 20° at Mach number 1.0.

2. When the relative displacement between the center of gravity and the center of pressure was increased (control system operative) from 1/4 to 1/2 inch, the trim angle of attack was generally doubled for altitudes below about 300,000 feet but had a negligible effect on the amplitude of the oscillation.

3. An increase in control-system threshold from 0.5 deg/sec to 1.0 deg/sec allowed the capsule to reach greater amplitudes of oscillation but did not appreciably affect the trim angle of attack.

4. For a 1/4-inch center-of-gravity offset and a 1.0 deg/sec threshold, the use of an initial roll rate of 1 rpm reduced the dispersion area from a circle of approximately 8.9 nautical miles in diameter for the nonrolling capsule to a circle of about 0.25 nautical mile in diameter for the rolling vehicle. For the rolling capsule, with a 1.0 deg/sec threshold, an increase in center-of-gravity offset from 1/4 to 1/2 inch about doubled the diameter of the dispersion circle.

5. The control system, in general, reduced the pitch and yaw rates to within the threshold after arbitrary disturbances were introduced in the angle of attack and in the rates. The time required to reduce these rates varied considerably with the altitude at which the disturbances were introduced.

6. With the control system inoperative at all times the capsule with an initial reentry angle of attack of 0° experienced maximum pitch and yaw rates at about Mach number 1.0, the point of first parachute deployment. The peak pitch rate was about 41 deg/sec and the peak yaw rate was about 24 deg/sec.

Langley Research Center,
National Aeronautics and Space Administration,
Langley Field, Va., July 15, 1960.

APPENDIX A

EQUATIONS OF MOTION, ASYMMETRY CONSIDERATIONS, AND DESCRIPTION OF CAPSULE CONTROL SYSTEM

EQUATIONS OF MOTION

The equations of motions used herein are basically those of reference 1 with the drogue parachute terms neglected and terms to include the effects of center-of-gravity offset and control-system torques included. The equations that describe the motion of the capsule with respect to the axes system of figure 1 are given as follows:

X-force equation:

$$\dot{u} = \frac{QA}{m} C_X \cos \alpha - g \frac{R_e^2}{R^3}(x \cos \psi \cos \theta + y \sin \theta + z \sin \psi \cos \theta) - qw + rv$$

Y-force equation:

$$\dot{v} = \frac{QA}{m} C_{Y_\alpha} \frac{v}{V_R} - g \frac{R_e^2}{R^3}(-x \cos \psi \sin \theta + y \cos \theta - z \sin \psi \sin \theta)$$

$$- ru + qw \tan \theta$$

Z-force equation:

$$\dot{w} = \frac{QA}{m} C_{Z_\alpha} \frac{w}{V_R} - g \frac{R_e^2}{R^3}(-x \sin \psi + z \cos \psi) - qv \tan \theta + qu$$

X-moment equation:

$$\dot{p} = \frac{QAd}{I_{X_b}}\left(C_{Z_\alpha} \frac{D}{d} \frac{w}{V_R} \cos \phi - C_{Y_\alpha} \frac{D}{d} \frac{v}{V_R} \sin \phi\right) + \frac{M_{X_b}}{I_{X_b}}$$

Y-moment equation:

$$\dot{q} = \frac{QAd}{I_{Y_b}}\left(C_{m_\alpha} \frac{w}{V_R} + C_{m_q} \frac{qd}{2V_R} + C_X \frac{D}{d} \sin \phi\right) - pr \frac{I_{X_b}}{I_{Y_b}} + rq \tan \theta$$

$$+ \frac{1}{I_{Y_b}}\left(M_{Y_b} \cos \phi - M_{Z_b} \sin \phi\right)$$

Z-moment equation:

$$\dot{r} = \frac{QAd}{I_{Y_b}}\left(C_{n_\alpha}\frac{v}{V_R} + C_{n_r}\frac{rd}{2V_R} - C_X\frac{D}{d}\cos\phi\right) - q^2\tan\theta + pq\frac{I_{X_b}}{I_{Y_b}}$$

$$+ \frac{1}{I_{Y_b}}\left(M_{Z_b}\cos\phi + M_{Y_b}\sin\phi\right)$$

Relationships used with these equations are as follows:

$$\dot{\phi} = p - q\tan\theta$$

$$\dot{\theta} = r$$

$$\dot{\psi} = \frac{-q}{\cos\theta}$$

$$\dot{x} = u\cos\theta\cos\psi - v\sin\theta\cos\psi - w\sin\psi$$

$$\dot{y} = u\sin\theta + v\cos\theta$$

$$\dot{z} = u\cos\theta\sin\psi - v\sin\theta\sin\psi + w\cos\psi$$

The angle of attack, the angle between the total velocity vector and the capsule longitudinal axis, is defined as

$$\sin\alpha = \frac{\sqrt{v^2 + w^2}}{V_R}$$

with the resultant velocity defined as

$$V_R = \sqrt{u^2 + v^2 + w^2}$$

Altitude is defined as

$$h = \sqrt{x^2 + y^2 + z^2} - R_e$$

where $R_e = 20.909 \times 10^6$ feet, an average value of the earth radius during the reentry. Latitude is defined as

$$\bar{\theta} = \tan^{-1} \frac{y}{\sqrt{x^2 + z^2}}$$

and for small changes in latitude, longitude is given by

$$\frac{\pi}{2} - \bar{\psi} = \tan^{-1} \frac{x}{z}$$

ASYMMETRY CONSIDERATIONS

Forces acting at a center of pressure that is not coincident with the center of gravity produce moments about the axes system located at the center of gravity. Displacements between the center of pressure and the center of gravity used in the calculations were 1/4 and 1/2 inch and an examination of the distances and the magnitude of the various derivatives indicated that for fore and aft displacements the derivatives were changed only in the third digit. Since these changes were within the accuracy of the knowledge of the derivatives, no changes were made in fore and aft displacement. Since the longitudinal force is large, small vertical or lateral displacements between the center of pressure and the center of gravity produce significant moments. Also the forces along the Y- and Z-axes produce rolling moments when there is a displacement. These moments vary with the angle ϕ as indicated in figure 1(b) and are shown in the equations of motion as functions of ϕ.

CONTROL-SYSTEM OPERATION

The test capsule has an automatic on-off reaction control system responding to pitch, yaw, and roll rates about the body axes. The body axes roll through an angle ϕ about the X-axis, which is coincident with the X_b-axis; thus, it is necessary to determine body axes rates from

$$q_b = q \cos \phi + r \sin \phi$$

$$r_b = r \cos \phi - q \sin \phi$$

$$p_b = p$$

The torques applied by the control system when the body axes rates exceed a given threshold are given in the following table:

Control	Torque, ft-lb	Threshold
Roll	$M_{X_b} = 0$	$(p_b - K) < p_{b_o} < (p_b + K)$
	$M_{X_b} = 6$	$p_b < p_{b_o} - K$
	$M_{X_b} = -6$	$p_b > p_{b_o} + K$
Pitch	$M_{Y_b} = 0$	$-K < q_b < K$
	$M_{Y_b} = 30$	$q_b < -K$
	$M_{Y_b} = -30$	$q_b > K$
Yaw	$M_{Z_b} = 0$	$-K < r_b < K$
	$M_{Z_b} = 30$	$r_b < -K$
	$M_{Z_b} = -30$	$r_b > K$

Two values of the threshold limit K were investigated, 0.5 deg/sec and 1.0 deg/sec. No time lag was incorporated in the system. Location of the jets is shown in figure 2. It was not possible to determine the amount of fuel consumed during control-system operation. The torques were applied as long as was necessary to reduce the rates to threshold values. Illustration of the regions of control-system operation is shown in sketch (a).

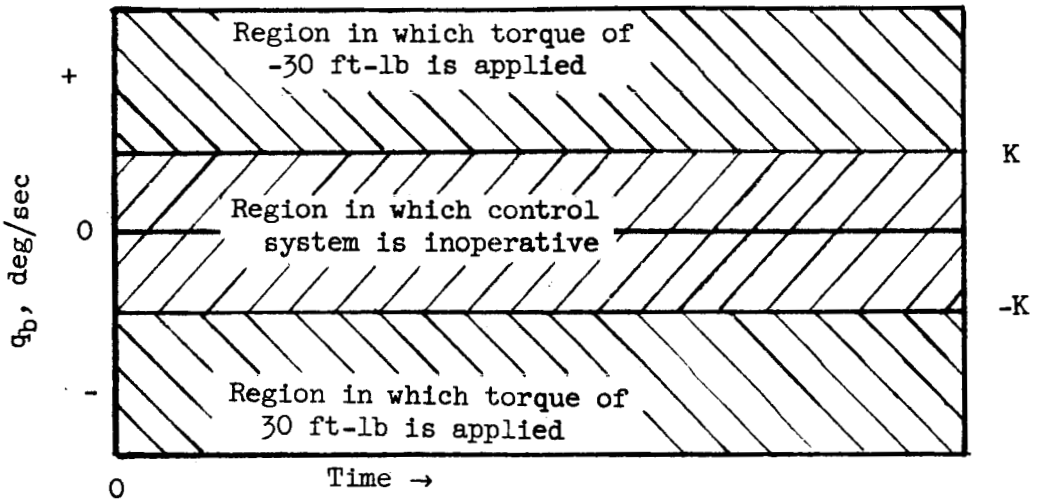

Sketch (a)

APPENDIX B

INITIAL CONDITIONS FOR CALCULATIONS

INITIAL CONDITIONS WITH HEADING CONSIDERED

Equations for Determination of Initial Conditions

It can be shown that the velocities along the X-, Y-, and Z-axes are given as

$$\dot{x} = V_R(\sin\delta\cos\bar{\theta}\cos\bar{\psi} + \cos\delta\cos H\sin\bar{\psi} + \cos\delta\sin H\cos\bar{\theta}\cos\bar{\psi})$$

$$\dot{y} = V_R(\sin\delta\sin\bar{\theta} - \cos\delta\sin H\cos\bar{\theta})$$

$$\dot{z} = V_R(-\cos\delta\cos H\cos\bar{\psi} + \cos\delta\sin H\sin\bar{\theta}\sin\bar{\psi} + \sin\delta\cos\bar{\theta}\sin\bar{\psi})$$

where δ is the inclination of the flight path with respect to the local horizontal and H is the heading angle measured in a plane tangent to the surface of the earth at a point located at $\bar{\psi}$ and $\bar{\theta}$. The angle H is positive when measured from the east toward the south. When $\bar{\psi} = \bar{\psi}_o = 90^o$, the equations for $\dot{x}$, $\dot{y}$, and $\dot{z}$ reduce to

$$\dot{x}_o = (V_R)_o\cos\delta_o\cos H_o$$

$$\dot{y}_o = (V_R)_o(\sin\delta_o\sin\bar{\theta}_o - \cos\delta_o\sin H_o\cos\bar{\theta}_o)$$

$$\dot{z}_o = (V_R)_o(\cos\delta_o\sin H_o\sin\bar{\theta}_o + \sin\delta_o\cos\bar{\theta}_o)$$

When the equations for $\dot{x}$, $\dot{y}$, and $\dot{z}$ given in appendix A are solved by the method of determinants, the velocities along the X-, Y-, and Z-axes are given by

$$u = \dot{x}\cos\theta\cos\psi + \dot{y}\sin\theta + \dot{z}\cos\theta\sin\psi$$

$$v = -\dot{x}\sin\theta\cos\psi + \dot{y}\cos\theta - \dot{z}\sin\theta\sin\psi$$

$$w = -\dot{x}\sin\psi + \dot{z}\cos\psi$$

Since at reentry it was desired to have the angle of attack zero, $u = V_R$ and $v = w = 0$. With these substitutions in the equations for u, v, and w, the angles ψ_o and θ_o are

$$\psi_o = \tan^{-1} \frac{\dot{z}_o}{\dot{x}_o}$$

$$\theta_o = \tan^{-1} \frac{\dot{y}_o}{\sqrt{(\dot{x}_o)^2 + (\dot{z}_o)^2}}$$

Conditions for Calculations

At reentry at an altitude of 450,000 feet with $\bar{\psi}_o = 90^\circ$, $\alpha_o = 0$, $H_o = 20.83^\circ$, $\delta_o = -1.594^\circ$, and $\bar{\theta}_o = 24.736^\circ$, the initial conditions are given as

$u_o = V_R = 25{,}461.46$ fps

$v_o = 0$

$w_o = 0$

$\theta_o = -19.542^\circ$

$\psi_o = 7.528^\circ$

$\phi_o = 0^\circ, 60^\circ, 180^\circ, 240^\circ$ (ϕ_o was varied to determine the dispersion for a given lateral displacement, D, between the center of pressure and center of gravity)

$D = 0, \frac{1}{4}, \frac{1}{2}$ inch (see fig. 1(b))

$p_o = 0, 1, 6$ rpm

$q_o = 0$

$r_o = 0$

$x_o = 0$

$y_o = 8.939 \times 10^6$ ft

$z_o = 19.398 \times 10^6$ ft

$R_e = 20.909 \times 10^6$ ft

INITIAL CONDITIONS FOR EQUATORIAL FLIGHT

For the study of the dynamic stability at various initial altitudes one trajectory was calculated along the equator without center-of-gravity offset (D = 0). The initial conditions for this trajectory are

$u_o = V_R = 25{,}461.46$ fps

$v_o = 0$

$w_o = 0$

$\theta_o = 0$

$\psi_o = -1.594^\circ$

$\phi_o = 0$

$\bar{\theta}_o = 0$

$\bar{\psi}_o = 90^\circ$

$p_o = 1$ rpm

$q_o = 0$

$r_o = 0$

$x_o = 0$

$y_o = 0$

$z_o = 21.359 \times 10^6$ ft

$R_e = 20.909 \times 10^6$ ft

INITIAL CONDITIONS AT SIX ALTITUDES ALONG EQUATORIAL TRAJECTORY

Six altitudes were selected from the reference case (fig. 19) at which ϕ was an even multiple of 360° in order to facilitate the introduction of disturbances in α, q_b, and r_b. Initial conditions for

these six cases are given in table II. The angle of attack was disturbed about 5° by changing w and ± 2 deg/sec disturbances were added to q_b and r_b, the sign being chosen to increase the amplitude of the motion.

REFERENCES

1. Lichtenstein, Jacob H.: Analytical Investigation of the Dynamic Behavior of a Nonlifting Manned Reentry Vehicle. NASA TN D-416, 1960.

2. Allen, H. Julian: Motion of a Ballistic Missile Angularly Misalined With the Flight Path Upon Entering the Atmosphere and Its Effect Upon Aerodynamic Heating, Aerodynamic Loads, and Miss Distance. NACA TN 4048, 1957.

3. Nicolaides, John D.: On the Free Flight Motion of Missiles Having Slight Configurational Asymmetries. Rep. No. 858, Ballistic Res. Labs., Aberdeen Proving Ground, June 1953.

4. Fletcher, Herman S., and Wolhart, Walter D.: Damping in Pitch and Static Stability of Supersonic Impact Nose Cones, Short Blunt Subsonic Impact Nose Cones, and Manned Reentry Capsules at Mach Numbers From 1.93 to 3.05. NASA TM X-347, 1960.

5. Fletcher, Herman S.: The Damping in Pitch and Static Stability of Six Supersonic-Impact Ballistic Configurations and Three High-Drag Reentry Capsules at a Mach Number of 6.83. NASA TM X-349, 1960.

TABLE I.- CONDITIONS FOR CALCULATION OF DYNAMIC STABILITY DURING REENTRY FROM AN ALTITUDE OF 450,000 FEET AND DISPERSION AT MACH NUMBER 1.0

p_o, rpm	ϕ_o, deg	c.g. offset, in.	K, deg/sec	Control-system operating range	Data presented in figure -
0	0	1/4	0.5	On at all times	4, 9, 11
0	0	1/4	1.0		9, 13
0	180	1/4	1.0		5, 13
1	0	1/4	0.5		6, 10, 11
1	0	1/4	1.0		10, 12
1	60	1/4	1.0		14
1	240	1/4	1.0		14
1	0	1/2	1.0		7, 12, 15
1	0	1/2	1.0	On to $A_{V_R} = 5.0$, off thereafter	7, 15
1	0	1/2	---	Off at all times	8, 16
0	0	1/4	---	Off at all times	17
1	0	1/4	---		17
6	0	1/4	---		17

TABLE II.- CONDITIONS FOR STUDY OF DYNAMIC STABILITY AND CONTROL-SYSTEM EFFECTIVENESS AT SIX ALTITUDES

[No center-of-gravity offset; p_o = 1 rpm]

Initial altitude, ft	Initial Mach number	Initial time, sec	Initial angle of attack, deg	V_R, fps	ϕ_o, radians	$\Delta\alpha$, deg	Δq_b, deg/sec	Δr_b, deg/sec	K, deg/sec	Data presented in figure -
407,146	20.999	60.012	4.166	25,513.618	2π	0	0	0	Off	20
	21.214		9.165	25,775.275		5	2	2	Off	
	21.214		9.165	27,775.275		5	2	2	1.0	
315,960	25.364	180.184	2.355	25,580.636	6π	0	0	0	Off	21
	25.553		7.361	25,771.427		5	-2	2	Off	
	25.553		7.361	25,771.427		5	-2	2	1.0	
219,188	23.923	300.447	0.630	24,109.377	10π	0	0	0	Off	22
	24.038		5.631	24,224.802		5	2	2	Off	
	24.038		5.631	24,224.802		5	2	2	1.0	
161,891	14.951	360.631	0.837	16,550.557	12π	0	0	0	Off	23
	15.027		5.837	16,635.035		5	-2	-2	Off	
	15.027		5.837	16,635.035		5	-2	-2	1.0	
96,730	3.150	421.484	1.793	3,145.587	14π	0	0	0	Off	24
	3.171		6.800	3,166.321		5	-2	2	Off	
	3.171		6.800	3,166.321		5	-2	2	1.0	
68,601	1.080	455.462	11.692	1,046.669	15π	0	0	0	Off	25
	1.104		16.698	1,070.076		5	-2	-2	Off	
	1.104		16.698	1.070.076		5	-2	-2	1.0	

CONFIDENTIAL

TABLE III.- ANGLES OF ATTACK AT M = 1.0

p_o, rpm	ϕ_o, deg	c.g. offset, in.	K, deg/sec	Altitude, ft	Angle of attack, deg (a)	
					Maximum	Minimum
0	0	1/4	1.0	66,148	1.24	0.98
	180	1/4		66,679	1.25	.98
1	0	1/4		66,249	1.00	.97
	60	1/4		66,387	.59	.59
	240	1/4		66,418	1.53	1.42
1	0	1/2		65,833	2.06	2.00
	60	1/2		66,251	2.10	1.94
	240	1/2		66,410	2.51	2.46

[a]These values are those that exist just prior to changing derivatives at M = 1.0.

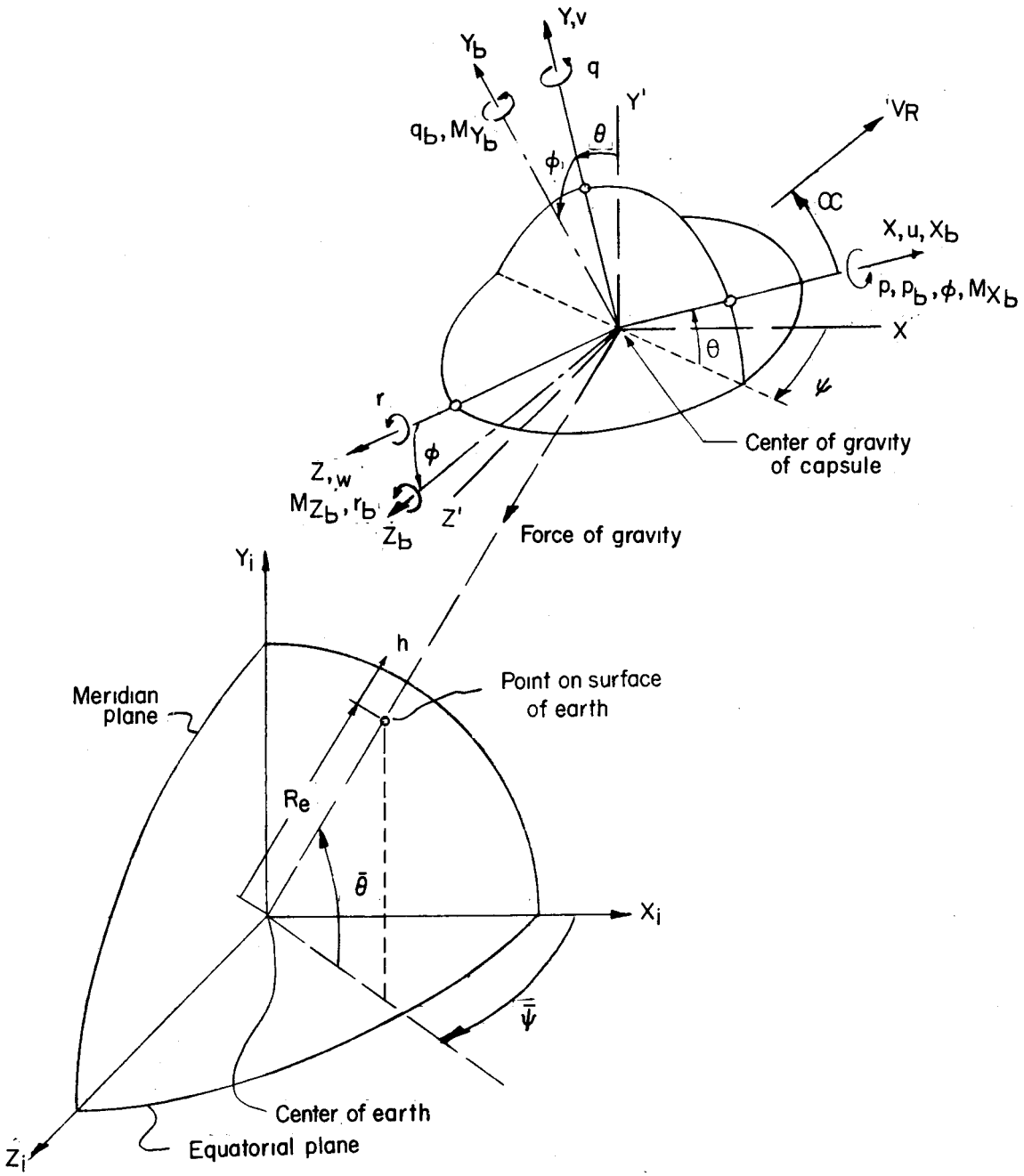

(a) General arrangement.

Figure 1.- System of axes. Positive velocities and displacements indicated.

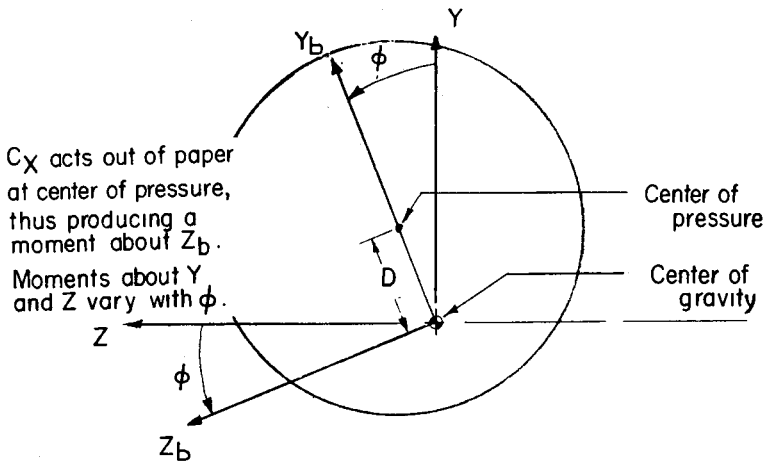

View along X-, X_b - axes
Moments about Y-and Z - axes

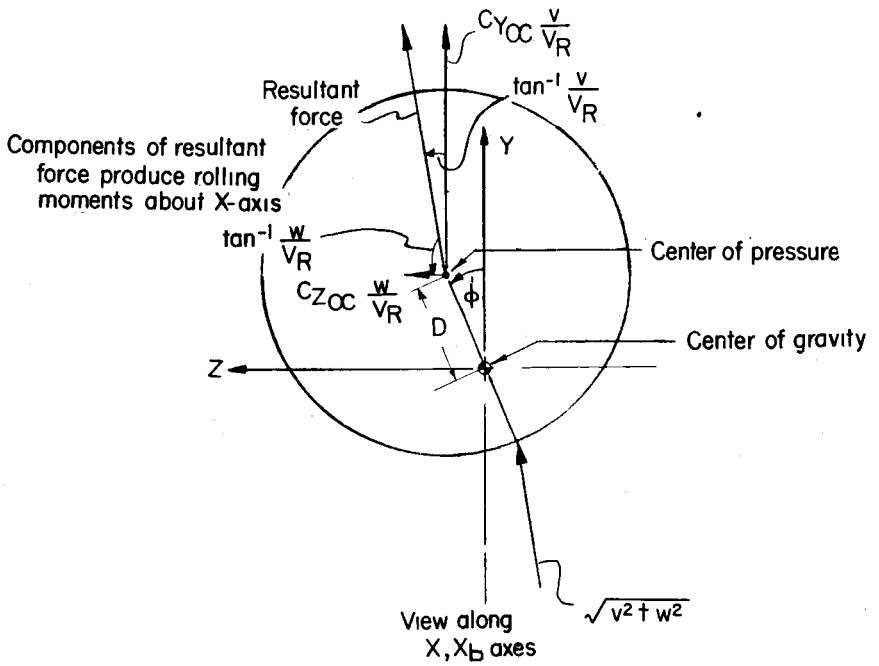

Moment about X - axis

(b) Moments arising from relative displacement between center of pressure and center of gravity.

Figure 1.- Concluded.

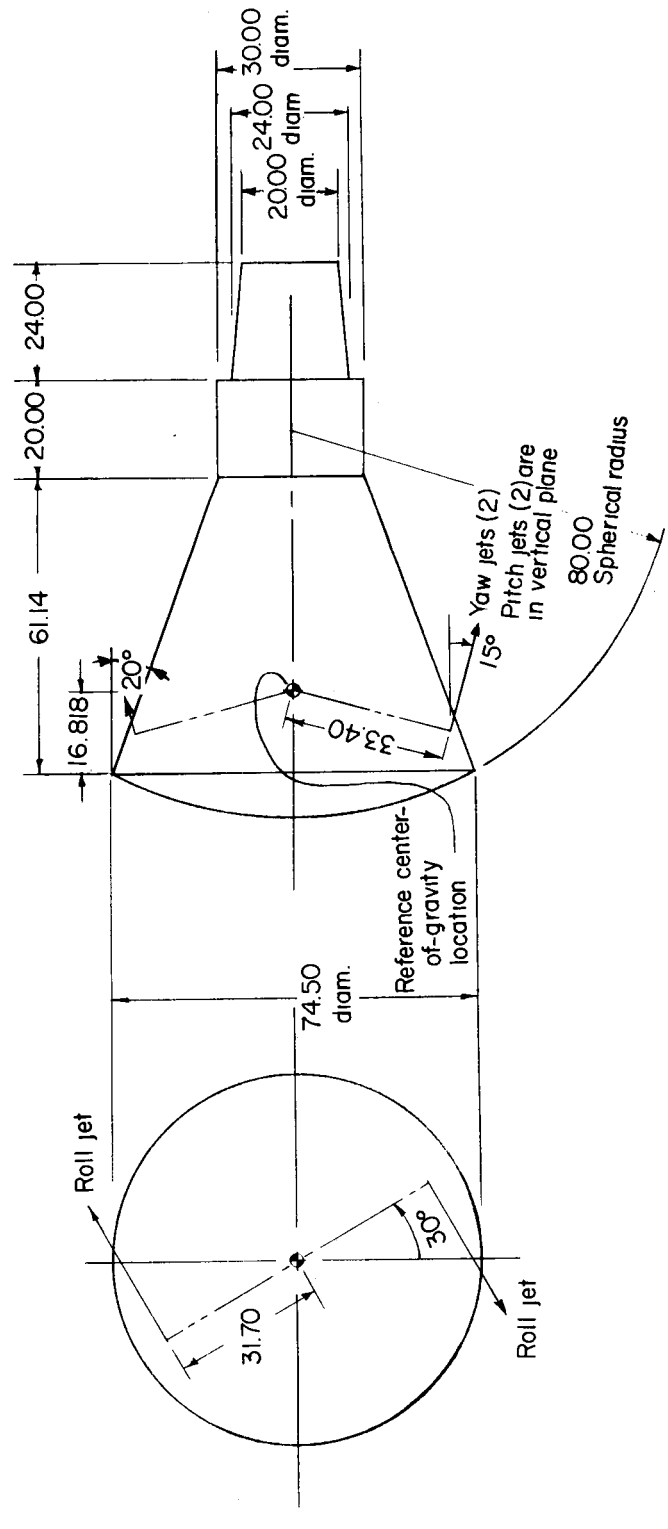

Figure 2.- Pertinent details of test configuration for which calculations were made. Dimensions are in inches unless otherwise noted.

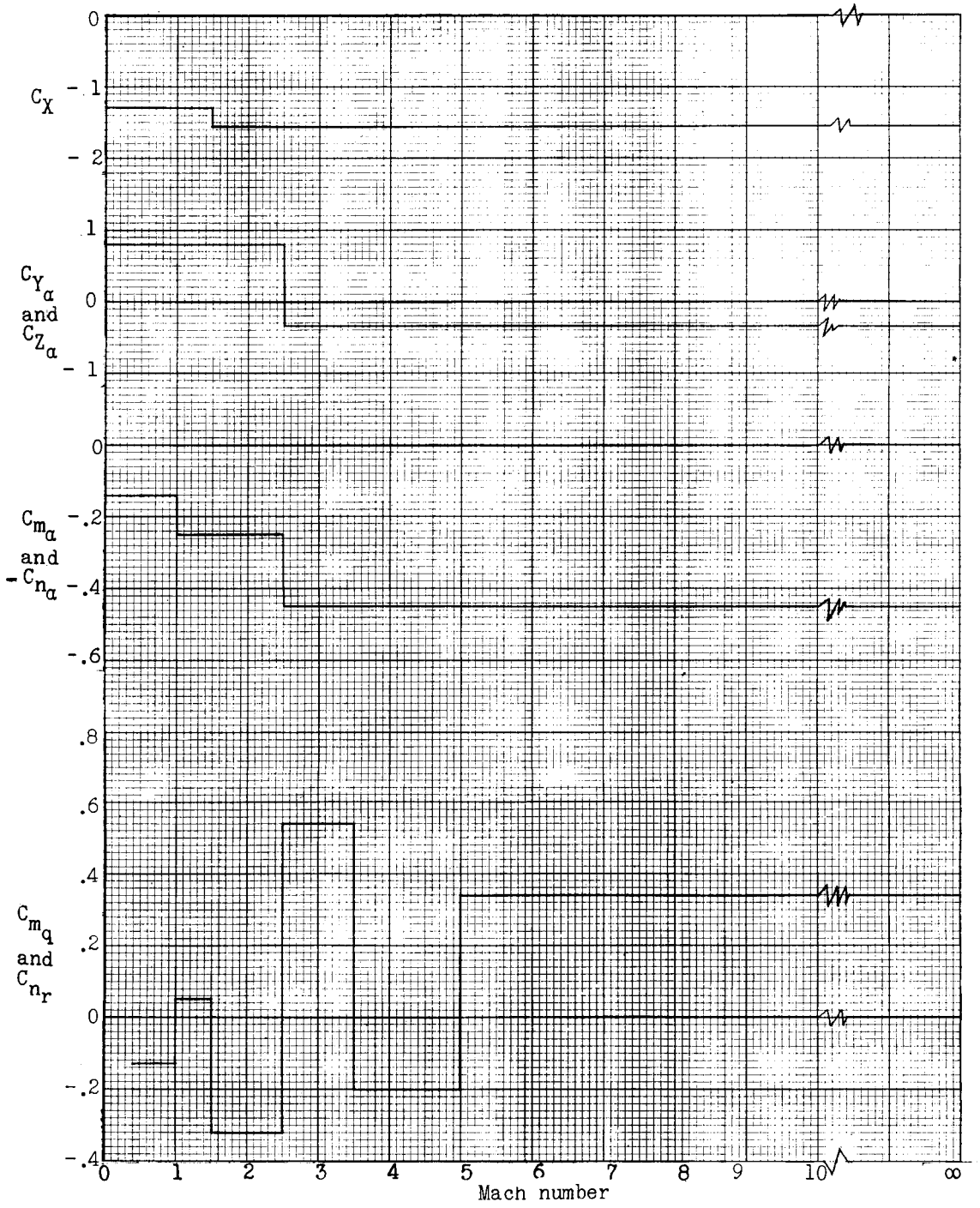

Figure 3.- Aerodynamic derivatives and C_X used in calculations.

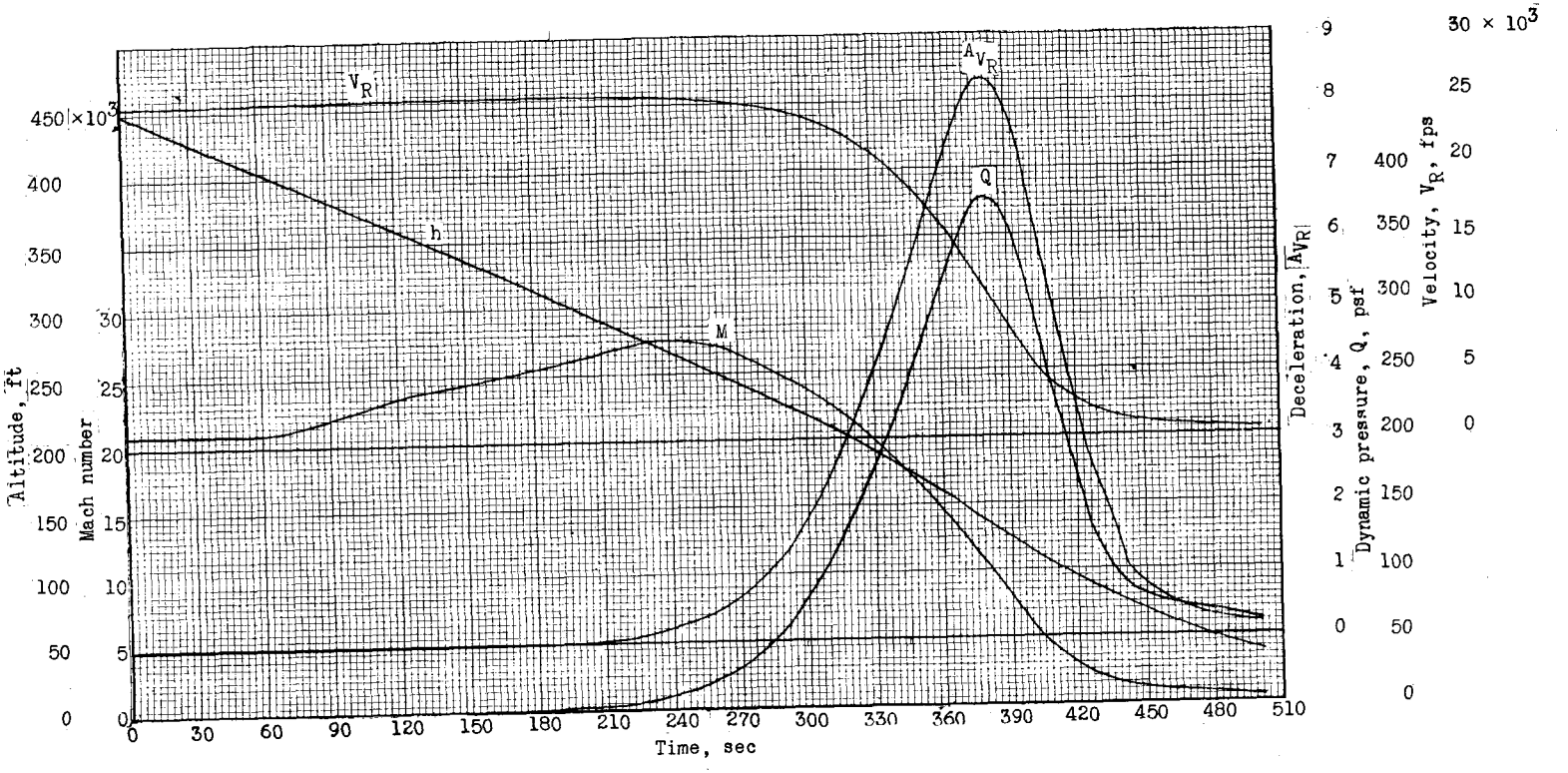

Figure 4.- Characteristics of a trajectory from reentry at 450,000-foot altitude. p_o = 0 rpm; ϕ_o = 0°; 1/4-inch center-of-gravity offset; K = 0.5 deg/sec threshold; control system operative at all times outside of threshold.

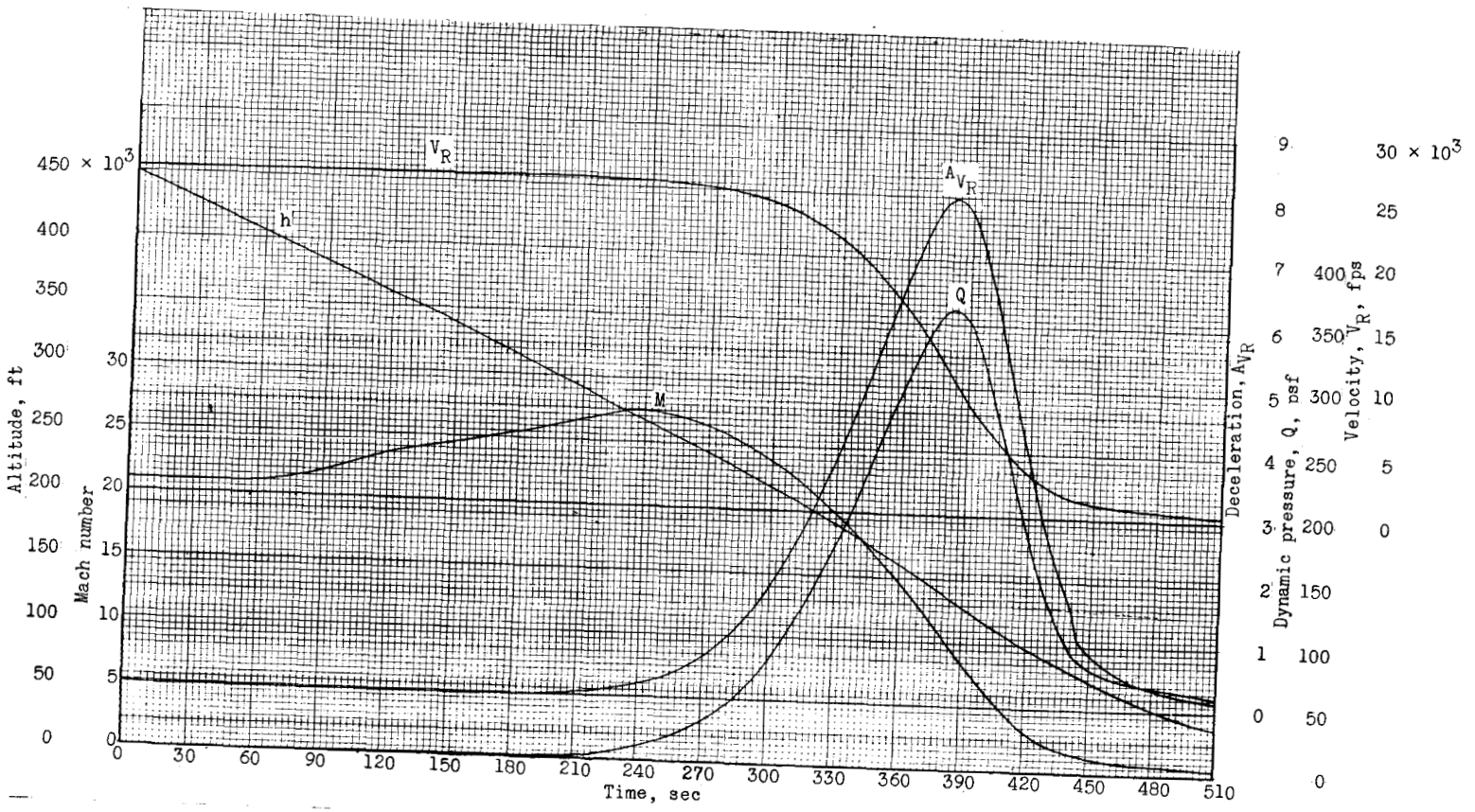

Figure 5.- Characteristics of a trajectory from reentry at 450,000-foot altitude. p_o = 0 rpm; ϕ_o = 180°; 1/4-inch center-of-gravity offset; K = 1.0 deg/sec threshold; control system operative at all times outside of threshold.

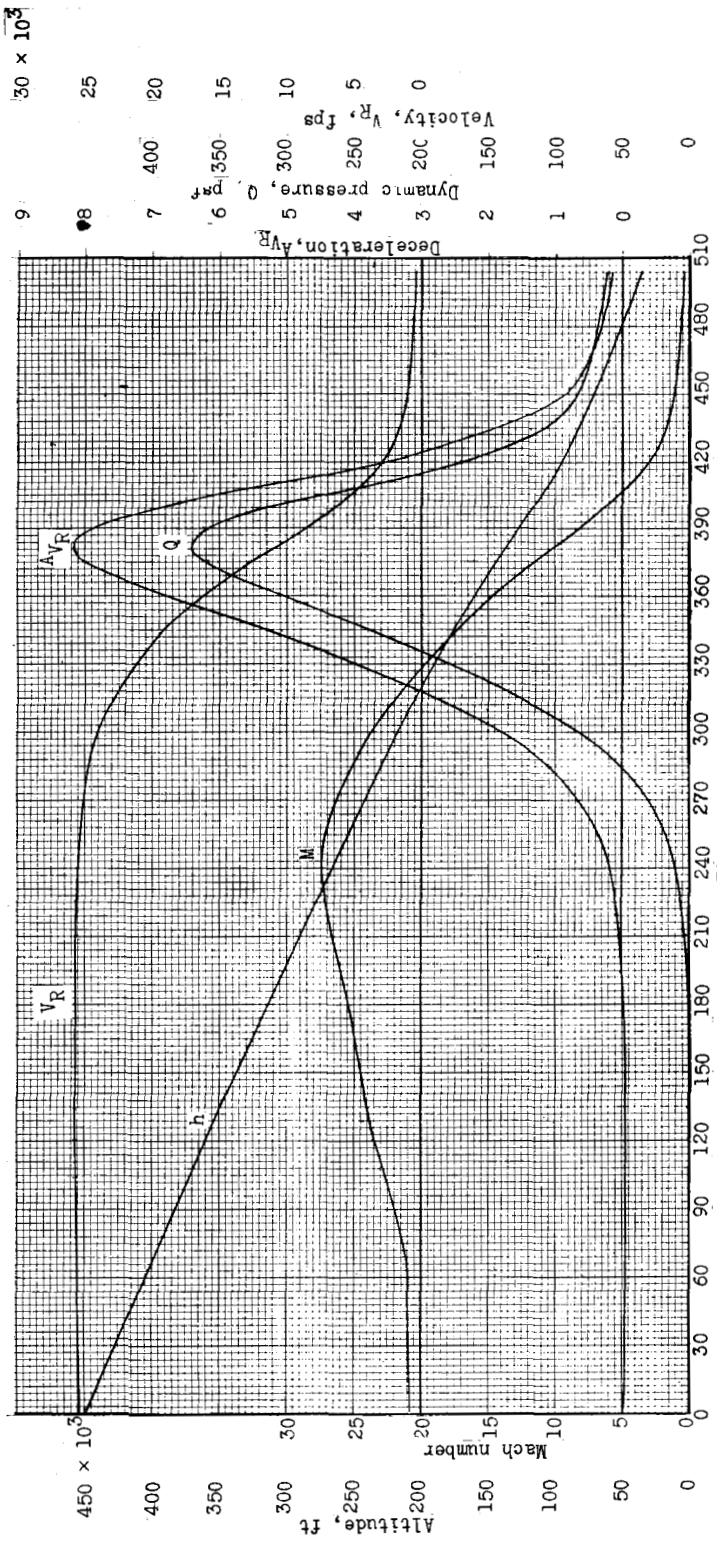

Figure 6.- Characteristics of a trajectory from reentry at 450,000-foot altitude. p_o = 1 rpm; ϕ_o = 0°; 1/4-inch center-of-gravity offset; K = 0.5 deg/sec threshold; control system operative at all times outside of threshold.

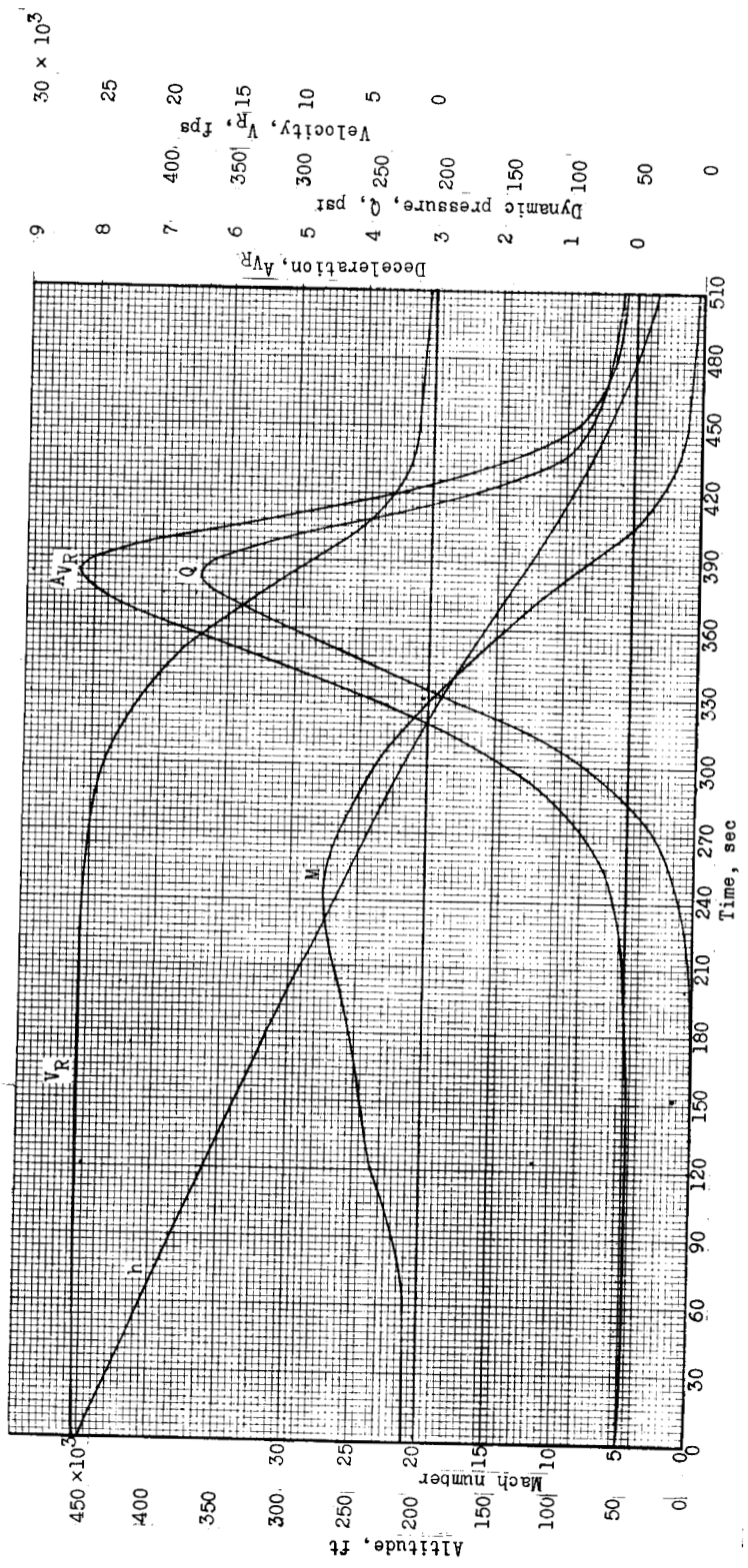

(a) Control system operative at all times outside of threshold with K = 1.0 deg/sec.

Figure 7.- Characteristics of a trajectory from reentry at 450,000-foot altitude. p_o = 1 rpm; ϕ_o = 0°; 1/2-inch center-of-gravity offset.

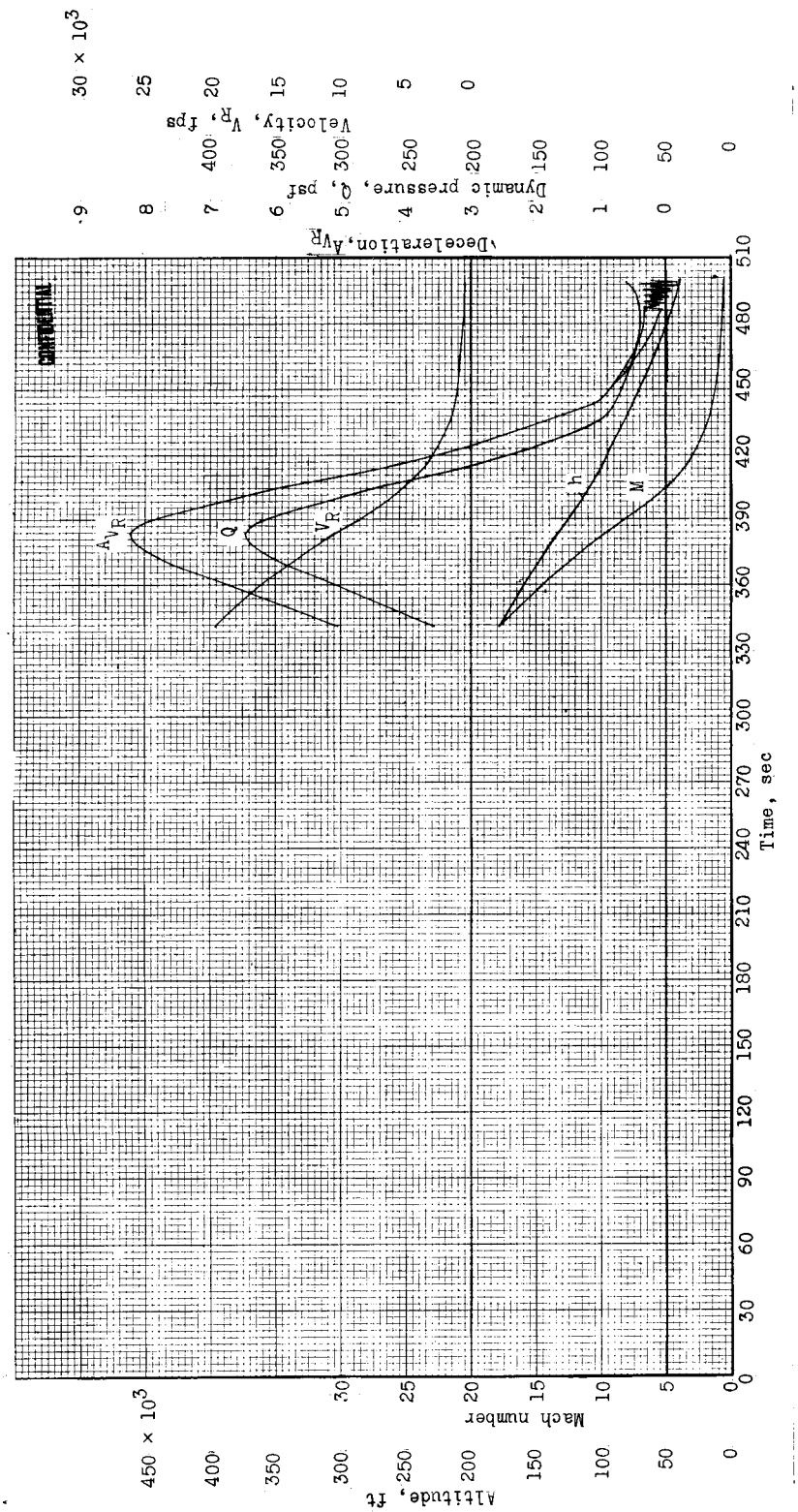

(b) Control system operative at all times outside of threshold with K = 1.0 deg/sec to A_{V_R} = 5.0; control system inoperative thereafter.

Figure 7.- Concluded.

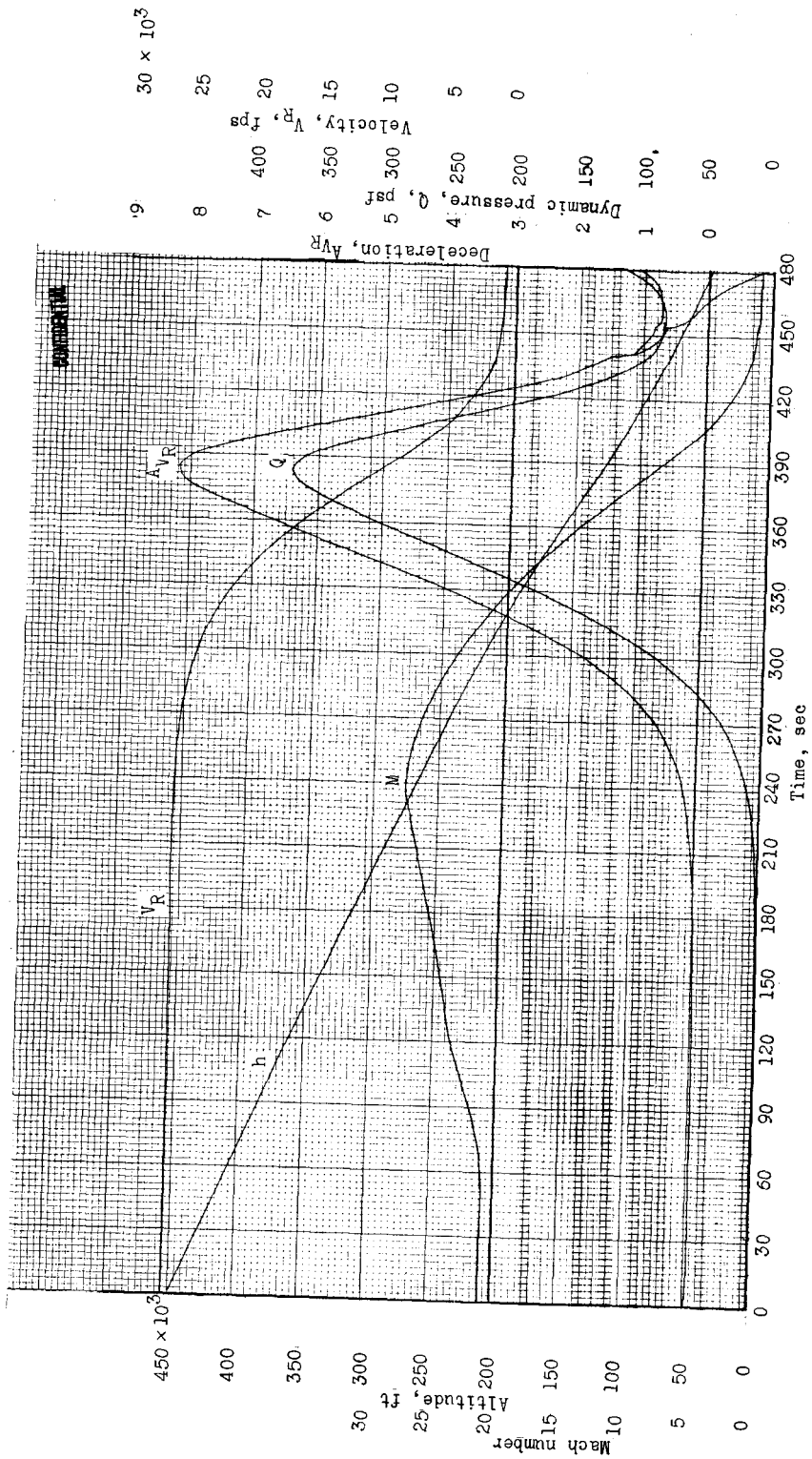

Figure 8.- Characteristics of a trajectory from reentry at 450,000-foot altitude. p_o = 1 rpm; ϕ_o = 0°; 1/2-inch center-of-gravity offset; control system inoperative at all times.

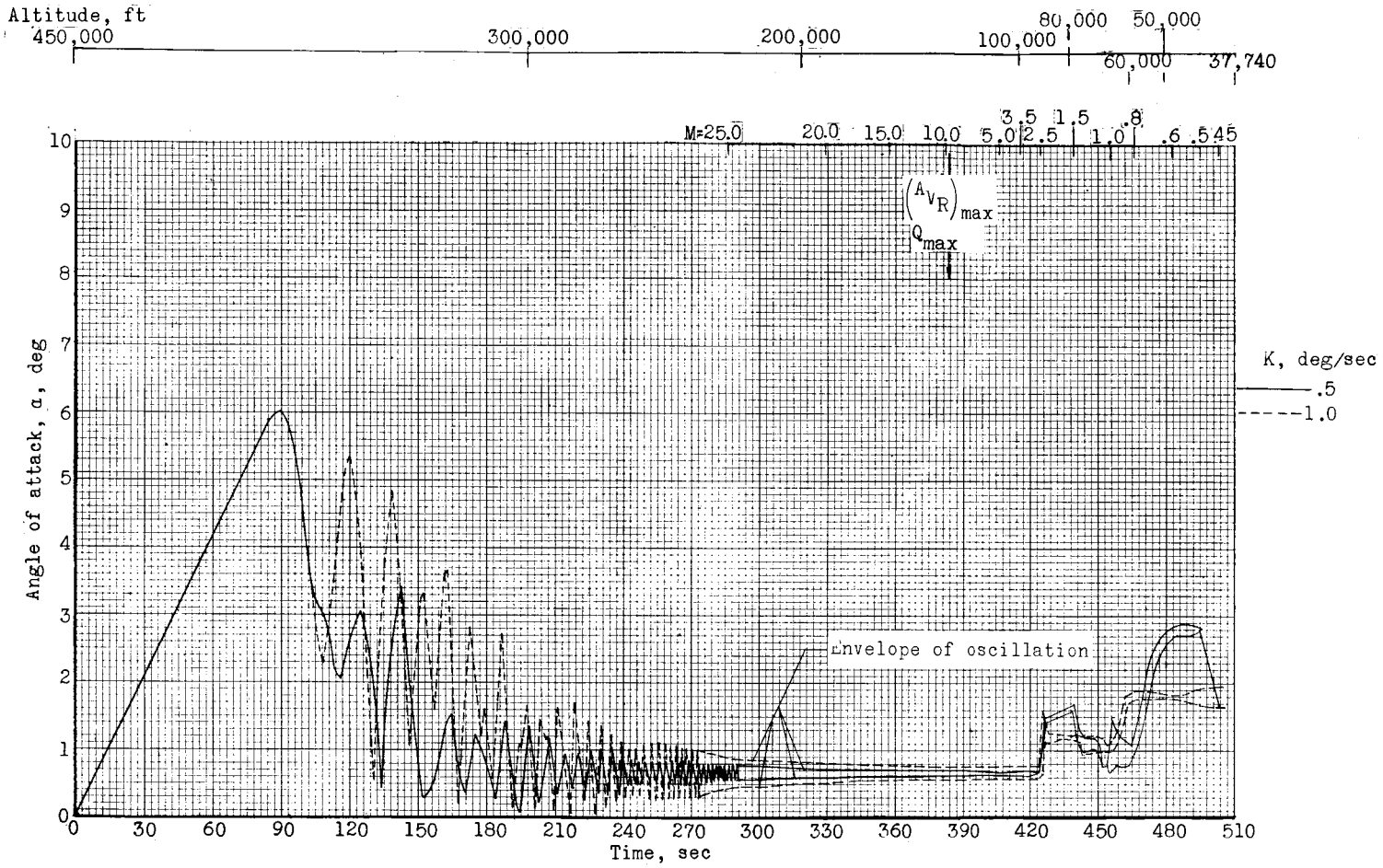

(a) α as a function of t for entire trajectory.

Figure 10.- Effect of control system threshold on variation of angle of attack with time. p_o = 1 rpm; $\phi_o = 0^o$; 1/4-inch center-of-gravity offset; control system operative at all times outside of threshold.

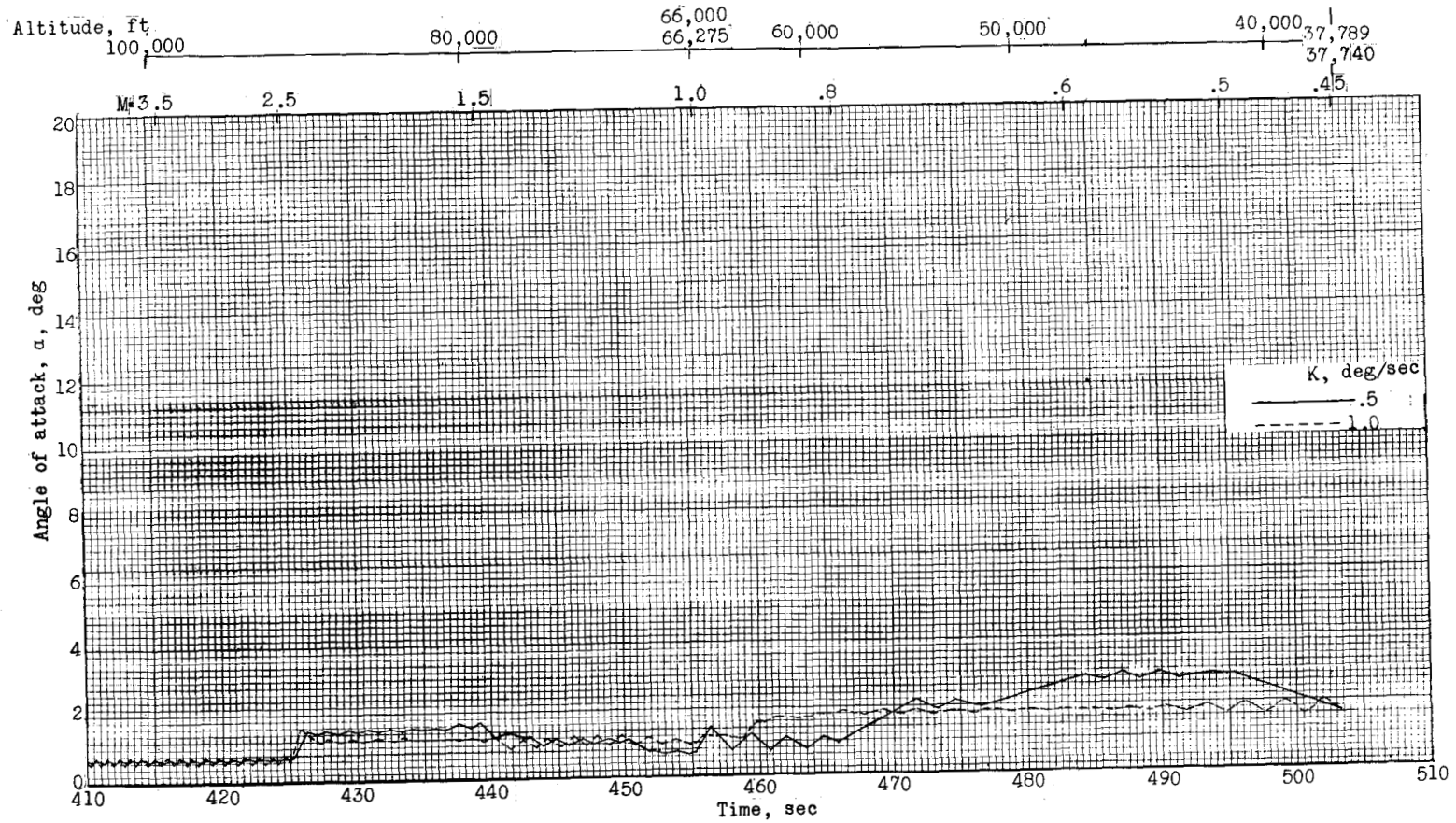

(b) α as a function of t for Mach numbers less than 3.5.

Figure 10.- Concluded.

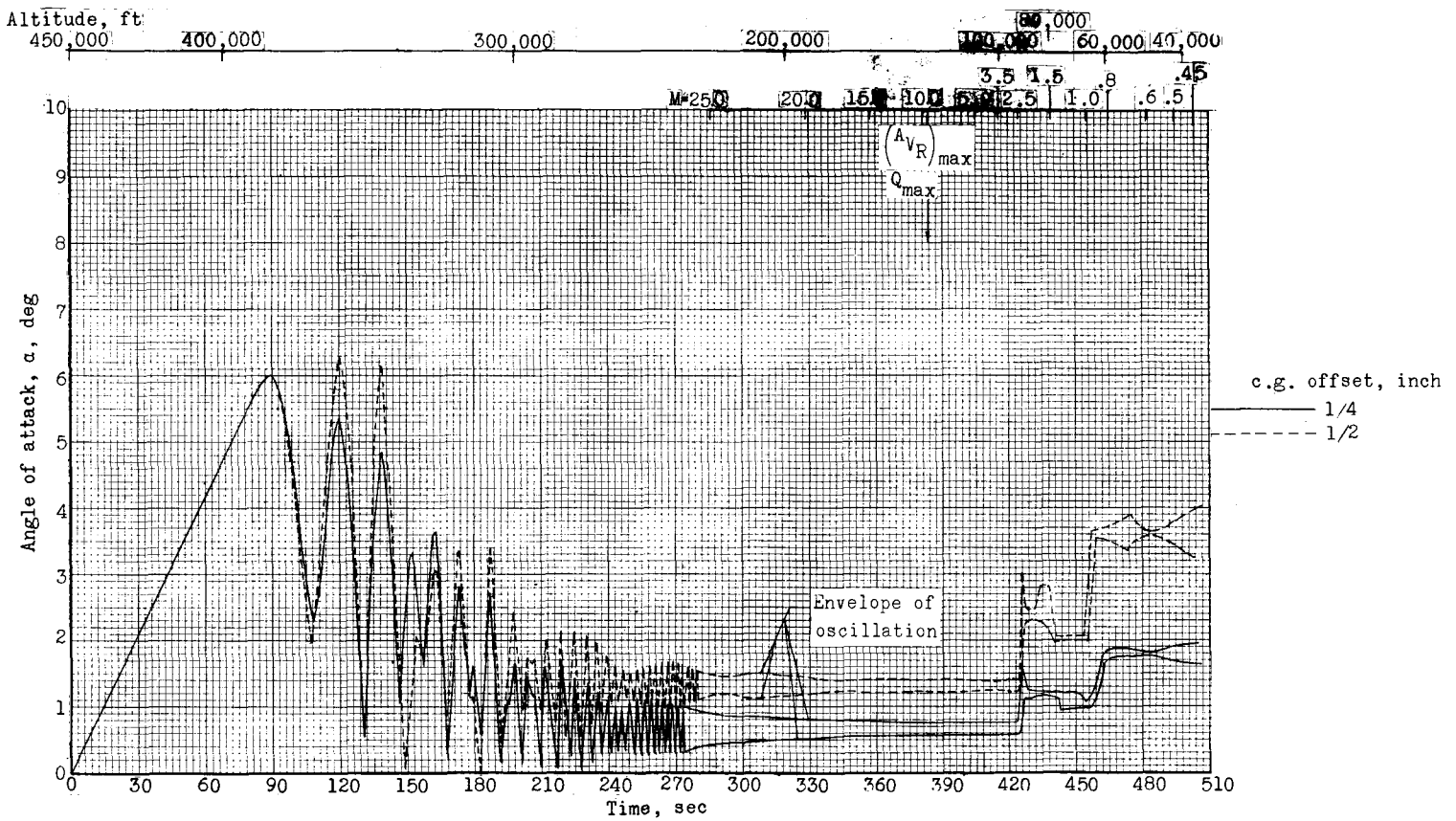

(a) α as a function of t for entire trajectory.

Figure 12.- Effect of center-of-gravity offset on variation of angle of attack with time. p_o = 1 rpm; $\phi_o = 0^o$; K = 1.0 deg/sec; control system operative at all times outside of threshold.

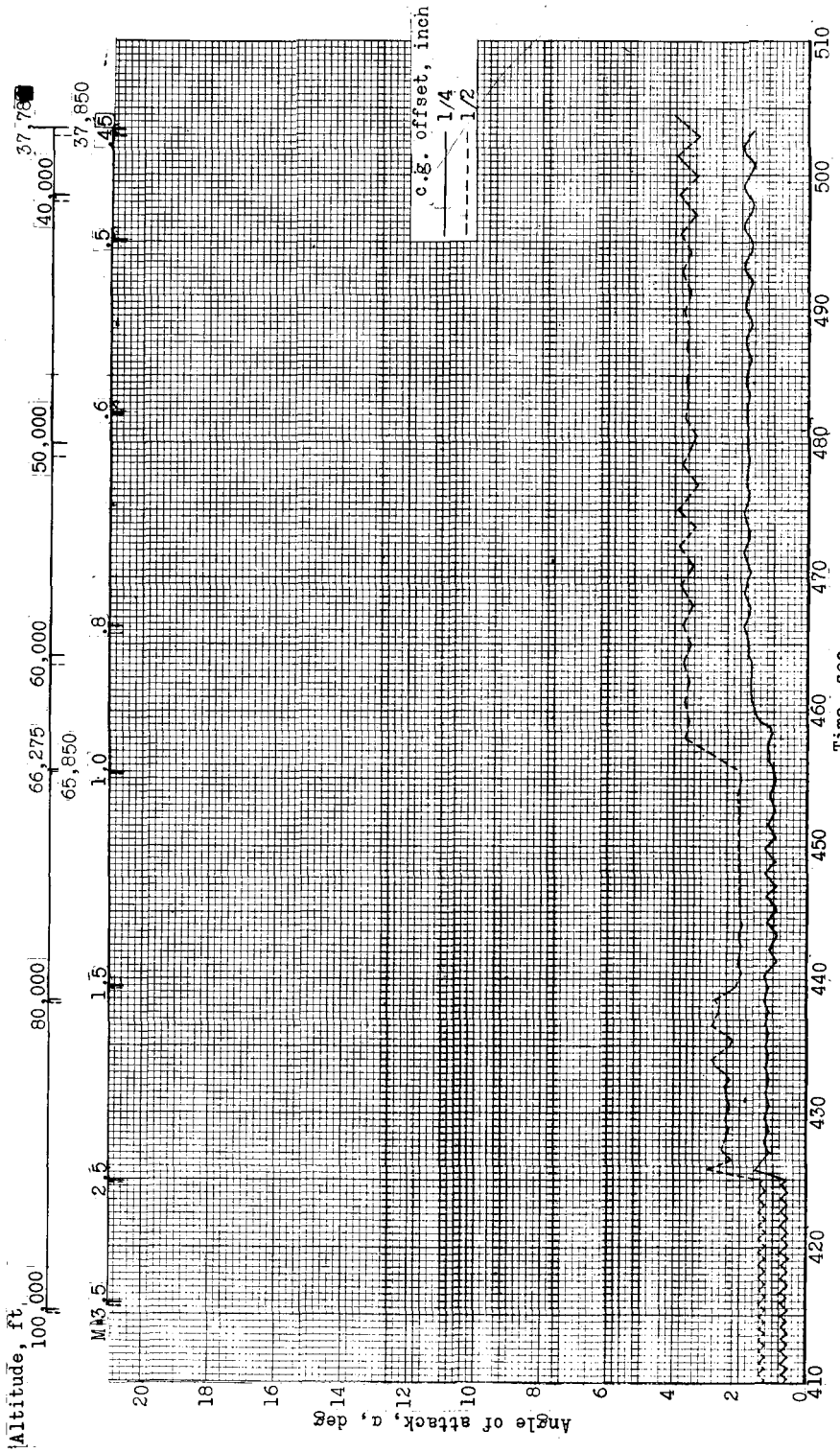

(b) α as a function of t for Mach numbers less than 3.5.

Figure 12.- Concluded.

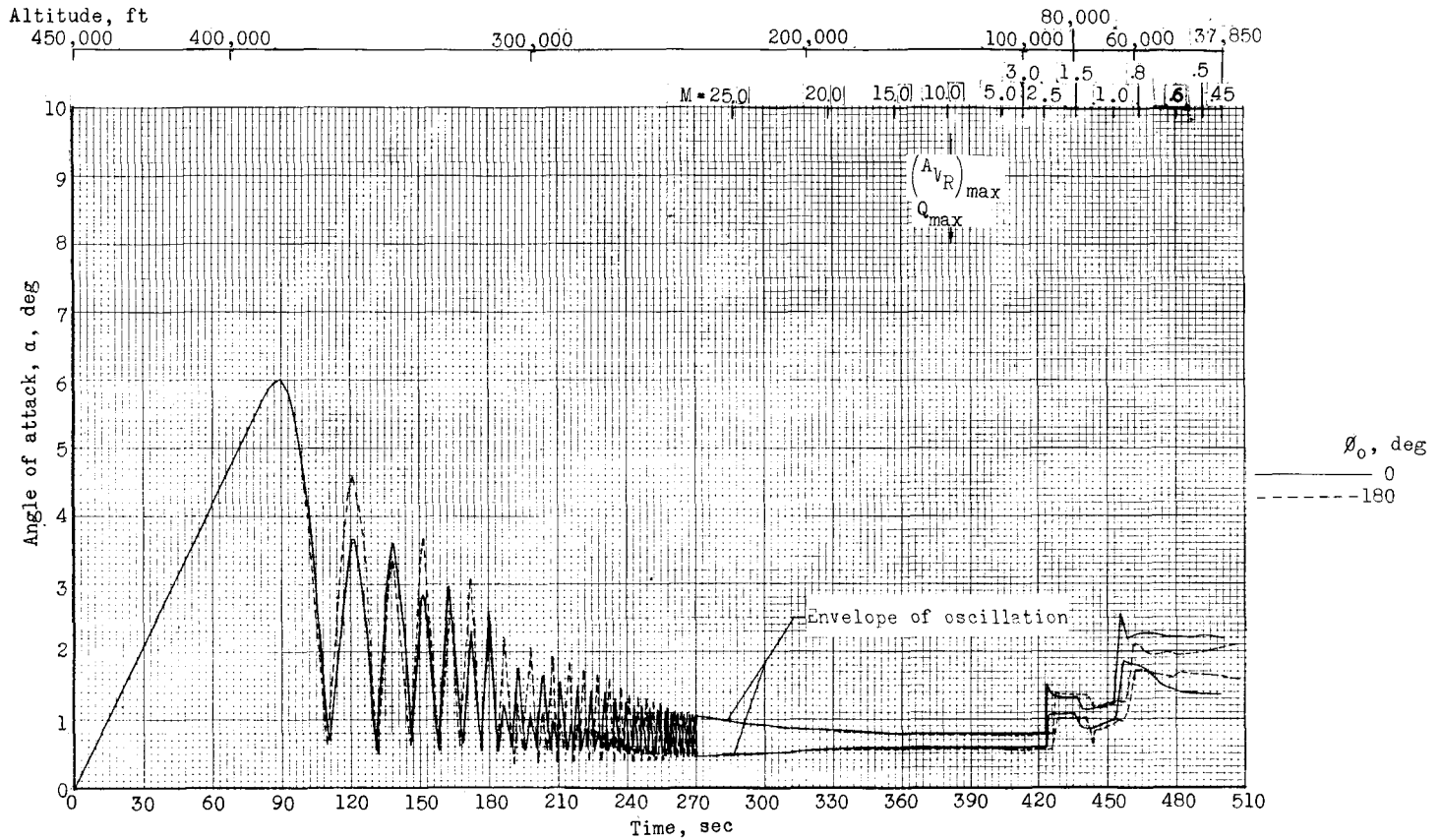

(a) α as a function of t for entire trajectory.

Figure 13.- Effect of initial roll angle on variation of angle of attack with time. p_o = 0 rpm; 1/4-inch center-of-gravity offset; K = 1.0 deg/sec; control system operative at all times outside of threshold.

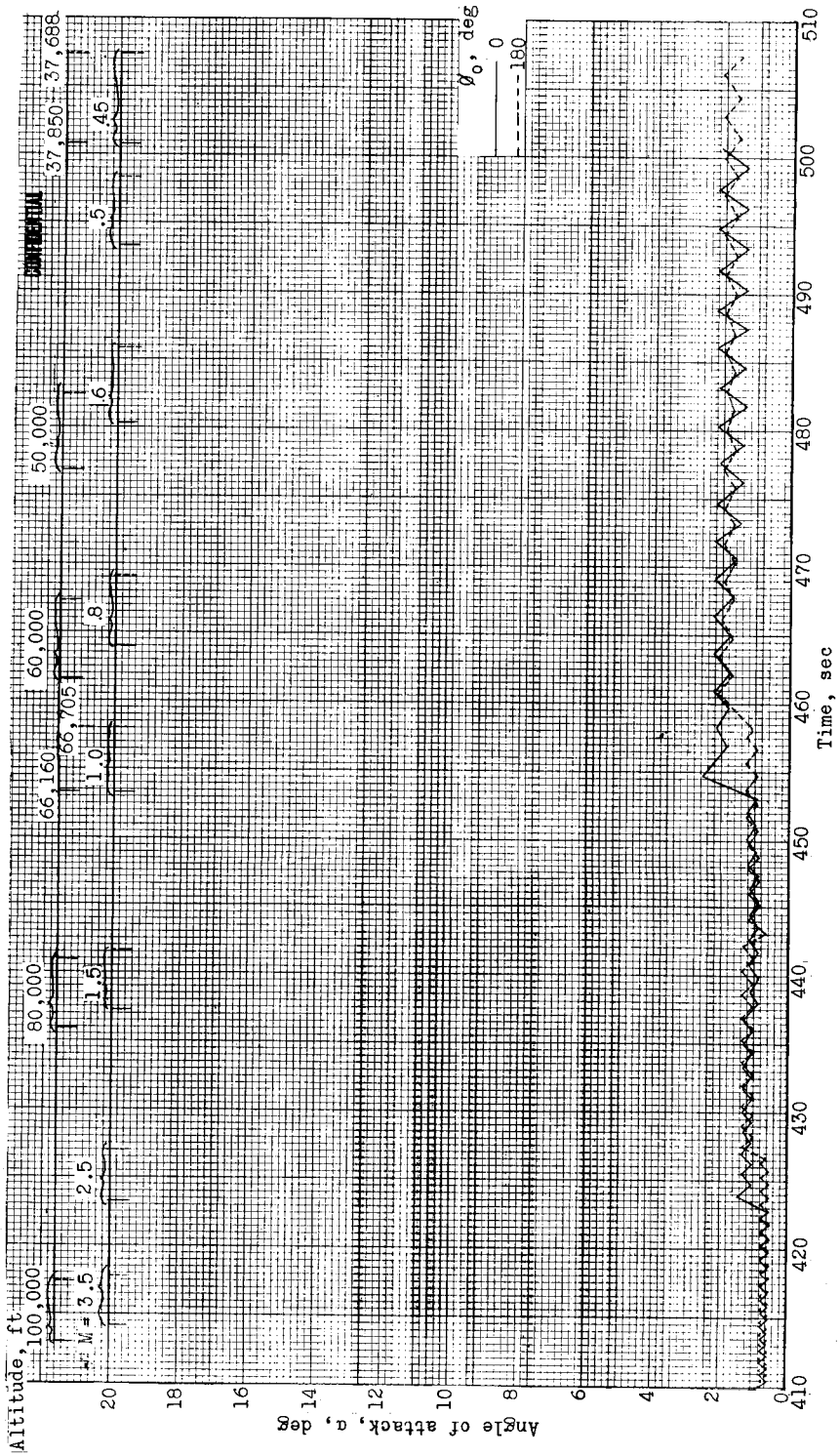

(b) α as a function of t for Mach numbers less than 3.5.

Figure 13.- Concluded.

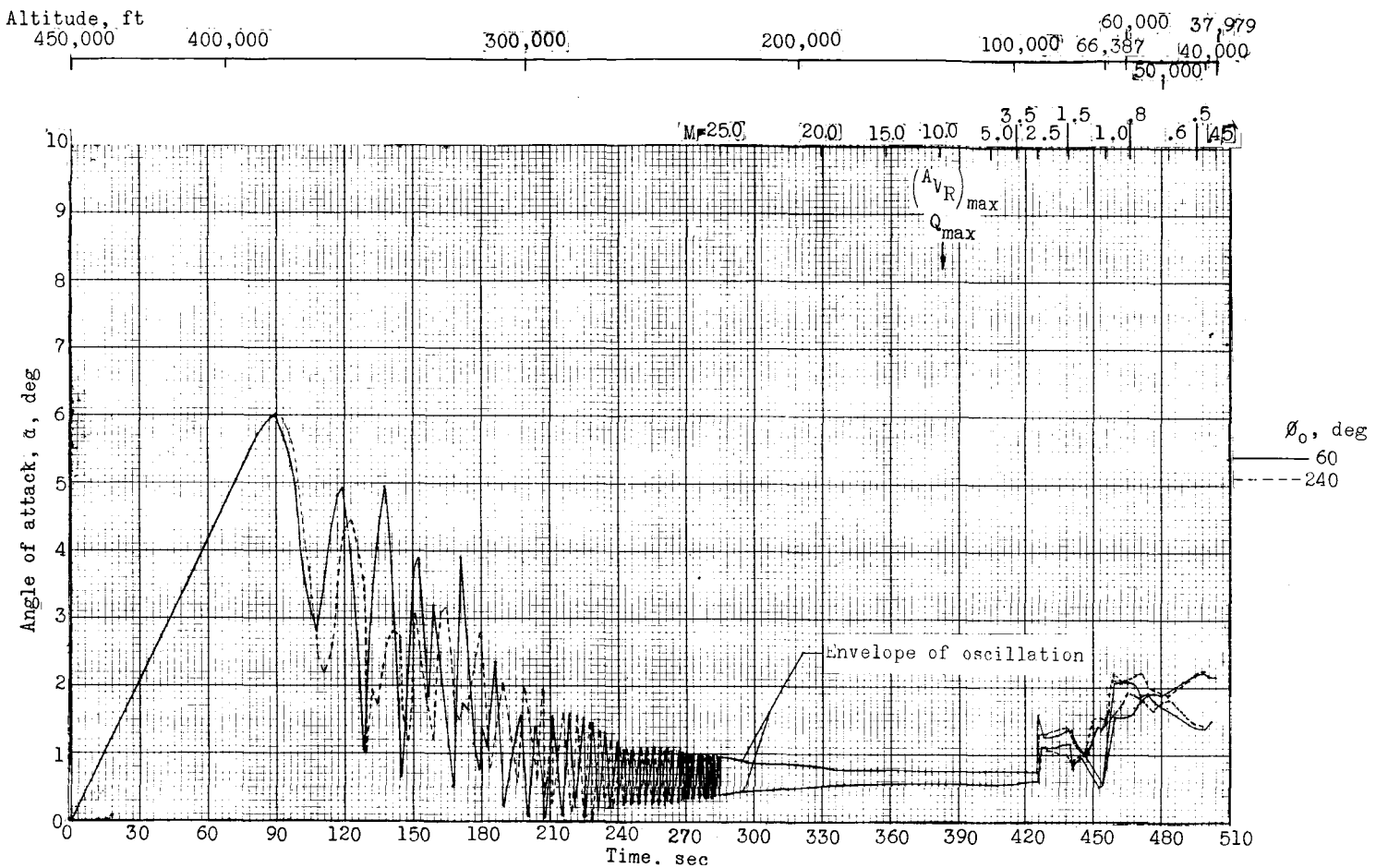

(a) α as a function of t for entire trajectory.

Figure 14.- Effect of initial roll angle on variation of angle of attack with time. p_o = 1 rpm; 1/4-inch center-of-gravity offset; K = 1.0 deg/sec; control system operative at all times outside of threshold.

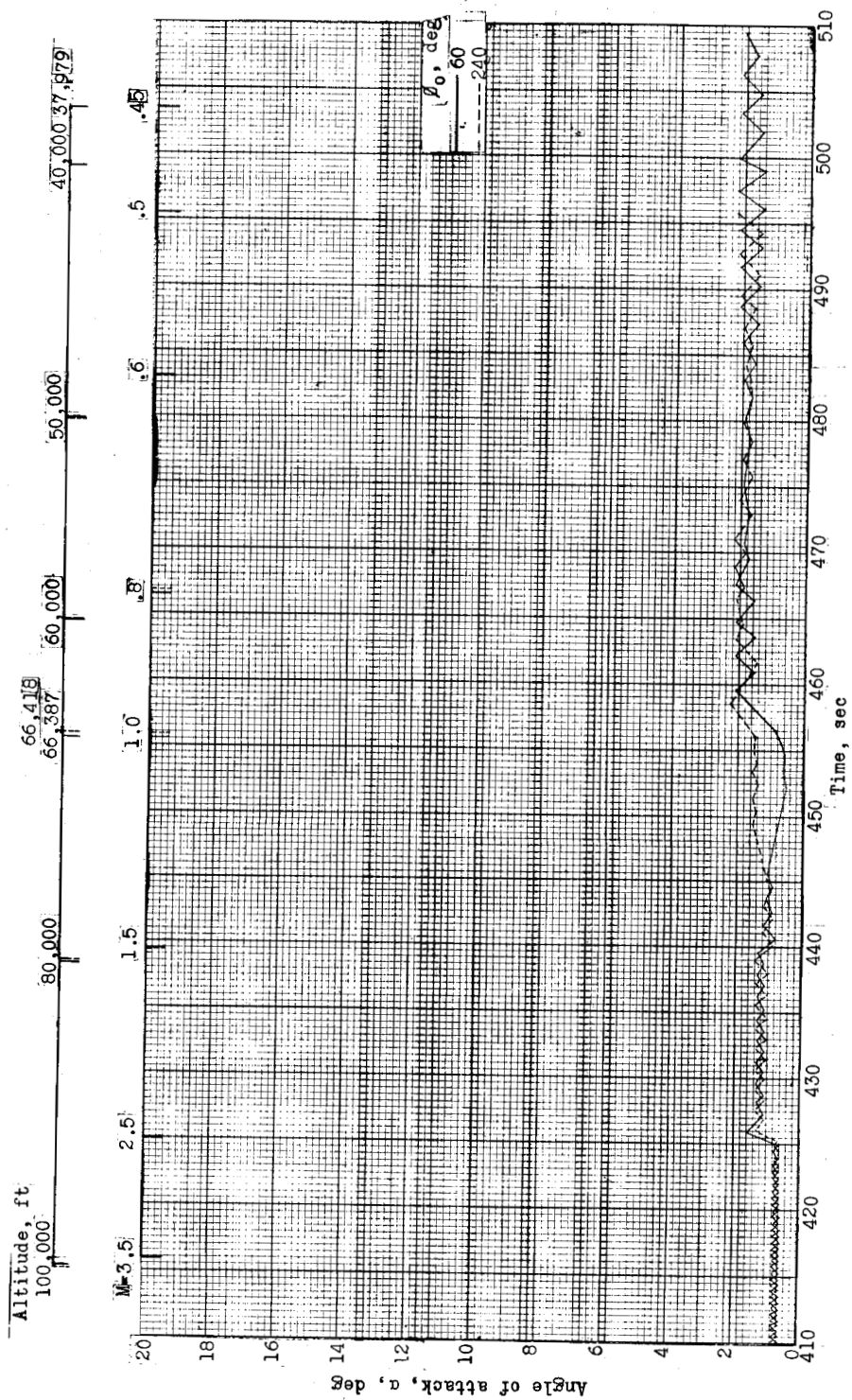

(b) α as a function of t for Mach numbers less than 3.5.

Figure 14.- Concluded.

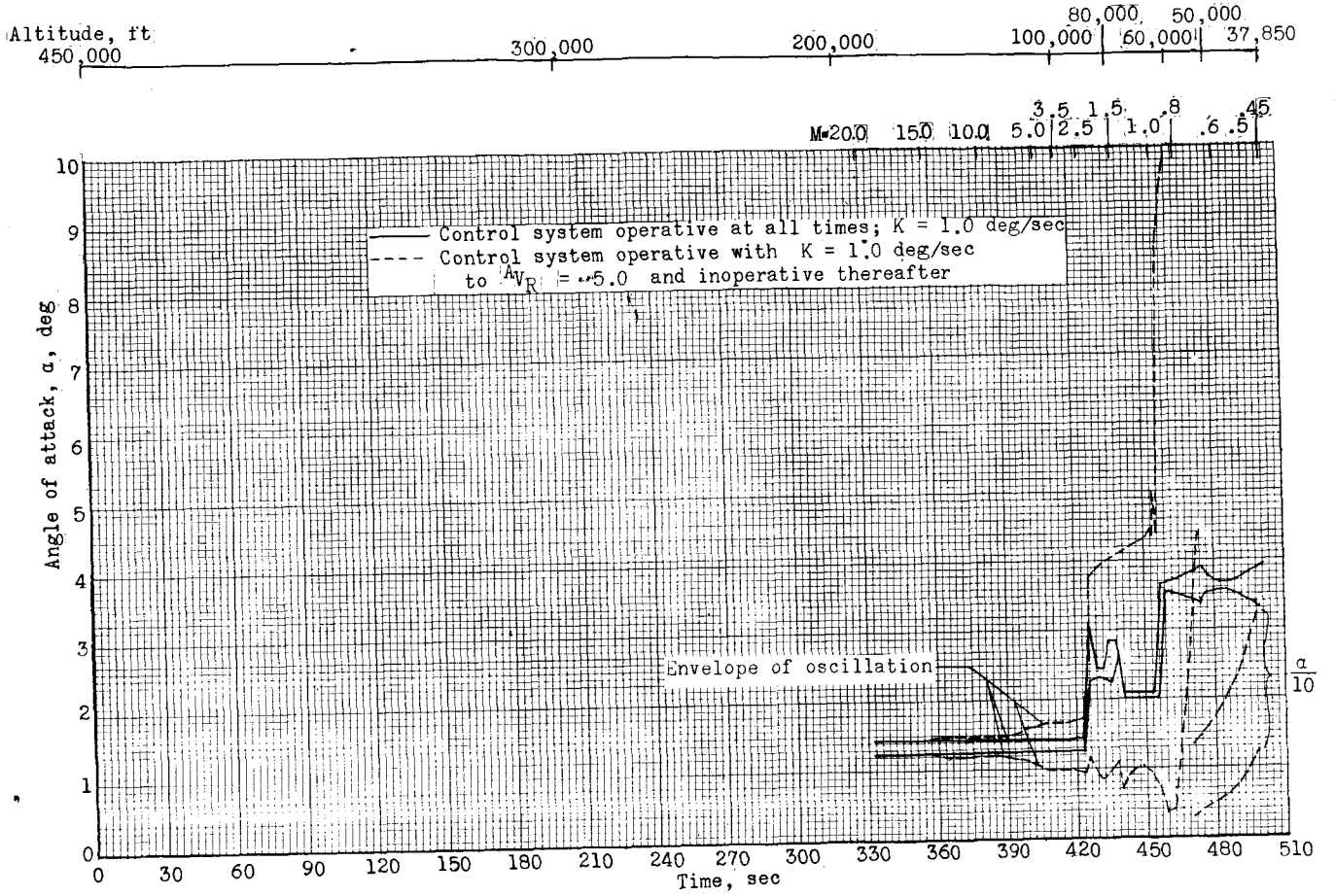

(a) α as a function of t from $A_{V_R} = 5.0$.

Figure 15.- Effect of cutting control system off at $A_{V_R} = 5.0$ on variation of angle of attack with time. p_o = 1 rpm; $\phi_o = 0^o$; 1/2-inch center-of-gravity offset.

CONFIDENTIAL

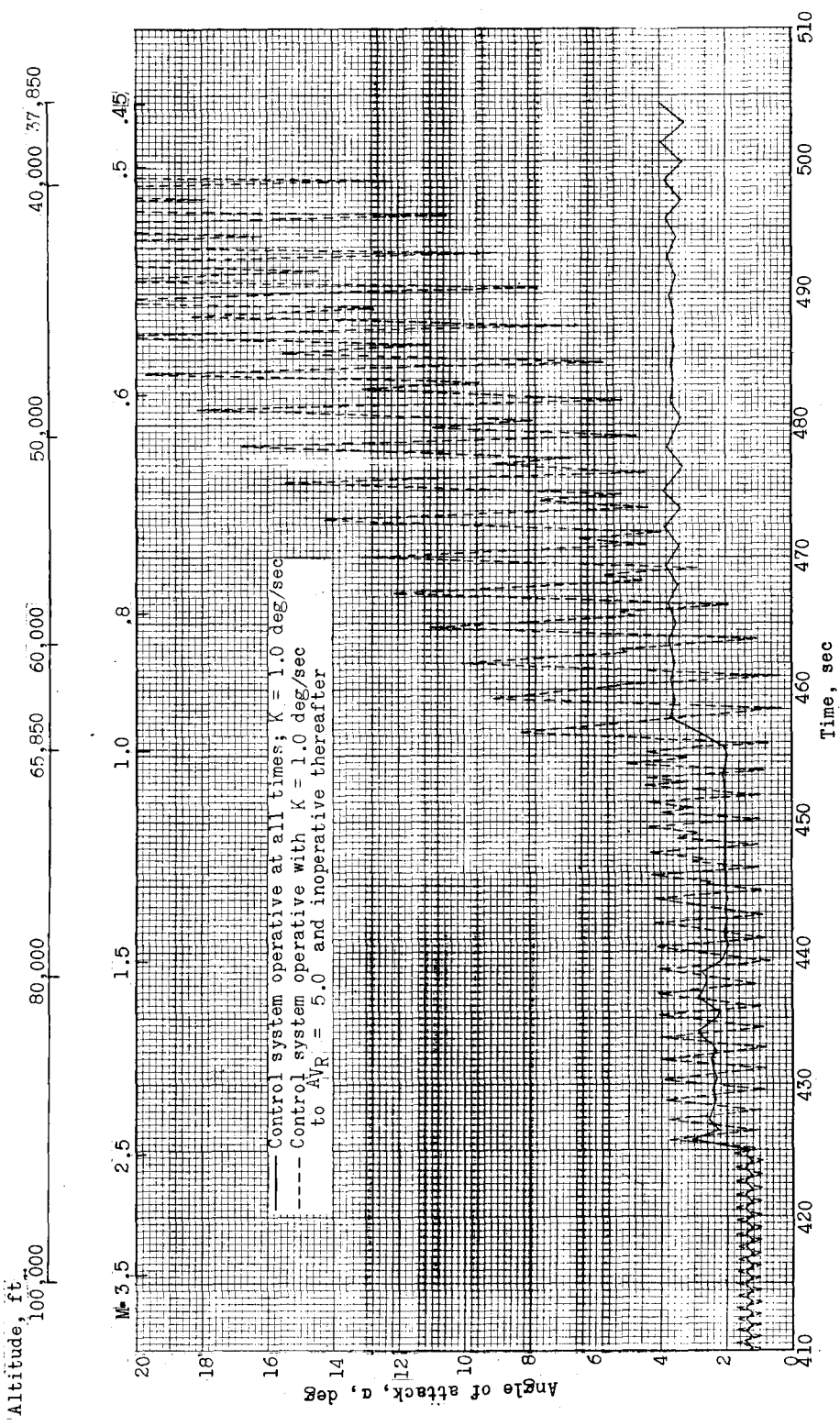

(b) α as a function of t for Mach numbers less than 3.5.

Figure 15.- Concluded.

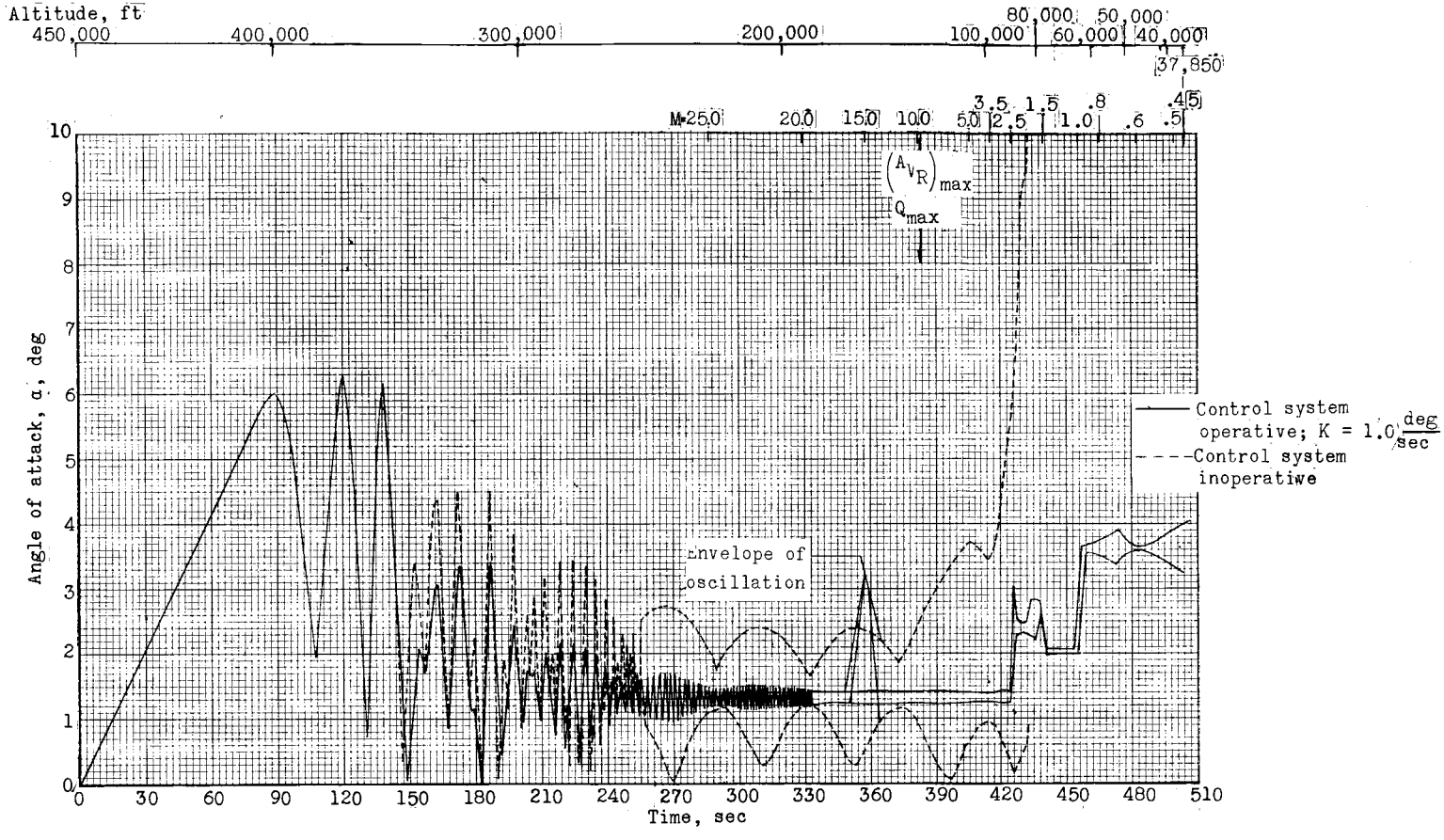

(a) α as a function of t for entire trajectory.

Figure 16.- Effect of control system operation on variation of angle of attack with time. p_o = 1 rpm; ϕ_o = 0°; 1/2-inch center-of-gravity offset.

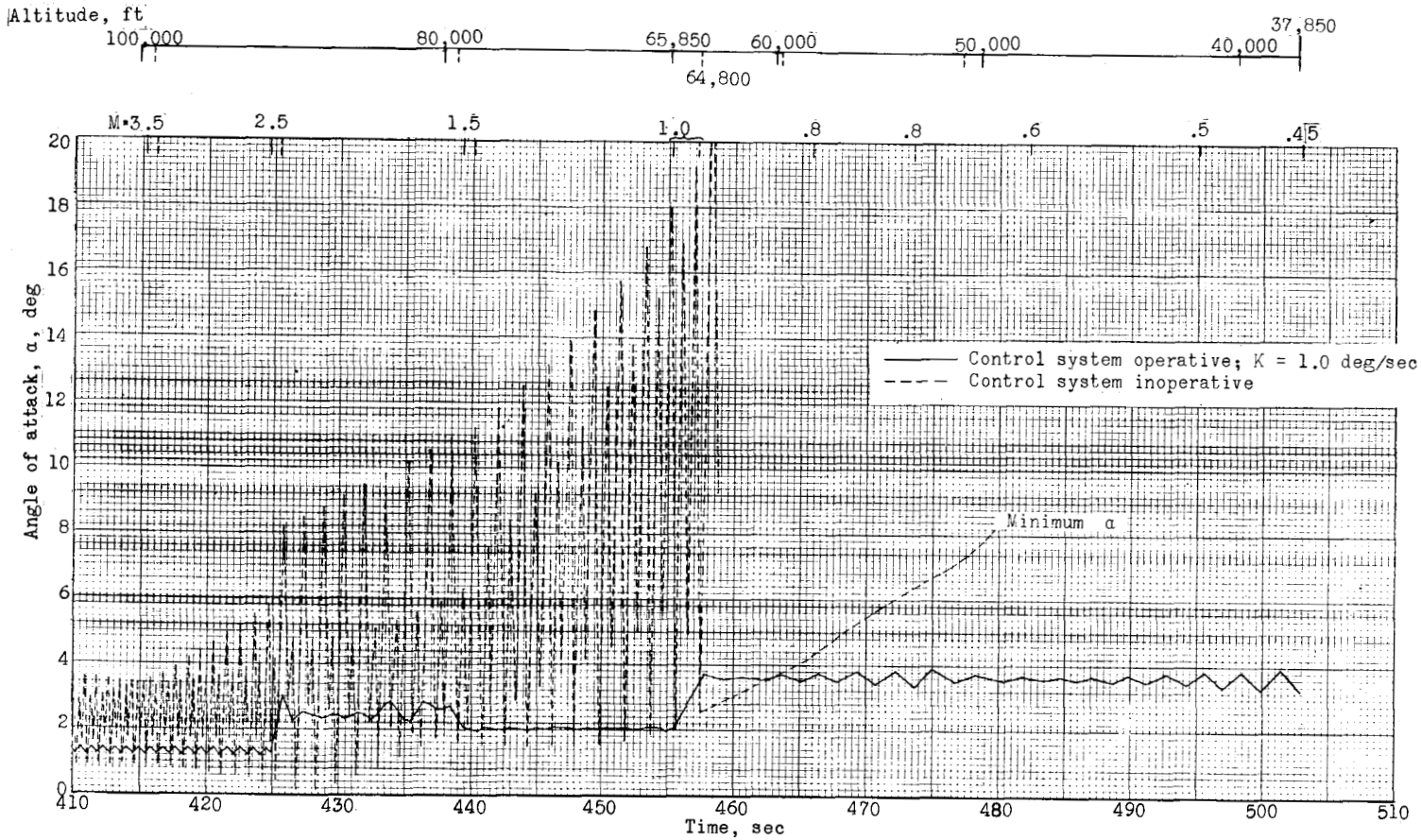

(b) α as a function of t for Mach numbers less than 3.5.

Figure 16.- Concluded.

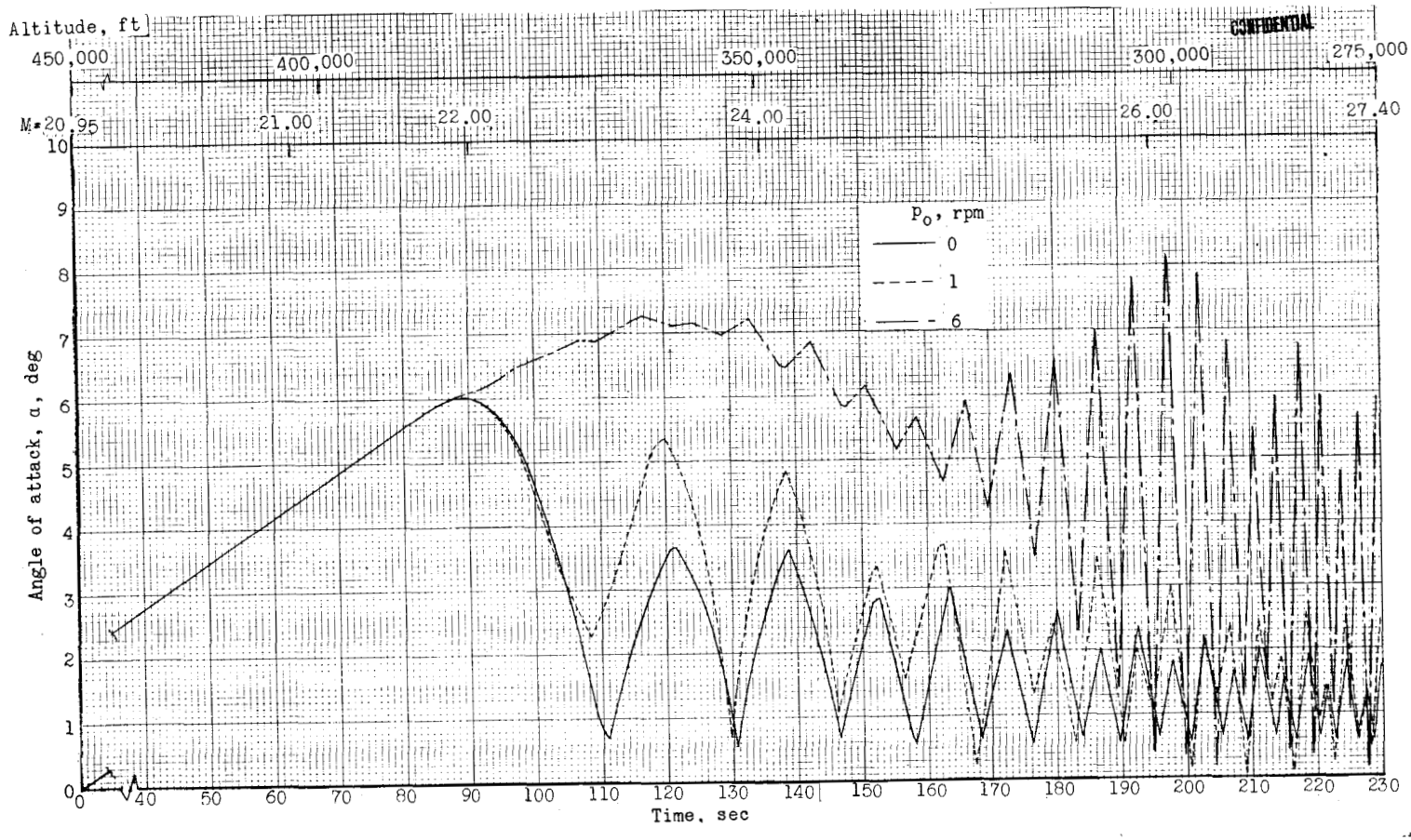

Figure 17.- Effect of initial roll rate on resonance in angle-of-attack variation with time. 1/4-inch center-of-gravity offset; control system inoperative.

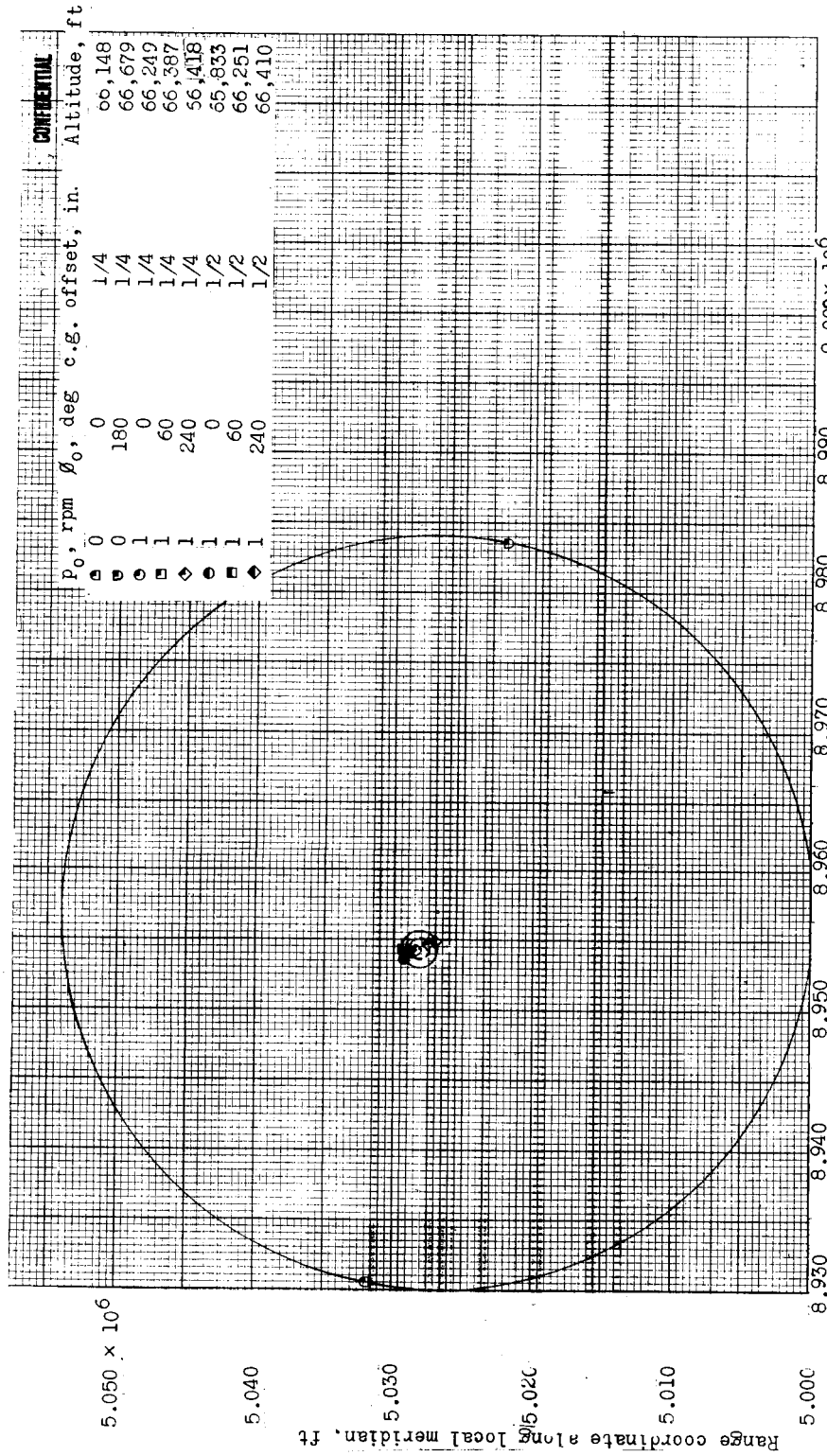

Figure 18.- Dispersion at M = 1.00 as affected by center-of-gravity offset. Control system operative with K = 1.0 deg/sec.

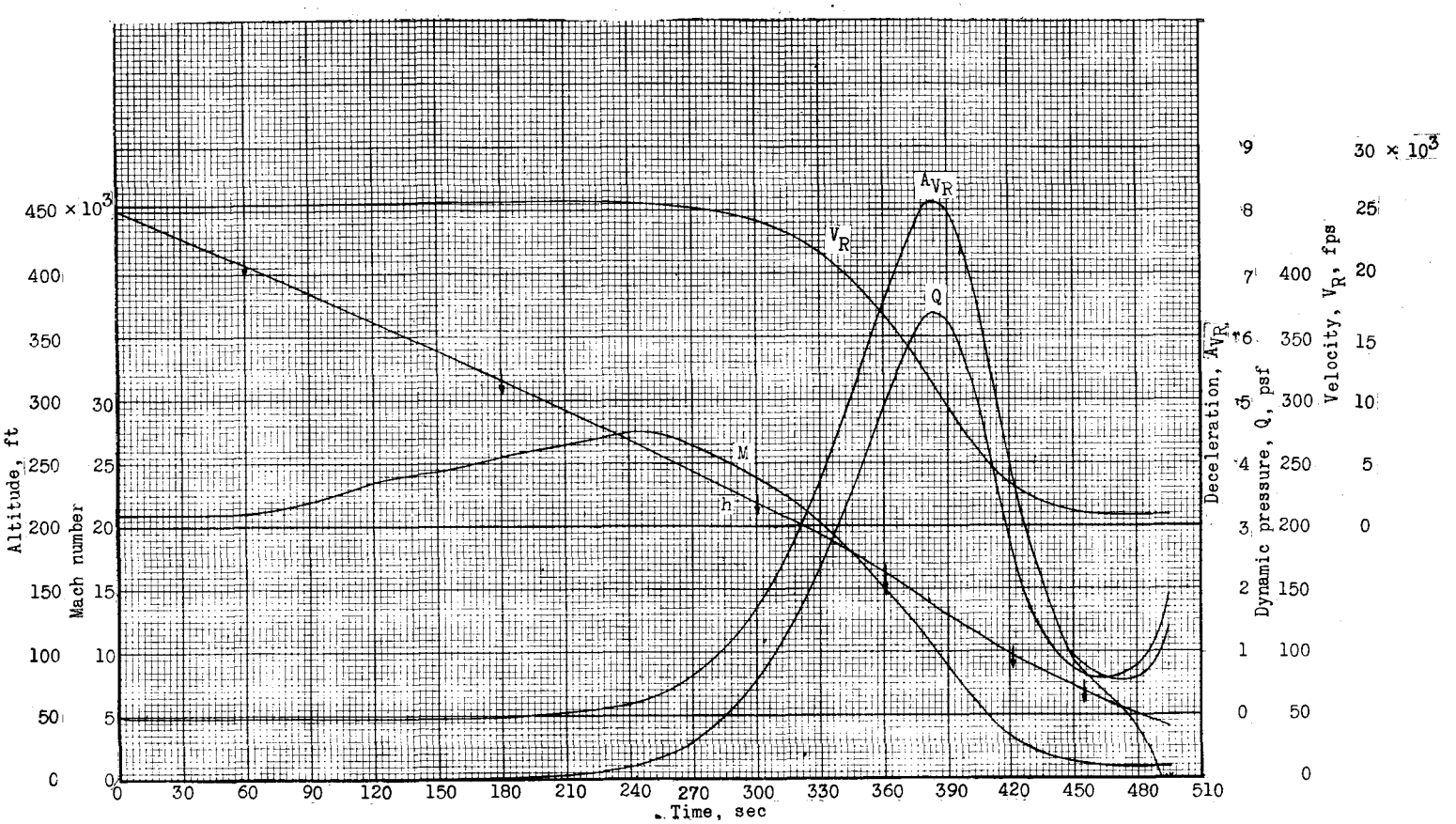

(a) Trajectory characteristics for one plane flight.

Figure 19.- Characteristics of reference case for study of dynamic stability at six altitudes. p_o = 1 rpm; no center-of-gravity offset; control system inoperative at all times. Arrows indicate initial altitudes of dynamic stability studies.

CONFIDENTIAL

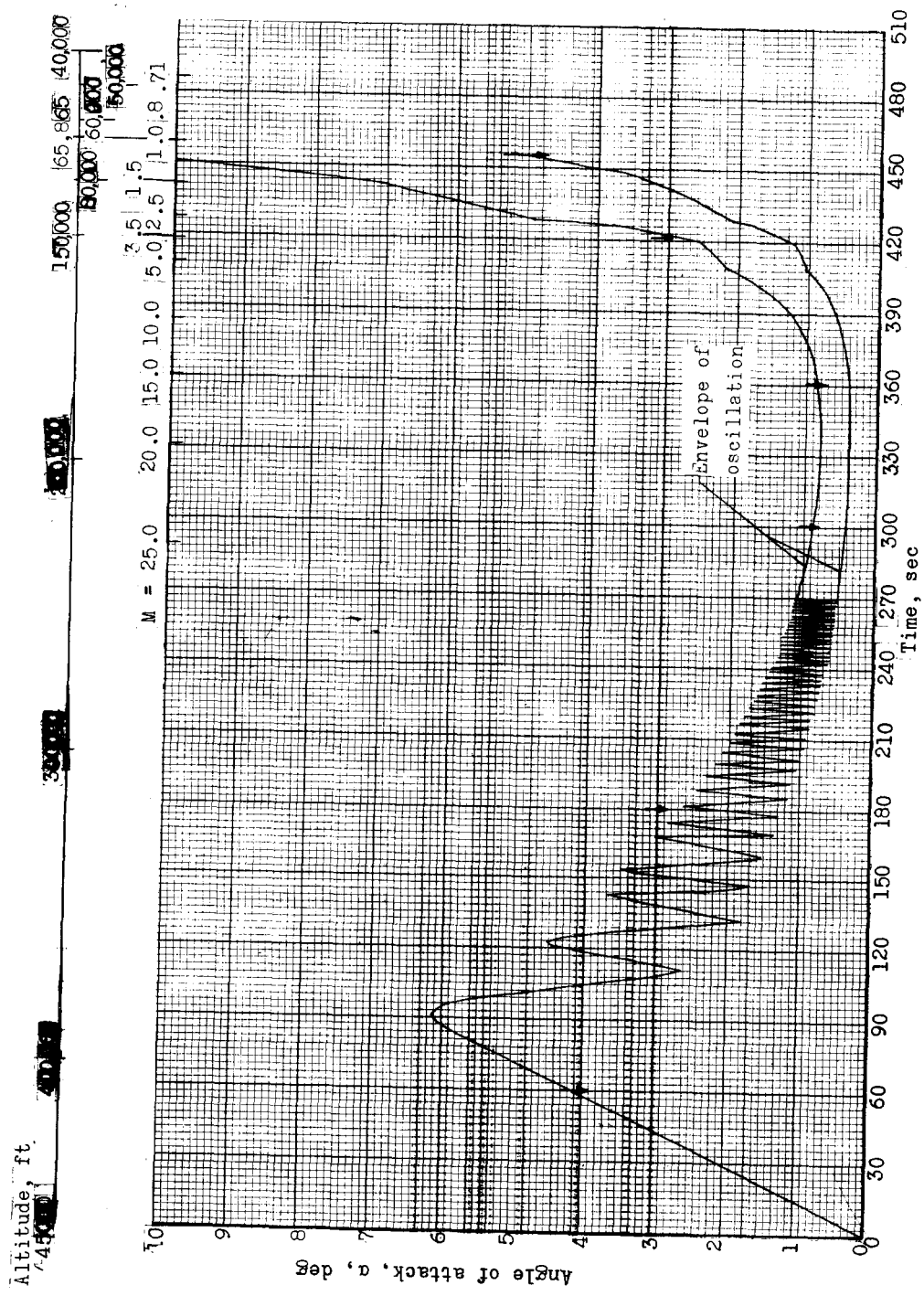

(b) α as a function of t for entire trajectory.

Figure 19.- Continued.

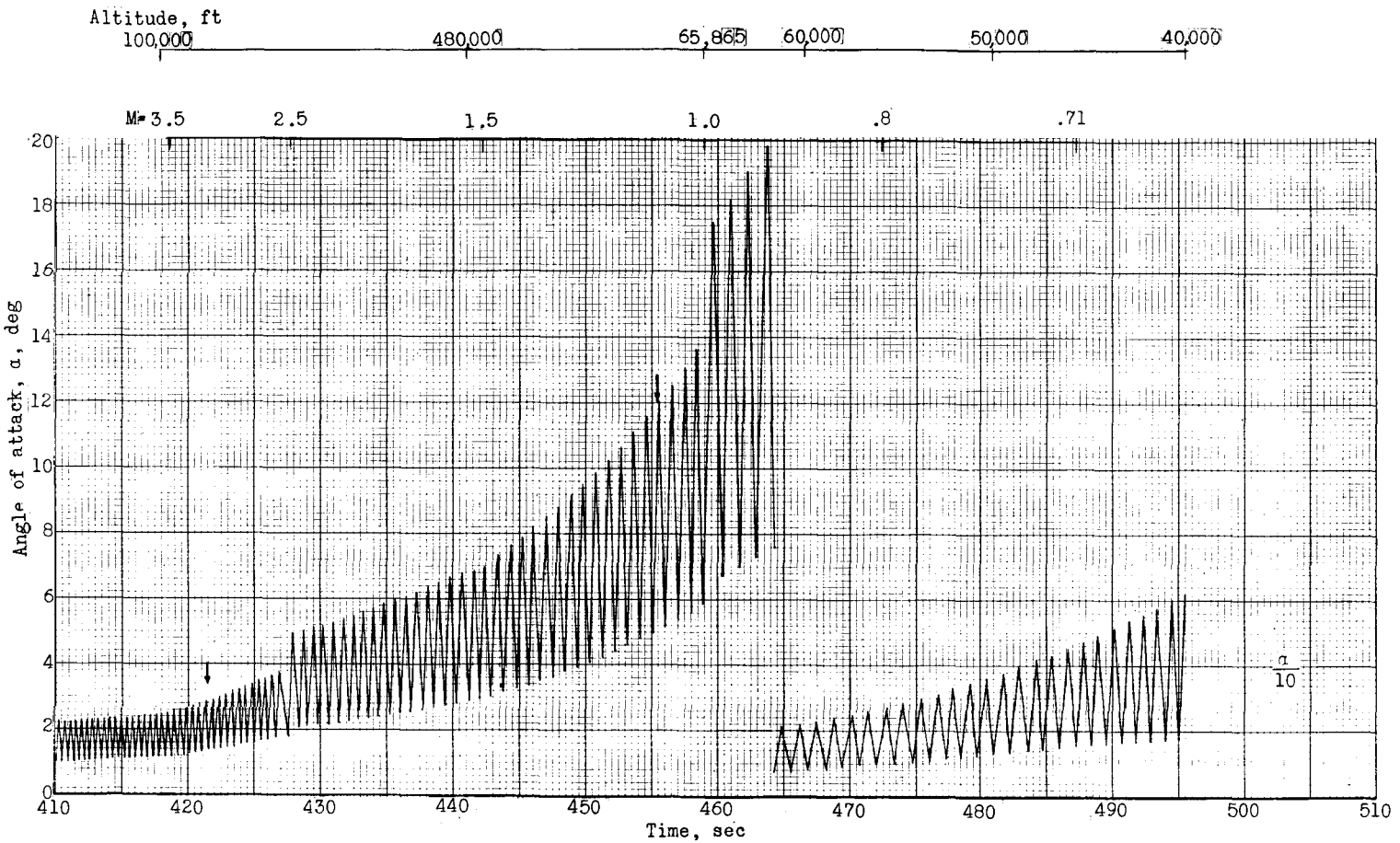

(c) α as a function of t for Mach numbers less than 3.5.

Figure 19.- Continued.

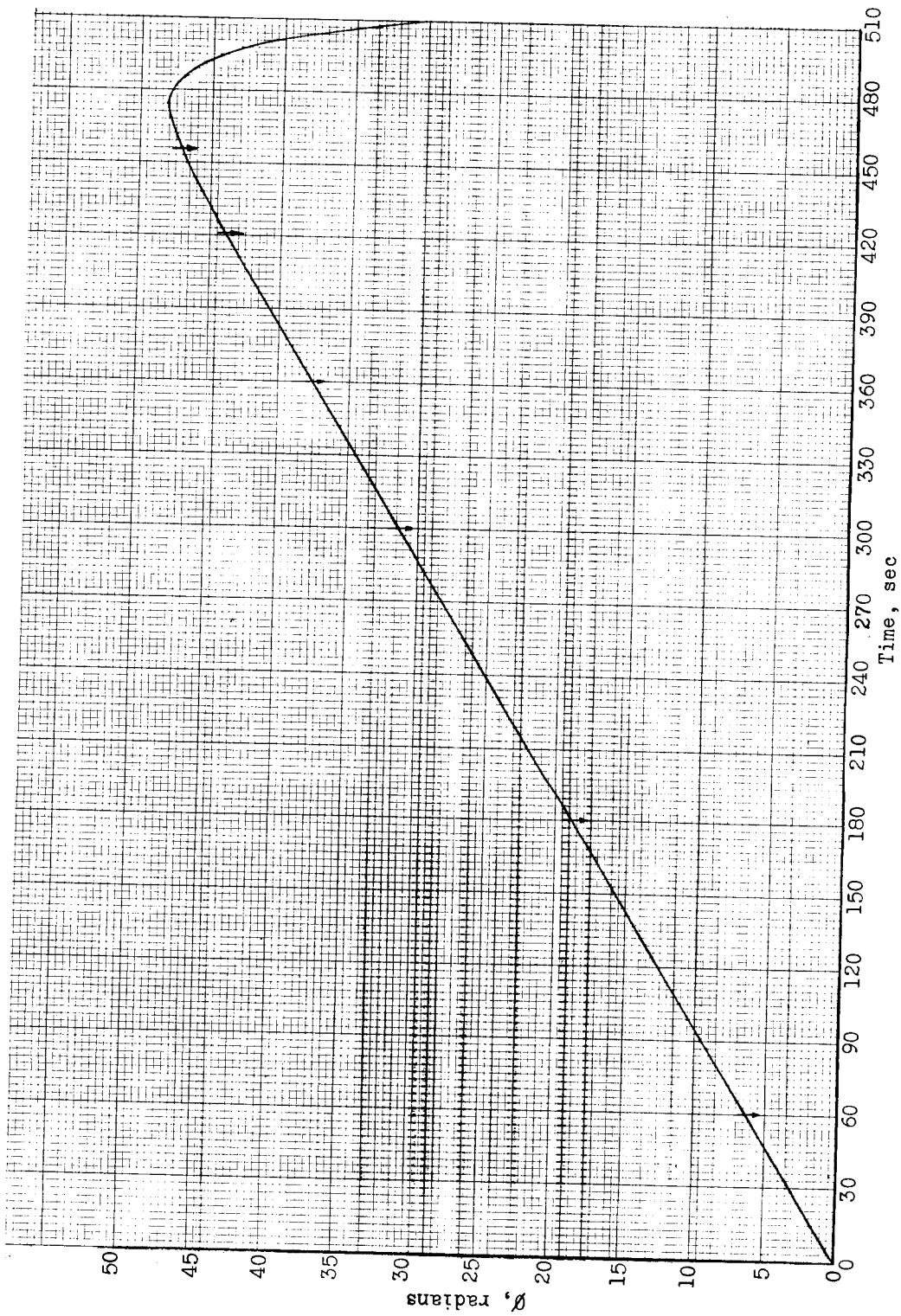

(d) ϕ as a function of t.

Figure 19.- Continued.

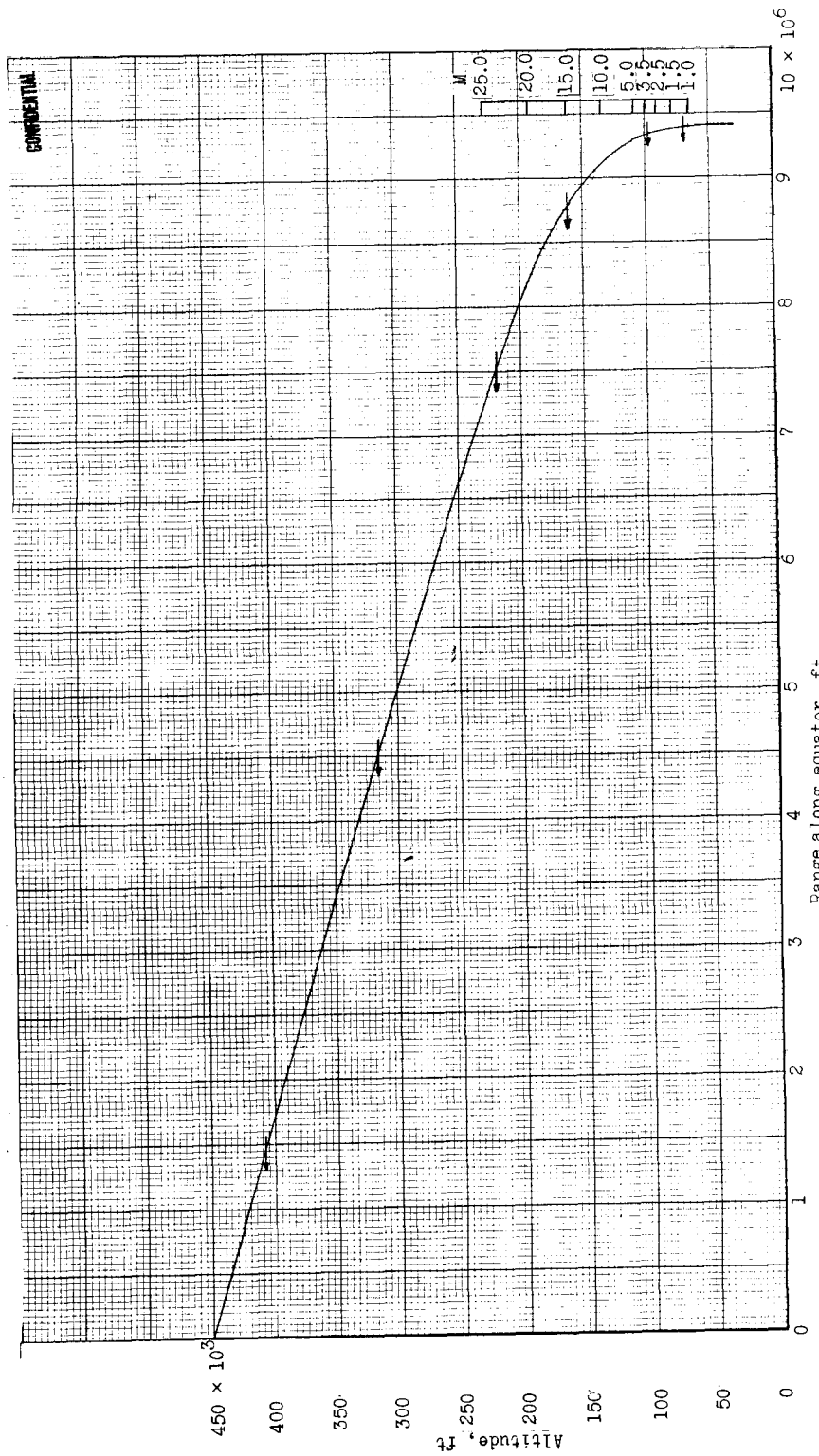

(e) Altitude as a function of range.

Figure 19.- Concluded.

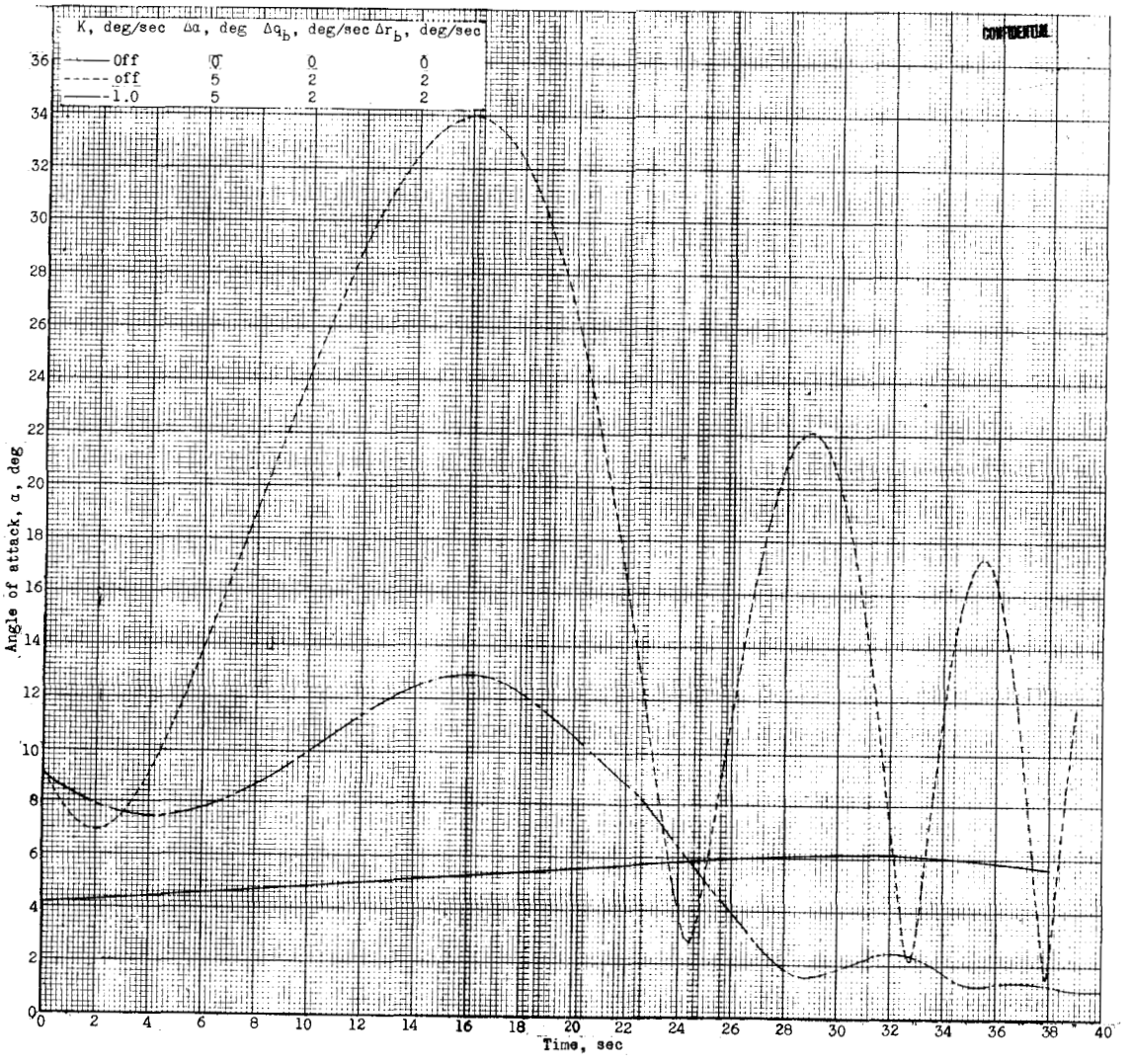

(a) α as a function of t.

Figure 20.- Effect of control-system operation on the variation of α, q_b, and r_b with time, with step disturbances in α, q_b, and r_b. Initial altitude, 407,146 feet.

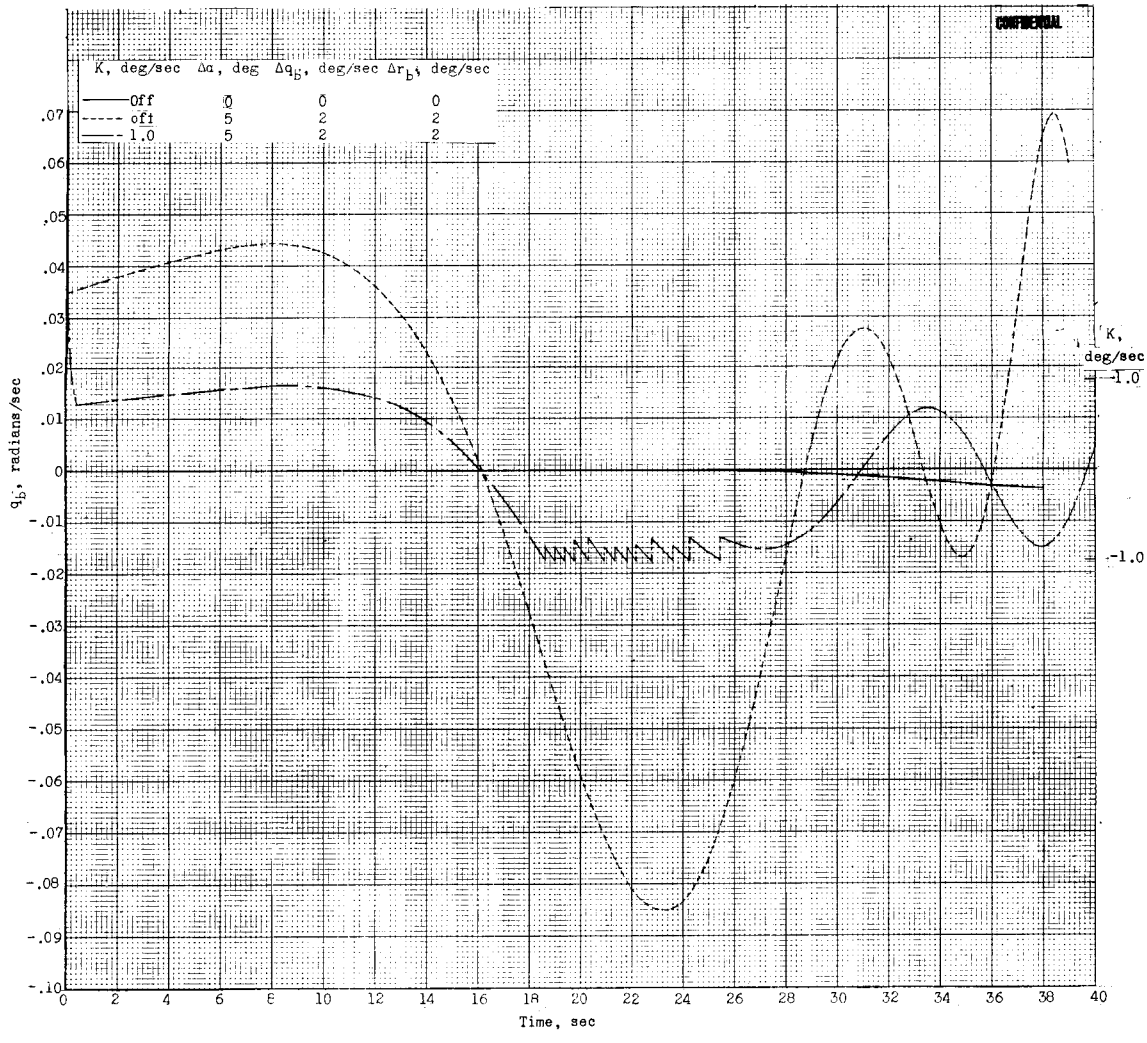

(b) q_b as a function of t.

Figure 20.- Continued.

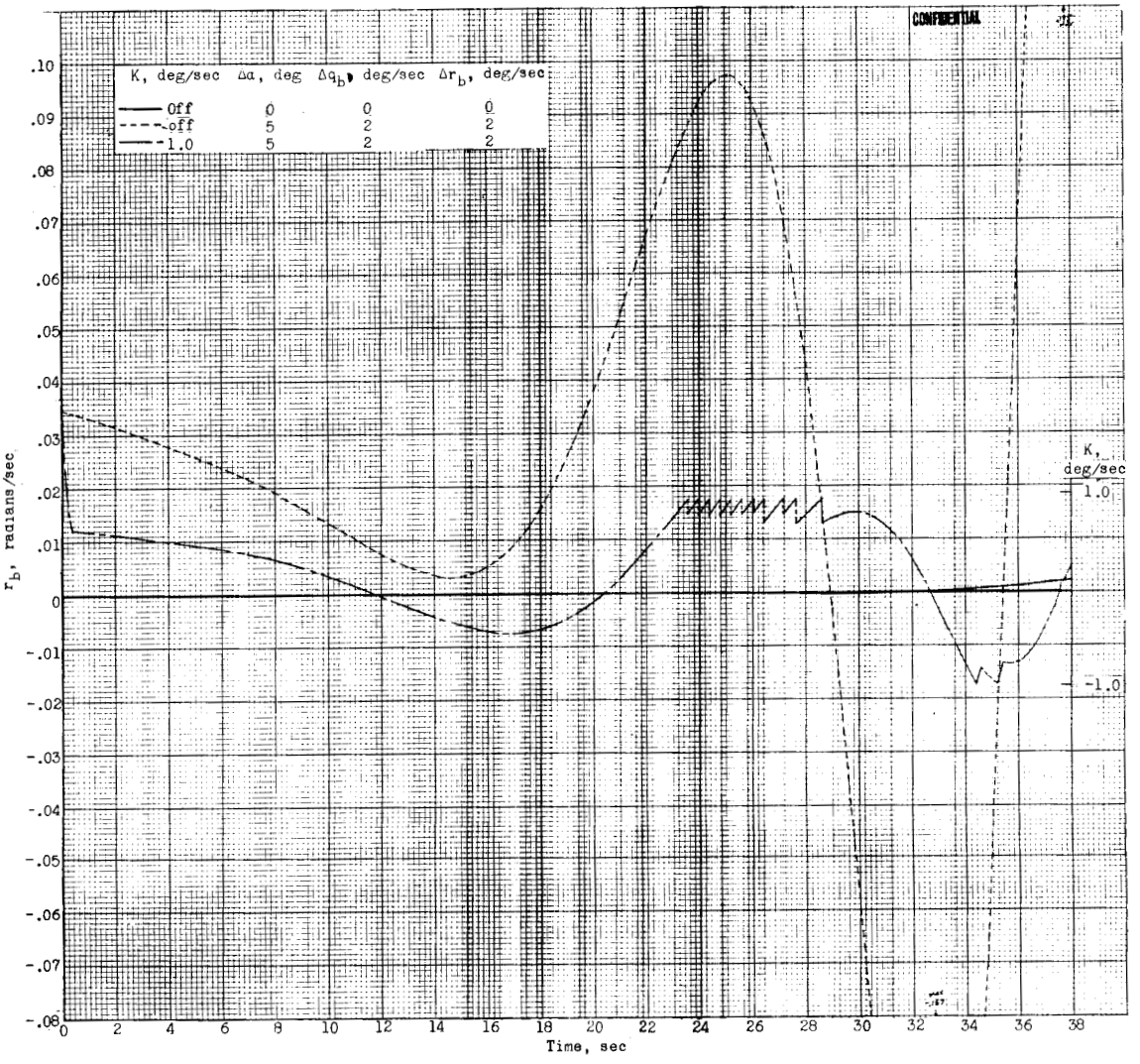

(c) r_b as a function of t.

Figure 20.- Concluded.

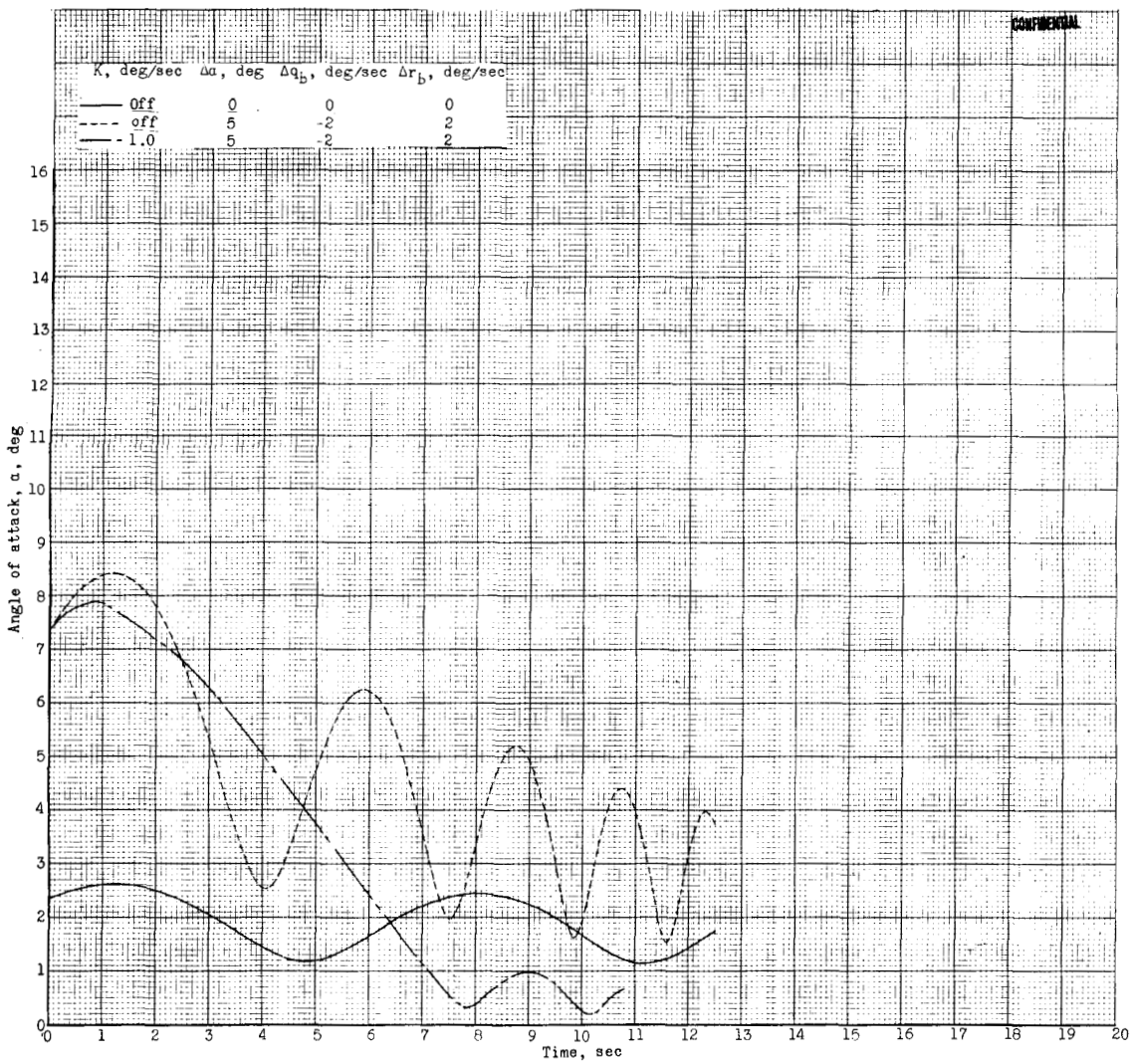

(a) α as a function of t.

Figure 21.- Effect of control-system operation on the variation of α, q_b, and r_b with time, with step disturbances in α, q_b, and r_b. Initial altitude, 315,960 feet.

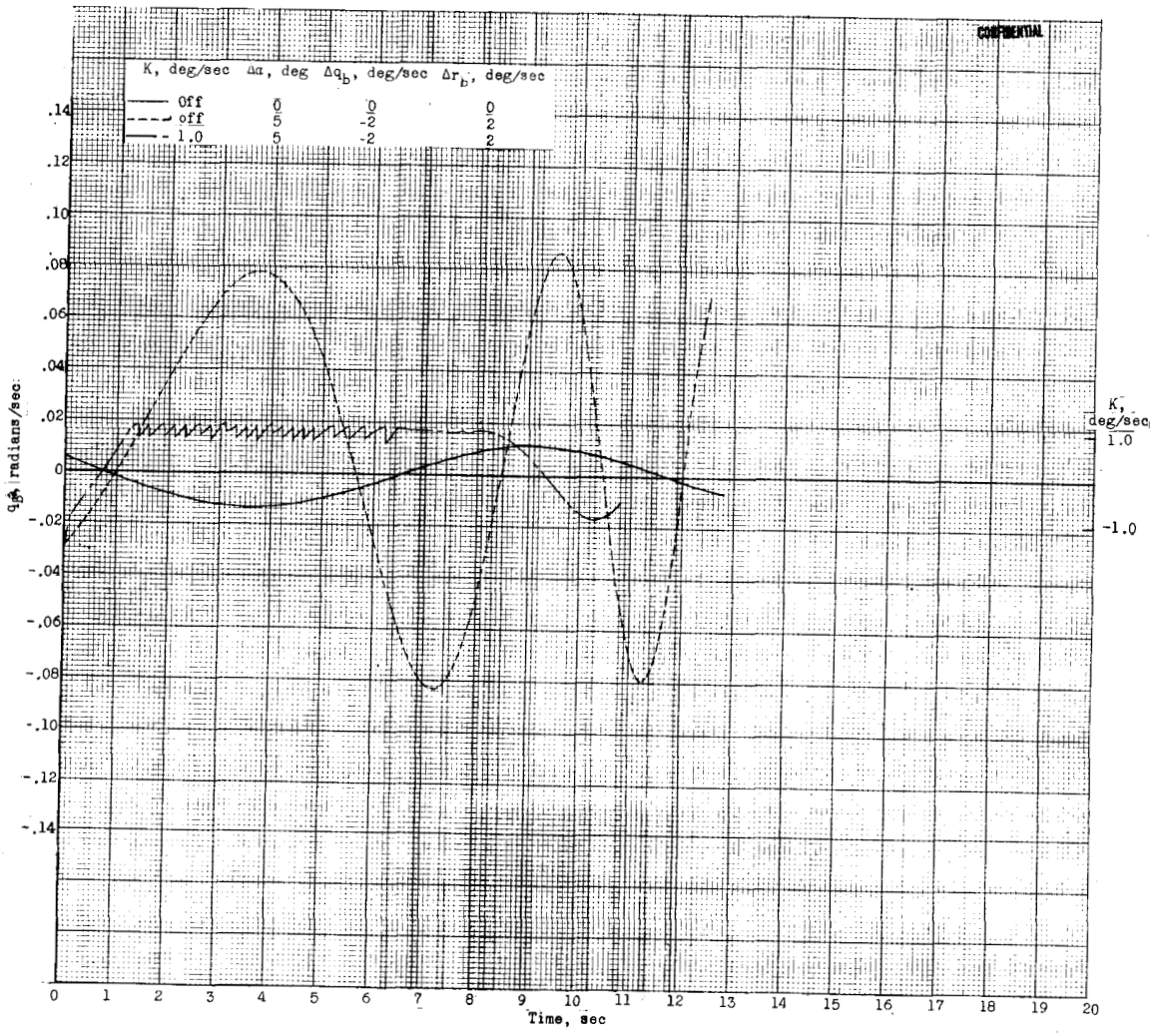

(b) q_b as a function of t.

Figure 21.- Continued.

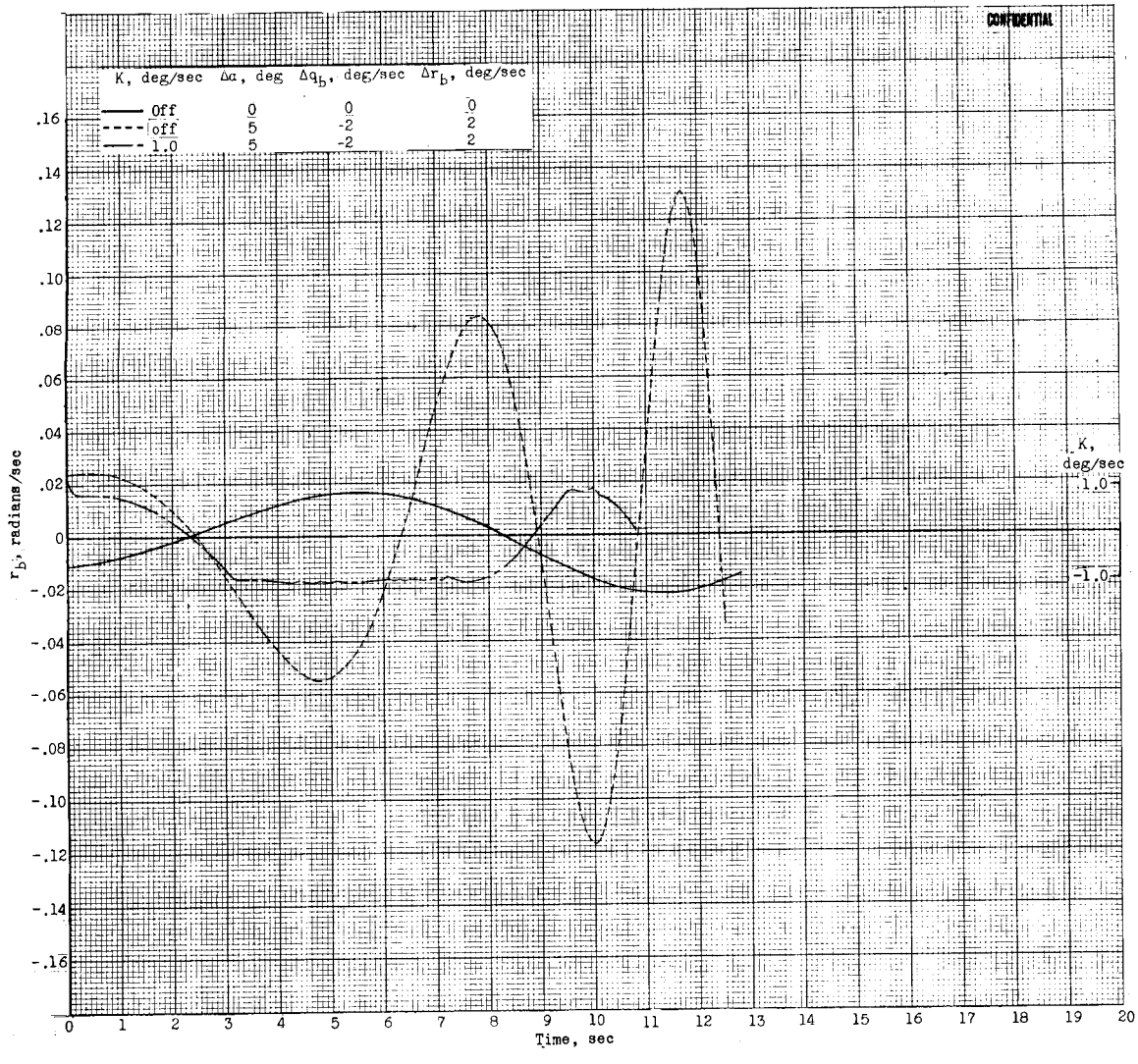

(c) r_b as a function of t.

Figure 21.- Concluded.

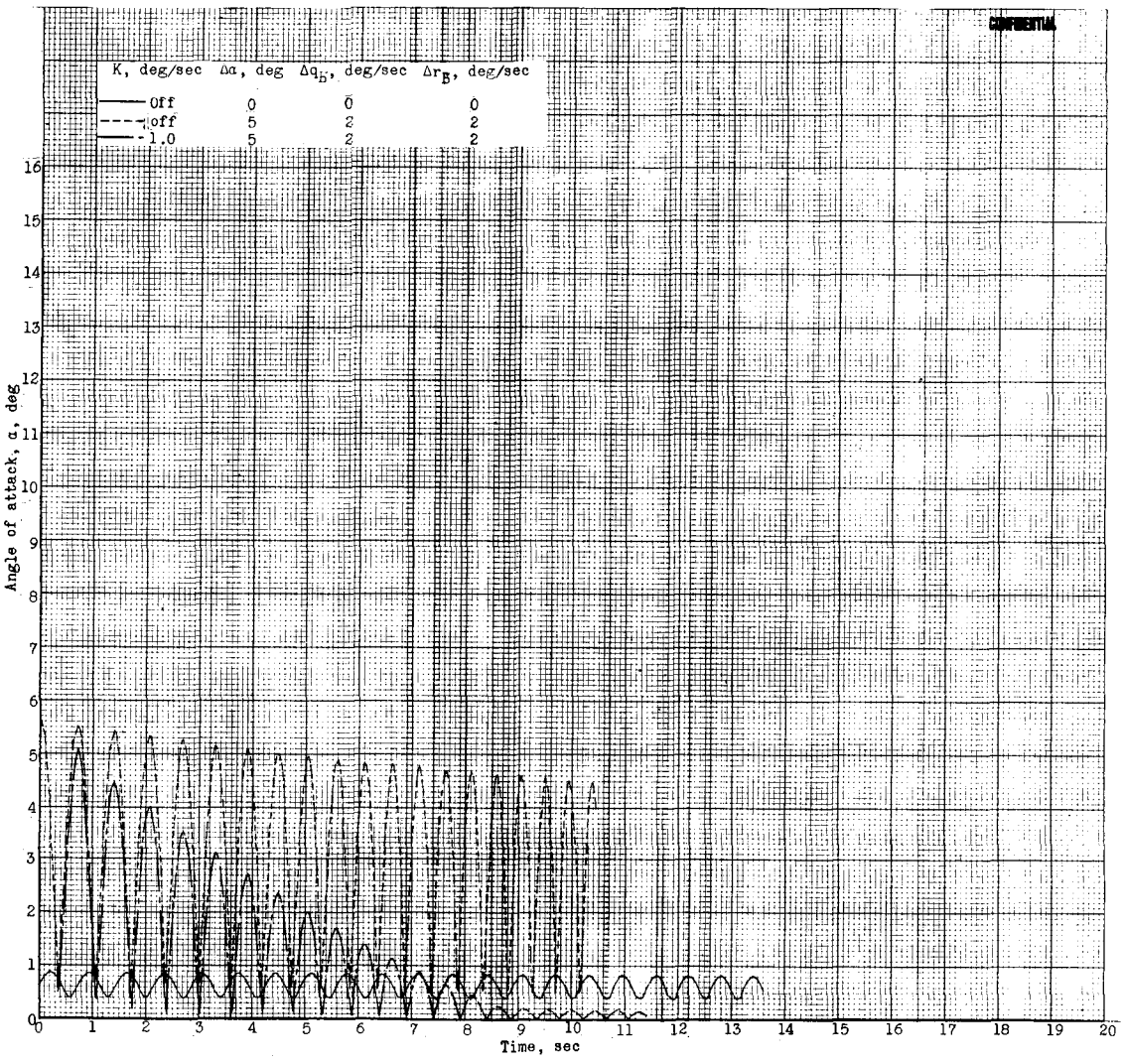

(a) α as a function of t.

Figure 22.- Effect of control-system operation on the variation of α, q_b, and r_b with time, with step disturbances in α, q_b, and r_b. Initial altitude, 219,188 feet.

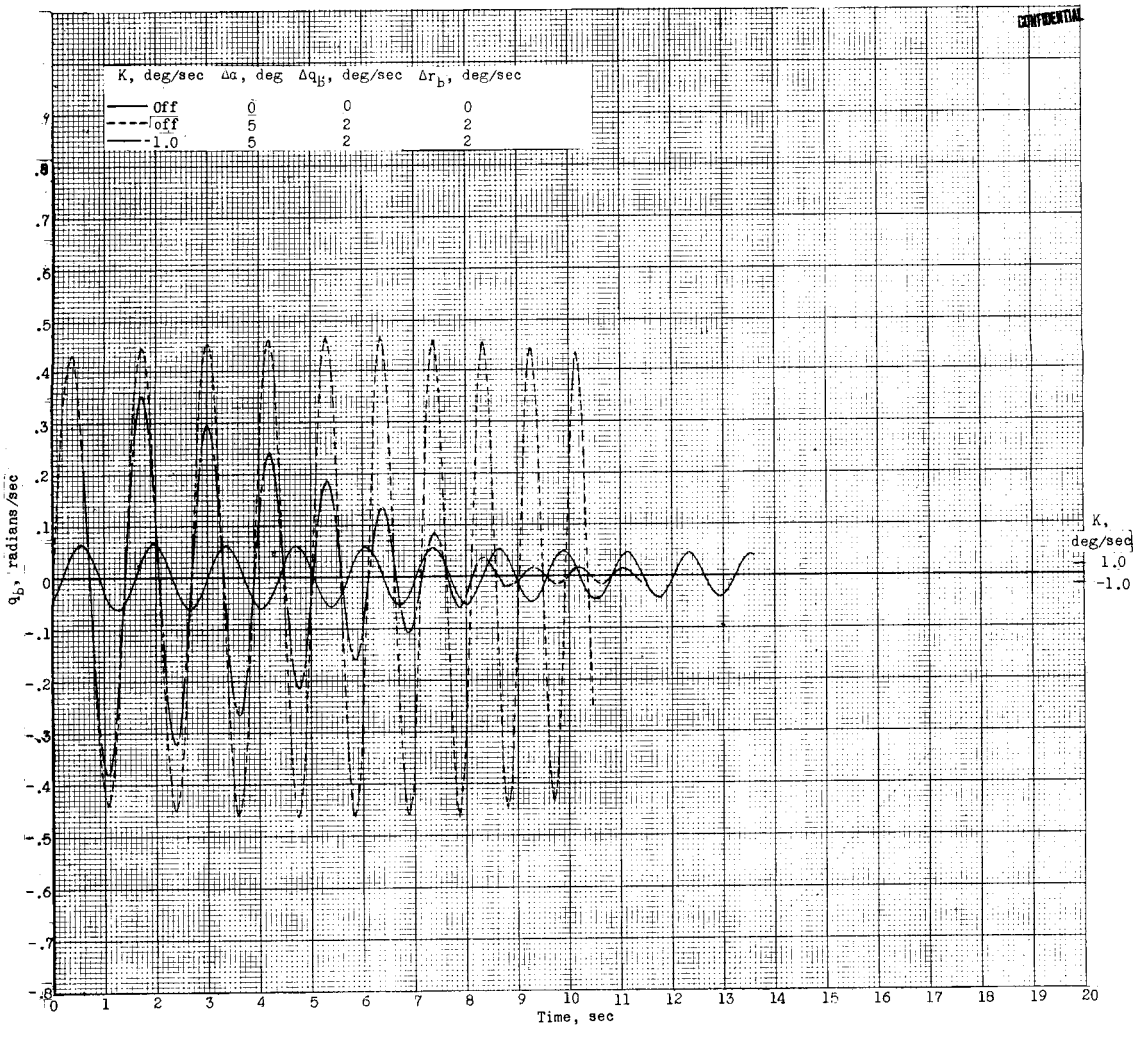

(b) q_b as a function of t.

Figure 22.- Continued.

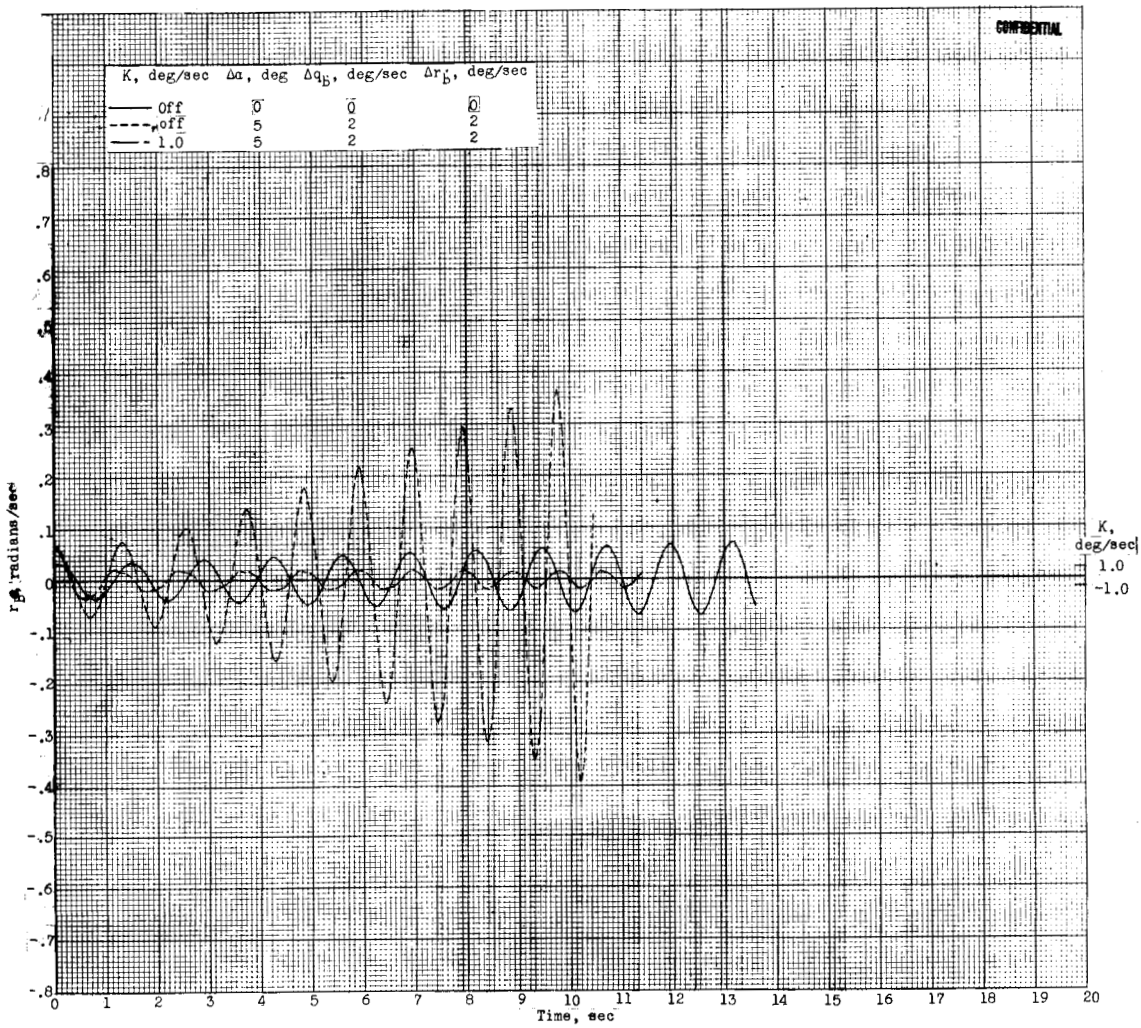

(c) r_b as a function of t.

Figure 22.- Concluded.

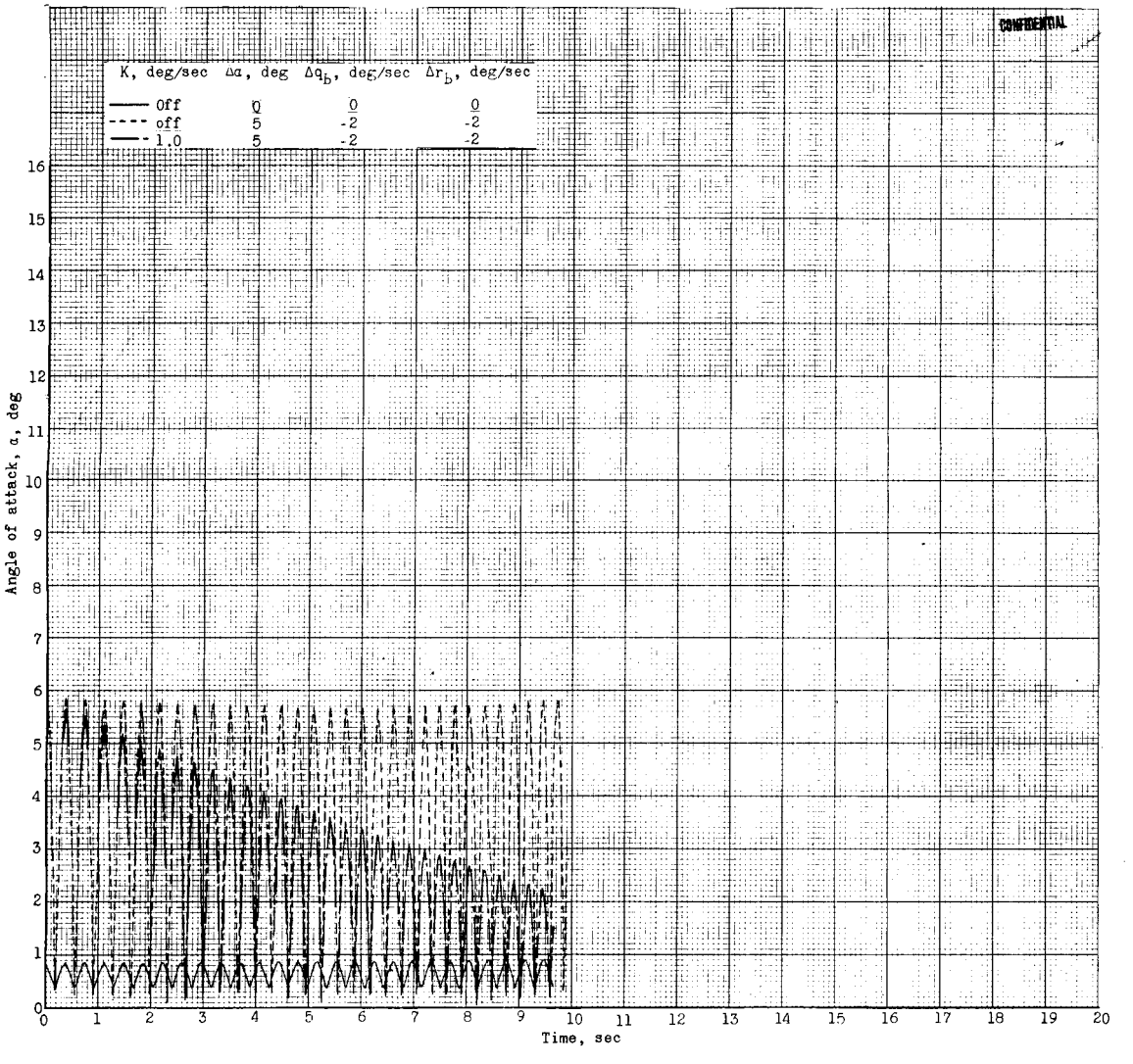

(a) α as a function of t.

Figure 23.- Effect of control-system operation on the variation of α, q_b, and r_b with time, with step disturbances in α, q_b, and r_b. Initial altitude, 161,891 feet.

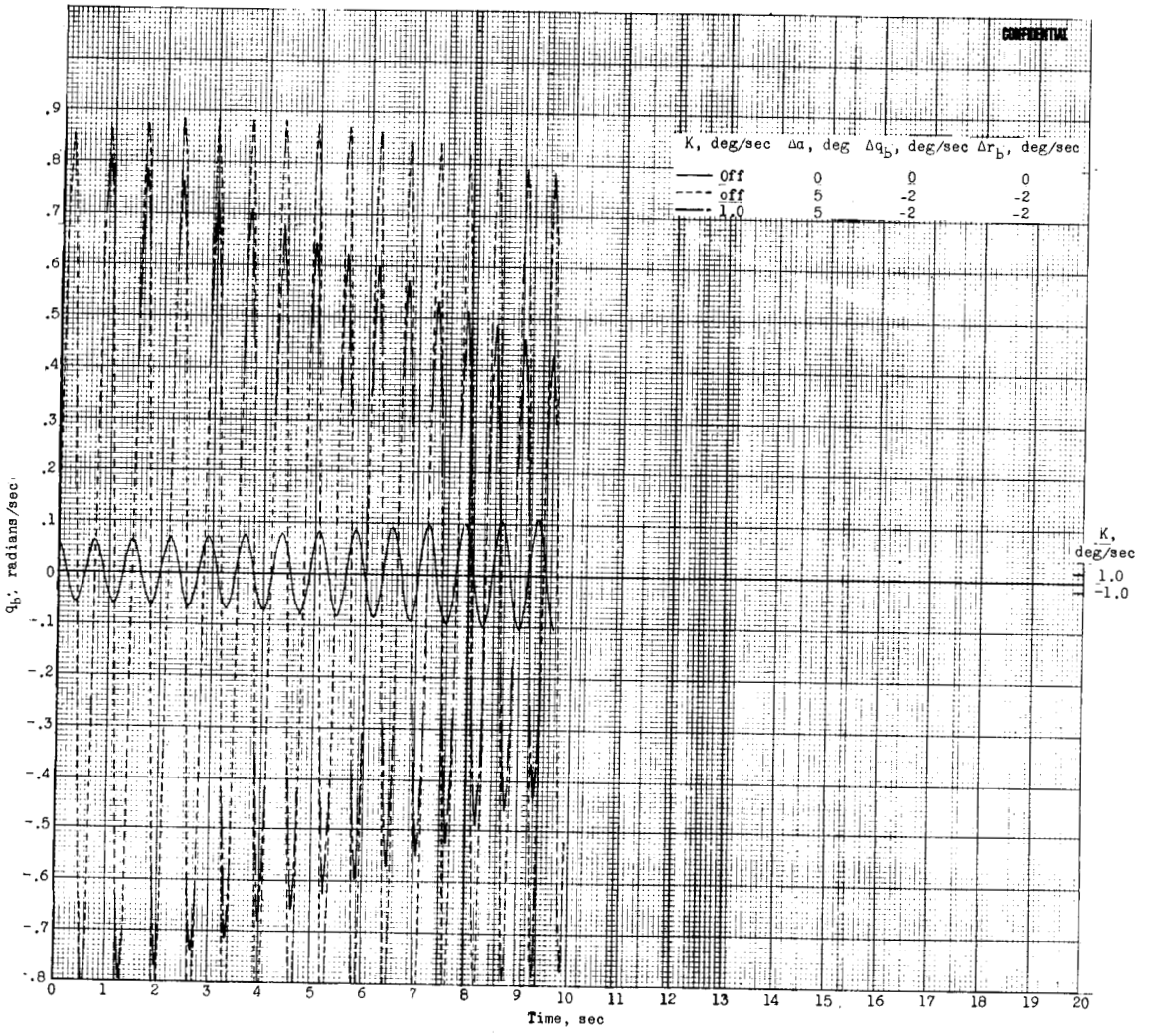

(b) q_b as a function of t.

Figure 23.- Continued.

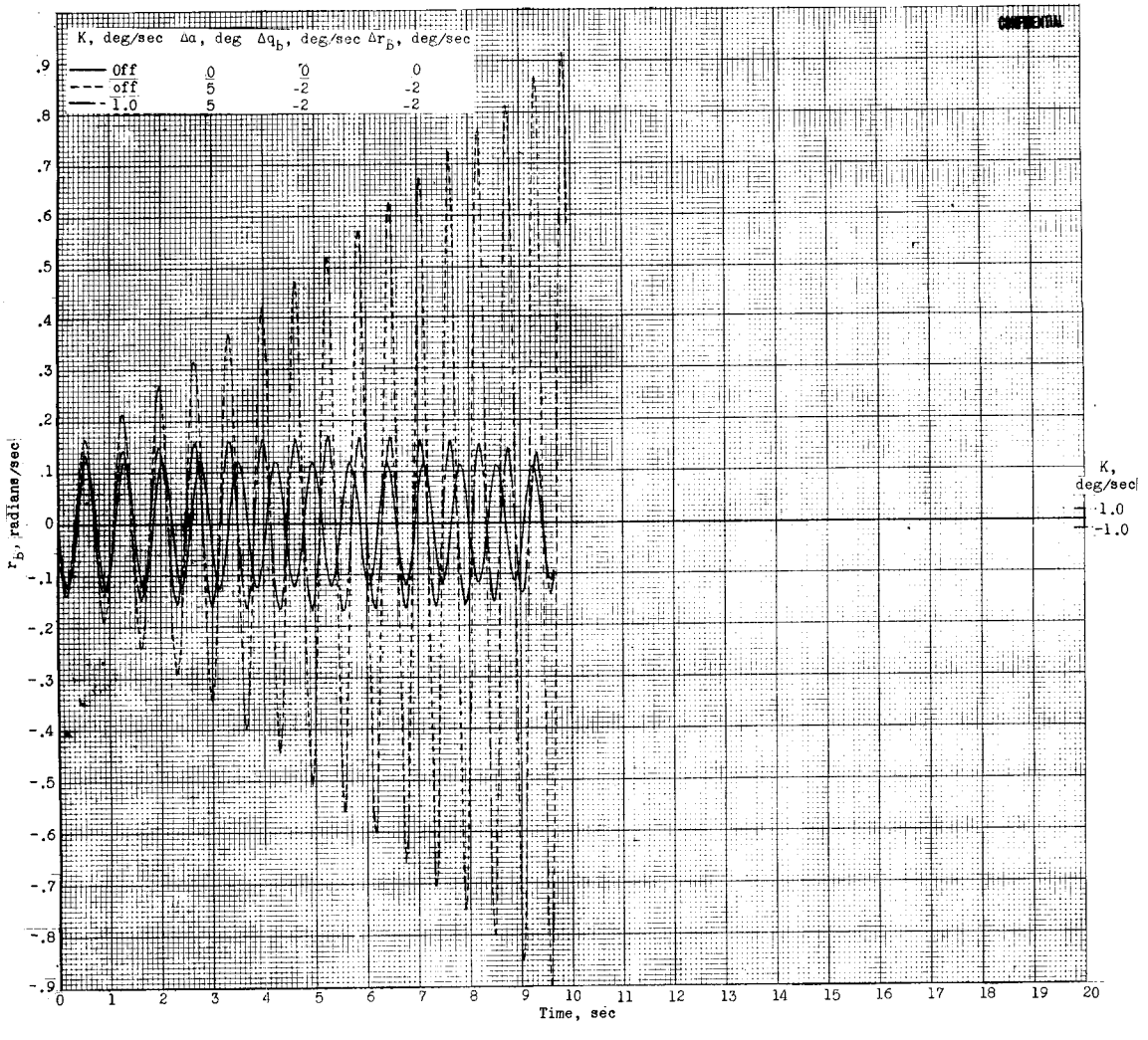

(c) r_b as a function of t.

Figure 23.- Concluded.

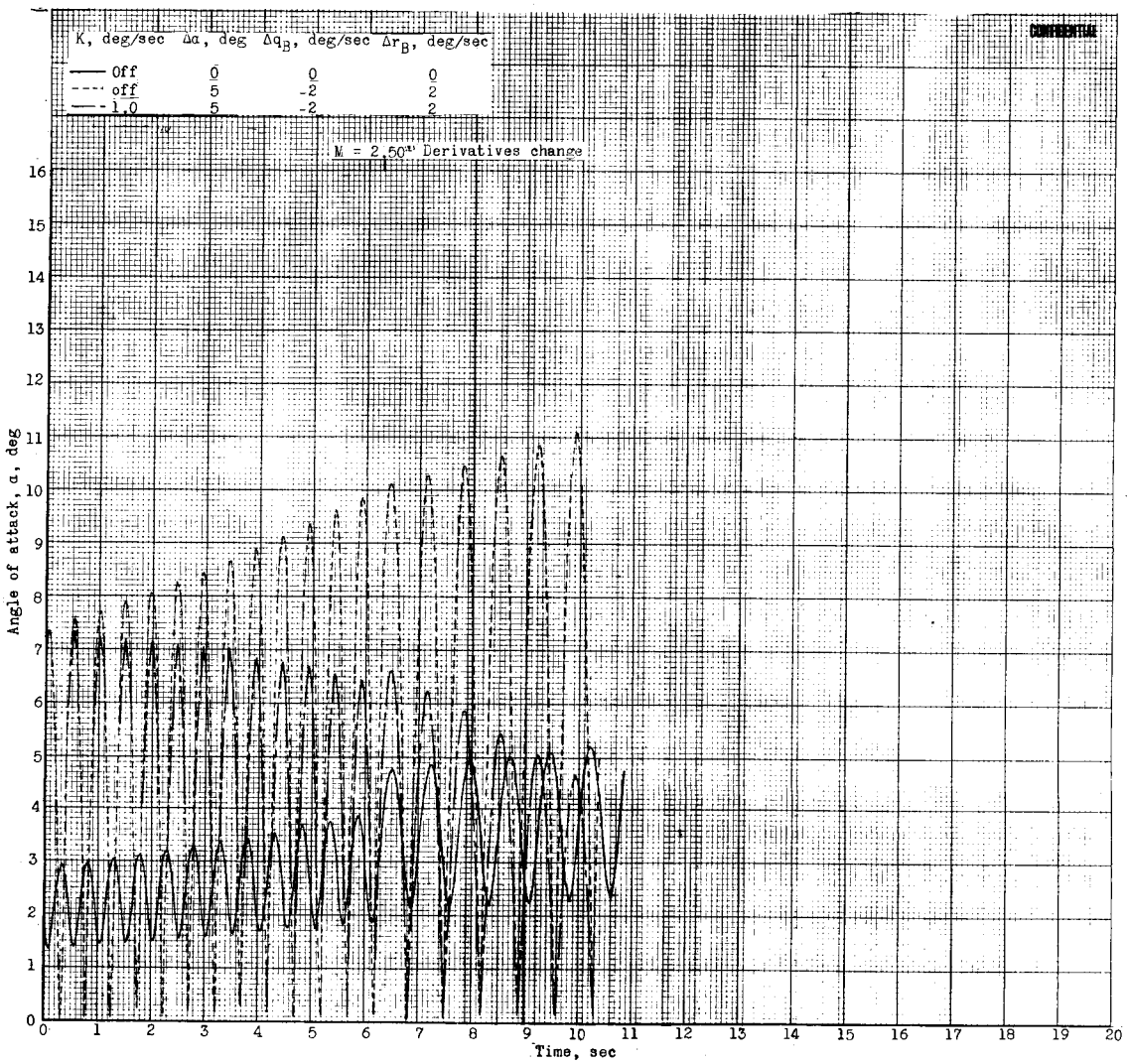

(a) α as a function of t.

Figure 24.- Effect of control-system operation on the variation of α, q_b, and r_b with time, with step disturbances in α, q_b, and r_b. Initial altitude, 96,730 feet.

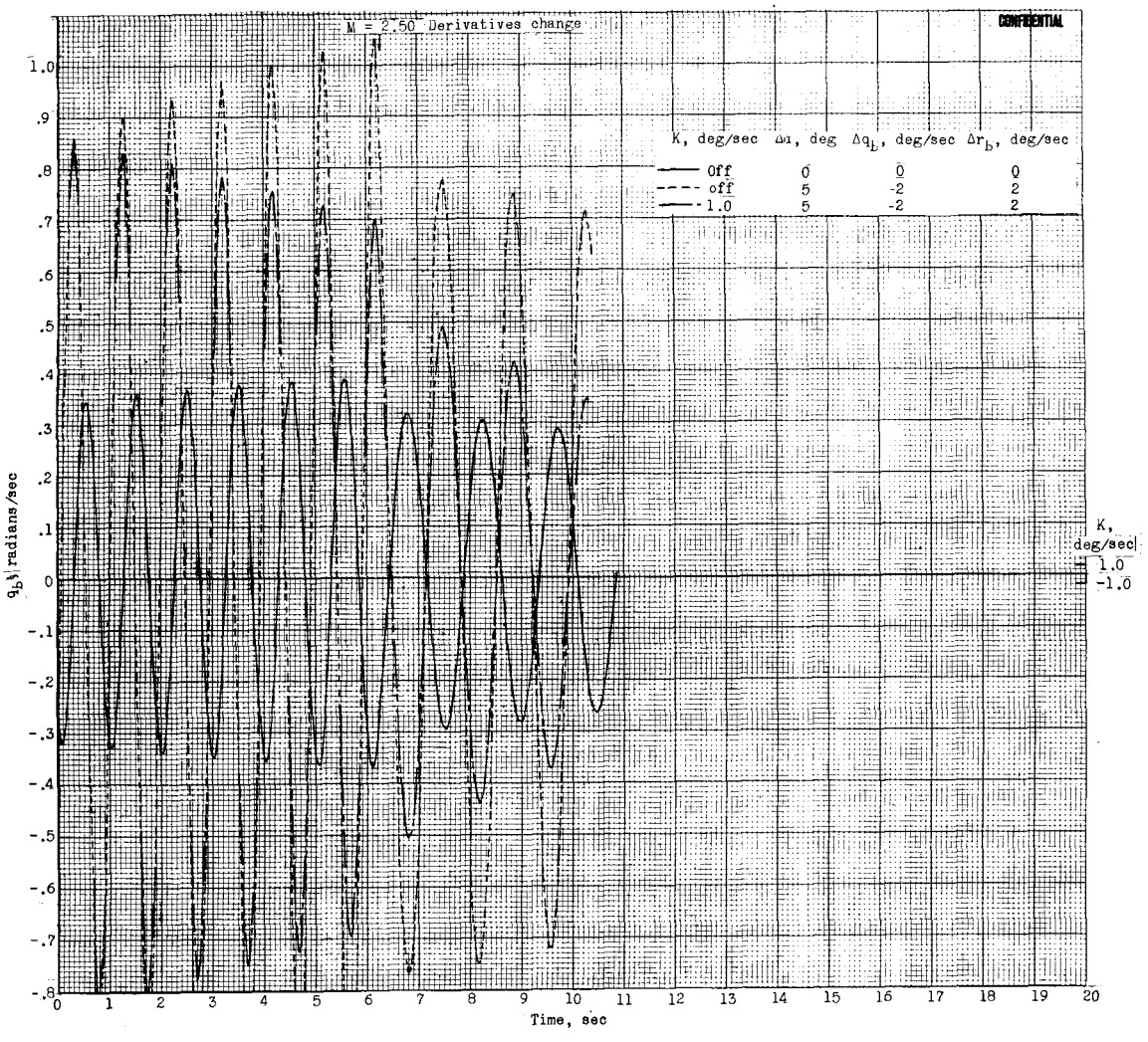

(b) q_b as a function of t.

Figure 24.- Continued.

(c) r_b as a function of t.

Figure 24.- Concluded.

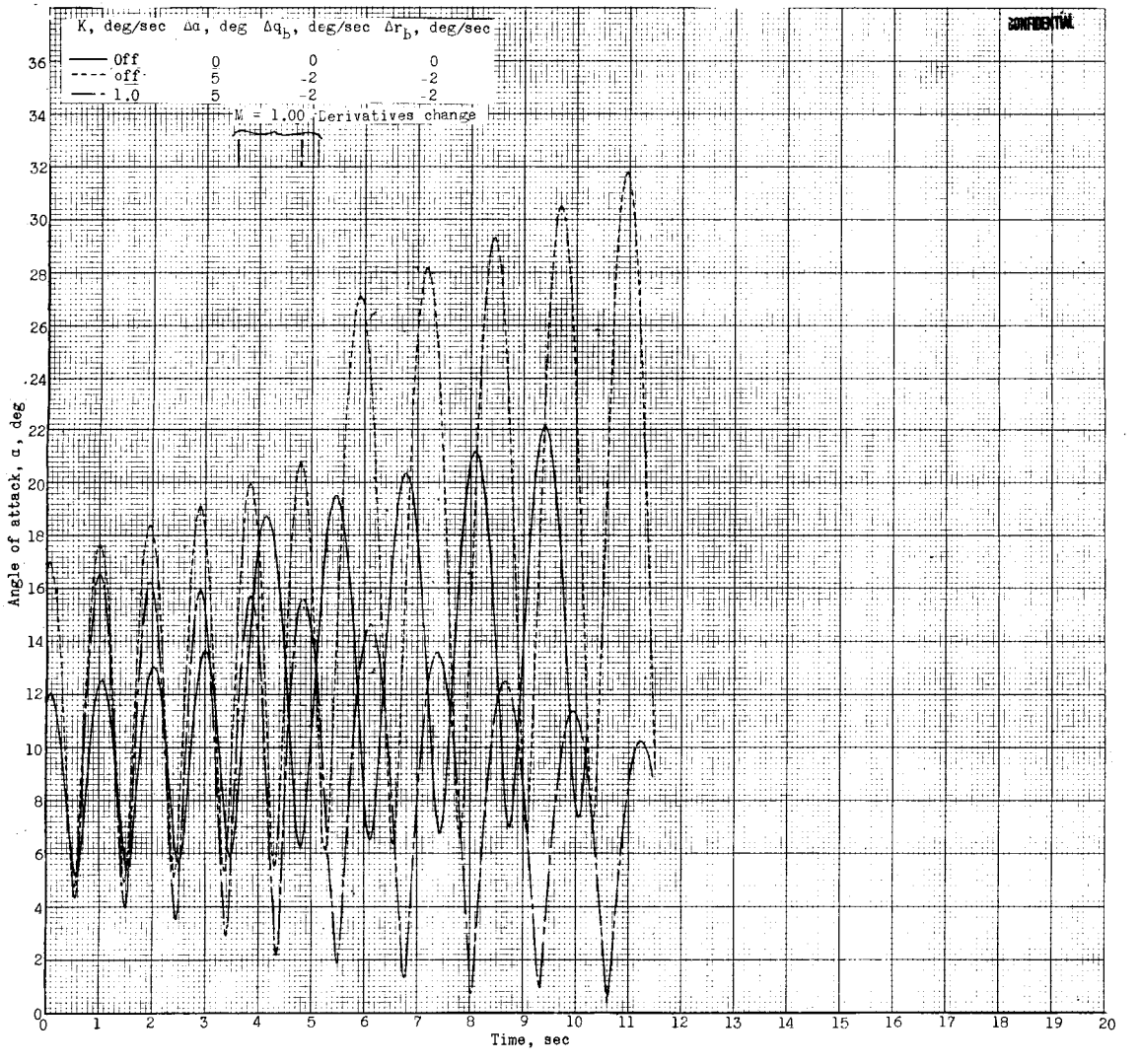

(a) α as a function of t.

Figure 25.- Effect of control-system operation on the variation of α, q_b, and r_b with time, with step disturbances in α, q_b, and r_b. Initial altitude, 68,601 feet.

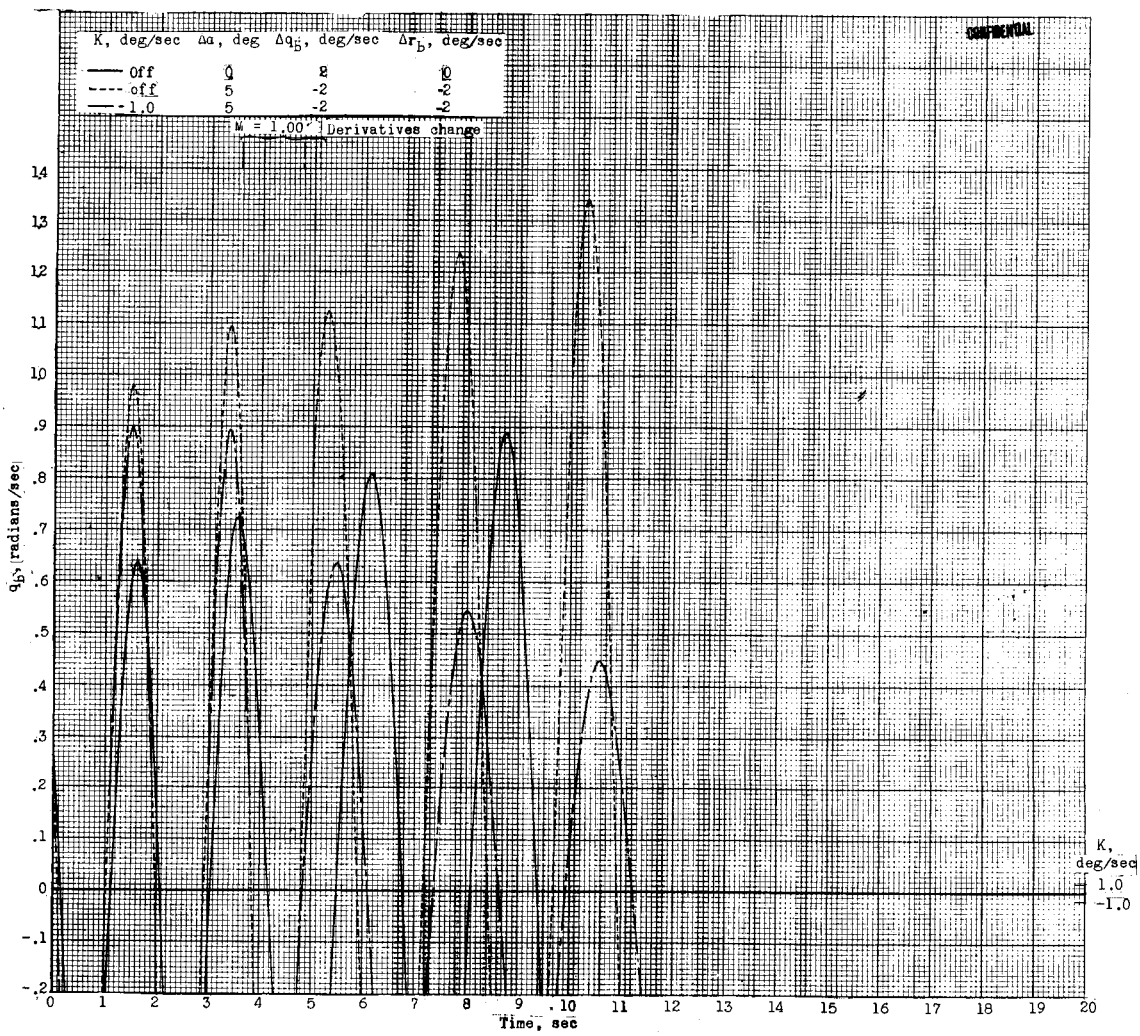

(b) q_b as a function of t.

Figure 25.- Continued.

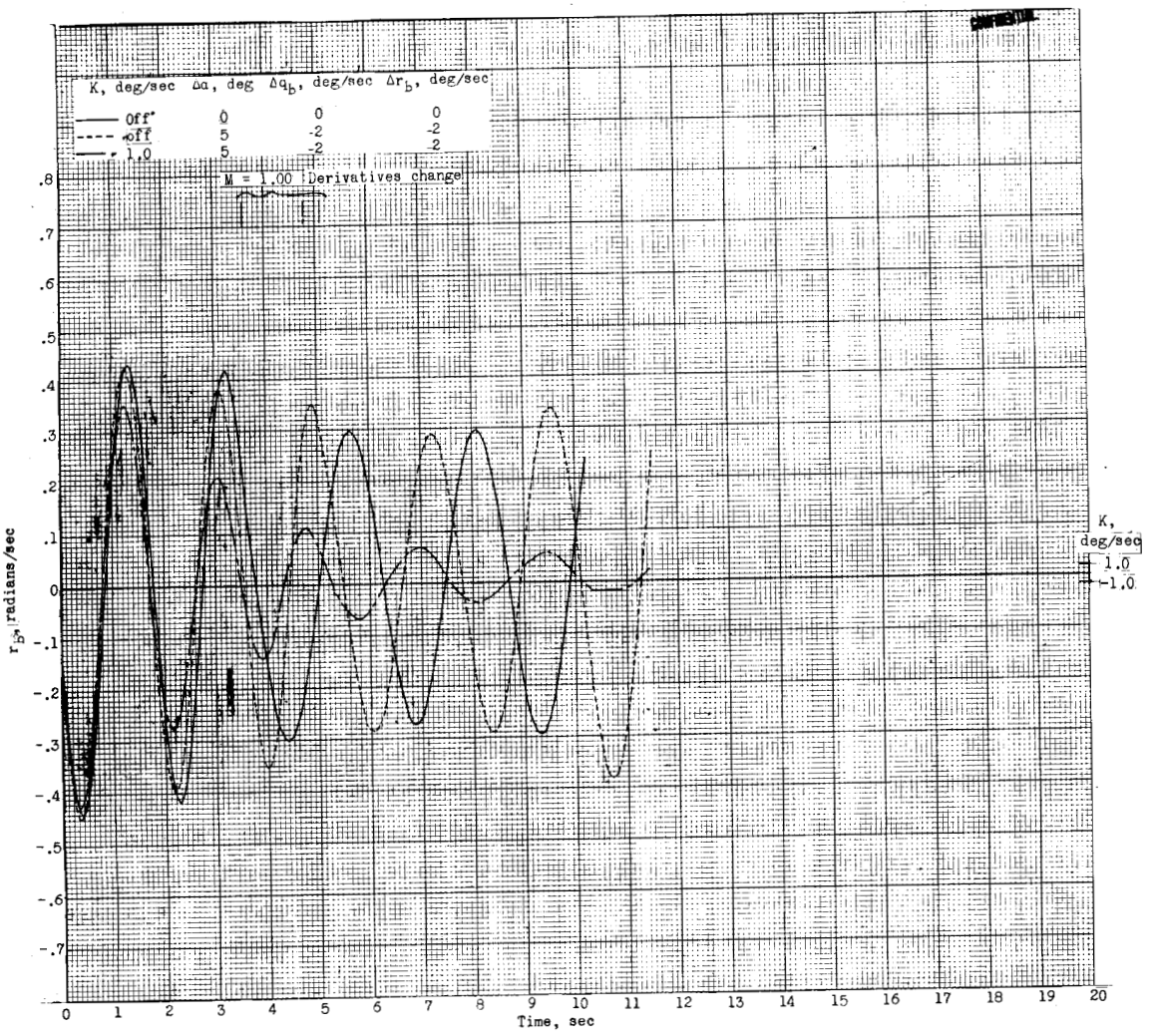

(c) r_b as a function of t.

Figure 25.- Concluded.